STUDIES OF TORSIONAL PROPERTIES OF DNA AND NUCLEOSOMES USING ANGULAR OPTICAL TRAPPING

A Dissertation

Presented to the Faculty of the Graduate School

of Cornell University

In Partial Fulfillment of the Requirements for the Degree of

Doctor of Philosophy

by

Maxim Y. Sheinin

May 2013

STUDIES OF TORSIONAL PROPERTIES OF DNA AND NUCLEOSOMES USING ANGULAR OPTICAL TRAPPING

Maxim Y. Sheinin, Ph. D.

Cornell University 2013

DNA *in vivo* is subjected to torsional stress due to the action of molecular motors and other DNA-binding proteins. Several decades of research have uncovered the fascinating diversity of DNA transformations under torsion and the important role they play in the regulation of vital cellular processes such as transcription and replication. Recent studies have also suggested that torsion can influence the structure and stability of nucleosomes – basic building blocks of the eukaryotic genome. However, our understanding of the impact of torsion is far from being complete due to significant experimental challenges. In this work we have used a powerful single-molecule experimental technique, angular optical trapping, to address several long-standing issues in the field of DNA and nucleosome mechanics. First, we utilized the high resolution and direct torque measuring capability of the angular optical trapping to precisely measure DNA twist-stretch coupling. Second, we characterized DNA melting under tension and torsion. We found that torsionally underwound DNA forms a left-handed structure, significantly more flexible compared to the regular B-DNA. Finally, we performed the first comprehensive investigation of the single nucleosome behavior under torque and force. Importantly, we discovered that positive torque causes significant dimer loss, which can have implications for transcription through chromatin.

BIOGRAPHICAL SKETCH

Maxim Yurievitch Sheinin was born to Yuri Sheinin and Vera Peshkova on July 31st, 1985 in Minsk, Belarus (then part of the Union of Soviet Socialist Republics). He attended School №20 (later Gymnasium №8) in Minsk in 1991-1996 and 1997-2000, Russian Embassy School in Vienna, Austria in 1996-1997, and Belarusian State University Lyceum in Minsk in 2000-2002, from which he graduated with a silver medal. In the year 2002 he enrolled in the Physics Department of Saint Petersburg State University (Saint Petersburg, Russia). In 2004 he joined the Sub-Department of Biological Physics. While in Saint Petersburg, he performed research on DNA spectroscopy at V. A. Fock Institute of Physics and at the Institute of Cytology of Russian Academy of Sciences. He graduated with honors with a Bachelor of Science degree in Physics in 2006, and subsequently enrolled in the graduate school at Cornell University. He joined Michelle Wang's single-molecule biophysics group in 2007. His graduate work focused on studies of torsional properties of DNA and nucleosomes using angular optical trapping. He graduated with a Master of Science in 2010 and a Doctor of Philosophy in 2013, both in Physics. In his spare time he enjoys playing soccer, reading, learning new languages, traveling, hiking, and spending time with family and friends.

To my parents, Vera and Yuri, and my wife, Anuttama

ACKNOWLEDGMENTS

First of all, I would like to thank my advisor, Michelle Wang, for her unwavering support during my graduate years. She has carefully nurtured the researcher in me, providing the freedom to explore fascinating new directions, while also guiding past the quicksand of failed projects. I have come to greatly admire her passion for science, extremely sharp mind, and work ethic. I have also greatly appreciated her willingness to listen and to be understanding under any circumstances.

I am also grateful to my Committee members John Lis, James Sethna, and Carl Franck for the advice they provided at various stages of my work. James Sethna has been especially helpful in fostering a deeper understanding of the theoretical aspects of my research, while John Lis has encouraged me in looking for biological implications of my findings. At several points in time I have also collaborated with both the Lis lab and the Sethna group; these experiences were exclusively positive.

I am thankful to my external collaborators, John Marko (Northwestern University) and Karolin Luger (Colorado State University). John Marko has been very generous in sharing with me his extensive knowledge on DNA mechanics, and Karolin Luger's help was instrumental during the final stage of my graduate work.

I would not have reached this stage without the help from people in the lab, and want to extend my sincere gratitude to all of them. Chris Deufel was the first person to introduce me to angular optical trapping; his enthusiasm and dedication inspired me throughout graduate school. I have worked closely with Scott Forth on several projects, and have learned a tremendous amount from him. I will also fondly remember his sense of humor and his mastery of the scientific prose. Jing Jin taught me the basics of molecular biology techniques, including PCR. Ben Smith, Dan

Johnson, and Michael Hall have always been willing to share their expertise with me, and our discussion on both scientific and non-scientific topics were always stimulating and enlightening.

I have relied extensively on James Inman's superb technical and computer skills, and drew support from his positive nature and "can-do" attitude. My research progress has been aided by the insightful discussions with Jie Ma, who has also been a very good friend outside the lab. I am thankful to Ming Li and Robert Forties for the help on the nucleosome project. Shanna Fellman's contribution to making the lab run smoothly cannot be overemphasized. I have been fortunate to work with many other bright people: Robert Fulbright, Mohammad Soltani, Jun Lin, Bo Sun, Thibault Roland, Yi Yang, Jessie Killian, SueYeon Chung, Ricky Chachra, Summer Saraf, Lucy Brennan. I am indebted to all of them.

My PhD journey at Cornell would not have been possible without the contribution of my teachers in college and school. I am especially grateful to my undergraduate advisor Nina A. Kasyanenko for fostering my interest in biophysics, and incidentally being the first person to mention the term "single-molecule biophysics" to me. I would also like to acknowledge my middle school physics teacher Maria K. Stogniy for lightning the flame of physics passion that has been with me throughout my studies.

Life always has its ups and downs, and I feel immensely fortunate to have friends at Cornell and around the world who shared the moments of happiness or sadness with me throughout graduate school: Emma Ravitch, Irina Kipenko, Andrei Andryeuski, Vitaliy Poleschuk, Petr Zaytsev, Avishek Chatterjee.

I would not be where I am without my family. My parents, Yuri Sheinin and Vera Peshkova, are the pillars I can always rely on, my best confidants, the people dearest to me. I love them very much. I am very thankful to my gradnparents, Marat and Eva Sheinin, and Rosa and the late

Vassiliy Peshkov, for their unconditional love and support. I am also grateful to my uncle's family: Vadim, Rimma, Eden, and Daniel Sheinin, for the warmth and hospitality of their house, which became almost like a second home to me. Finally, my deepest love and gratitude go to my wife, Anuttama Sheela Mohan. You have brought into my life a sense of purpose that goes beyond myself and has transformed my world. Your love is the best thing that happened to me.

TABLE OF CONTENTS

LIST OF FIGURES

LIST OF TABLES

CHAPTER 1

GENOME UNDER TORSION

*Parts of this chapter have been modified from Annual Review of Biophysics, Volume 42. Forth, S., Sheinin, M. Y., Inman, J., and Wang, M. D. *Torque Measurement at the Single Molecule Level.*

Introduction

Immediately after the remarkable discovery of the double-helical nature of DNA (Watson and Crick, 1953b) scientists realized that DNA rotation must be an intrinsic feature of the most basic genetic processes. For example, it was pointed out that unwinding of DNA strands required during replication will necessitate these strands to rotate relative to each other (Watson and Crick, 1953a). Topological challenges associated with DNA processing were further highlighted by the observation that DNA *in vivo* can exist in a circular form (Dulbecco and Vogt, 1963), and this circular DNA can be torsionally stressed (Vinograd et al., 1965). Decades of biochemical research on DNA under torsion (more often referred to as supercoiled DNA) have provided a lot of insight into its physical properties (Vologodskii and Cozzarelli, 1994) and biological roles (Kanaar and Cozzarelli, 1992). Its importance has been underscored by the discovery of a whole class of enzymes – topoisomerases – responsible for the regulation of supercoiling (Wang, 1985). Seminal paper by Liu & Wang (Liu and Wang, 1987) suggested that groove-tracking enzymes such as RNA polymerase can generate DNA supercoiling during translocation, a hypothesis soon to be corroborated both *in vitro* (Tsao et al., 1989) and *in vivo* (Wu et al., 1988).

The 1990s witnessed the advent of single-molecule techniques into biology. These high-precision biophysical tools have been used to quantitatively explore the structure and function of biomolecules with an unprecedented level of detail (Bustamante et al., 2000). Specifically, our understanding of DNA supercoiling has greatly benefited from single-molecule approaches, as they enable precise control and manipulation of the torsional state of DNA, a feat that is very challenging to achieve using biochemical means (Forth et al., 2013; Koster et al., 2010).

In this introductory Chapter I will discuss in detail our current state of knowledge regarding DNA supercoiling from both physical and biological perspectives. I will emphasize the contribution made by single-molecule techniques and specifically angular optical tweezers. This discussion will set the stage for my experimental results presented in subsequent Chapters.

DNA Topology and Mechanics

The study of DNA supercoiling began as a purely biological endeavor, but has since then greatly benefited from the contributions from mathematics and physics, which have provided a quantitative foundation of the discipline. In particular, concepts from topology, a branch of mathematics that studies properties of an object preserved under continuous deformation, have been borrowed to describe the behavior of supercoiled DNA as first observed in the biochemical experiments. Later on, analytical mechanics and statistical physics have provided the theoretical apparatus to explain single-molecule data on DNA under tension and torque.

Topological concepts are most intuitively understood when considering a closed circular DNA molecule. If one were to place one of the strands on a surface, than the other strand will be constrained by the DNA helical geometry to pierce that surface a defined number of times (Figure 1.1a). This number, called the linking number (Lk), is a topologically conserved quantity – that is, it cannot be changed by any continuous deformation of the molecule, but only by the breaking of one or two strands. Linking number of a DNA molecule with a given length of N bp in the absence of torsion (relaxed) is

$$Lk_0 = \frac{N}{p}, \tag{1.1}$$

where p is the helical pitch in bp/turn (Figure 1.1b).

When torsion is present (DNA is supercoiled), the linking number of the molecule will deviate from its relaxed value by the linking number difference ΔLk:

$$\Delta Lk = Lk - Lk_0. \tag{1.2}$$

It is common to characterize DNA supercoiling by normalizing linking number difference (Figure 1.1b) and using the degree of supercoiling (also called supercoiling density) σ:

$$\sigma = \frac{\Delta Lk}{Lk_0}. \tag{1.3}$$

Linking number can be further subdivided into two quantities, twist (Tw) and writhe (Wr):

$$Lk = Tw + Wr. \tag{1.4}$$

Twist (Tw) reflects the helical winding of two strands around each other, while writhe (Wr) is a measure of the coiling of the DNA axis about itself (Figure 1.1c). Both Tw and Wr are non-integer quantities and are not topologically invariant.

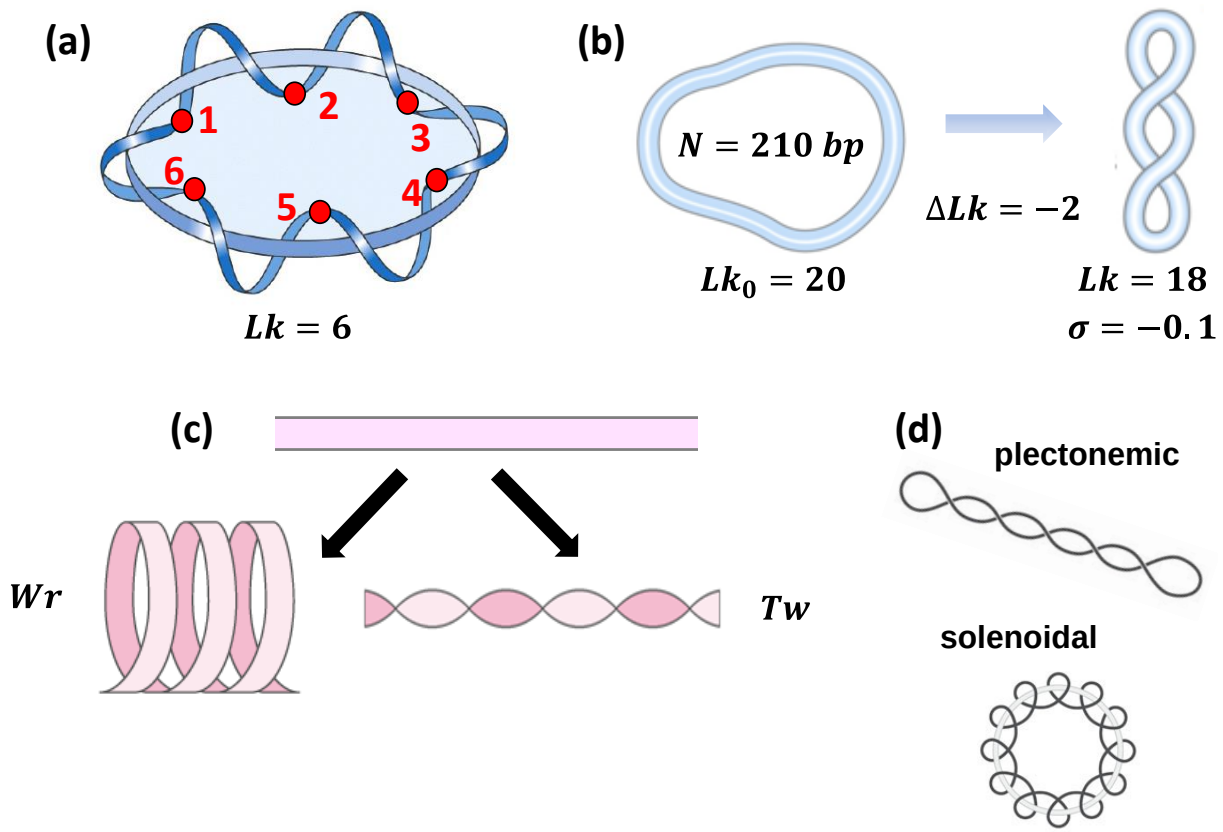

Figure 1.1: DNA topology basics.

(a) Illustration of the concept of the linking number *Lk*.

(b) A relaxed 210 bp circular DNA possesses a relaxed linking number of 20 (according to Equation 1.1). Changing *Lk* by –2 will result in a supercoiled conformation with degree of supercoiling $\sigma = -0.1$ (from Equation 1.3).

(c, top) A band representing relaxed DNA.

(c, bottom) Torsion can be manifested in two ways: as the coiling of the DNA axis about itself (writhe *Wr*) or the twisting of the axis (twist *Tw*). Adapted from Lehninger Principles of Biochemistry, 4th edition (Nelson and Cox, 2005).

(d) Two forms of DNA supercoiling: plectonemic (top) and solenoidal (bottom). Adapted from (Travers and Muskhelishvili, 2007) with permission from Nature Publishing Group.

In a relaxed DNA linking number purely consists of Tw; added linking number will be redistributed between Tw and Wr. Previous research has demonstrated that in a circular DNA about 75% of the degree of supercoiling is partitioned into Wr (Vologodskii and Cozzarelli, 1994). Increasing Wr changes three-dimensional conformation of the DNA molecule, creating supercoils. Free DNA in solution usually forms plectonemic supercoils: extended interwound loops. Alternatively, in the presence of certain proteins DNA can wrap around in a reel-like fashion, creating solenoidal supercoils (Nelson and Cox, 2005). Importantly, this arrangement provides for a much tighter compaction and has been implemented in the chromatin organization of eukaryotes (discussed below).

So far the discussion has been limited to circular DNA. However, topological concepts can be applied to a linear DNA as well, provided the angular orientation of its ends is fixed (DNA is torsionally constrained). In this case, common to single-molecule experiments, two external variables, tension and torsion, control the state of the DNA molecule.

A linear DNA molecule in solution will adopt a random coil conformation that maximizes its entropy (Strick et al., 2003). The size of the random coil globule is dependent on the length of the DNA and its persistence length L_p. Persistence length of DNA (or any other polymer) is defined as:

$$L_p = \frac{B}{k_B T}, \tag{1.5}$$

where B is the bending modulus and $k_B T$ is the thermal energy. Persistence length is the characteristic scale of bending fluctuations: DNA remains essentially straight for length $L < L_p$ ≈50 nm (Garcia et al., 2007).

DNA behavior under moderate tension (0.1-10 pN) is primarily dominated by entropy and is well described by the Marko-Siggia Worm-Like Chain (WLC) model (Bustamante et al., 1994; Marko and Siggia, 1995):

$$F = \frac{k_B T}{L_p}\left(\frac{1}{4(1 - z/L_o)^2} - \frac{1}{4} + \frac{z}{L_o}\right), \tag{1.6}$$

where F is the force, z is the end-to-end extension, and L_o is the DNA contour length.

At high force (>10 pN) enthalpic contribution has to be taken into account, as the backbone of the molecule slightly lengthens. This is commonly accomplished using Odijk approximation (Equation 1.7) (Odijk, 1995) or modified Marko-Siggia model (Equation 1.8) (Wang et al., 1997):

$$\frac{z}{L} = 1 - \frac{1}{2}\sqrt{\frac{k_B T}{F L_p}} + \frac{F}{K}, \tag{1.7}$$

$$F = \frac{k_B T}{L_p}\left(\frac{1}{4\left(1 - \frac{z}{L_o} + \frac{F}{K}\right)^2} - \frac{1}{4} + \frac{z}{L_o} - \frac{F}{K}\right), \tag{1.8}$$

where K is the DNA stretch modulus. At forces above 65 pN DNA undergoes a structural transition, which involves the lengthening of the molecule by about 70% (Smith et al., 1996). Recent experiments have demonstrated that depending on the experimental conditions (temperature, DNA sequence, ionic strength) this overstretching transition is accompanied by a mixture of DNA melting, peeling of ssDNA, and formation of a new base-paired state (S-DNA) (King et al., 2013; Zhang et al., 2013).

Complementing tension with torsion opens up new ways to modify DNA structure, as has been elucidated by single-molecule experiments (Strick et al., 2003). DNA responds as an elastic

spring to small angular deviations, so that torque τ changes linearly with twist θ:

$$\tau = \frac{k_B T C}{L_0}(\theta - \theta_0), \tag{1.9}$$

where C is the DNA torsional persistence length (defined as DNA torsional modulus divided by the thermal energy), and θ_0 is the equilibrium twist (35°/bp) (Bryant et al., 2003). This can be also rewritten in terms of the degree of supercoiling:

$$\tau = \omega_0 k_B T C \sigma, \tag{1.10}$$

where ω_0 is the natural twist (≈1.8 nm^{-1}).

One should note that torsional persistence length in Equations (1.9) and (1.10) is a force-dependent entity. As has been shown theoretically by Moroz and Nelson (Moroz and Nelson, 1997), thermal fluctuations cause some of the additional Lk to be converted into Wr instead of Tw. The effective force-dependent C can be approximately calculated as follows (Marko, 2007):

$$C(F) = C\left[1 - \frac{C}{4L_p}\sqrt{\frac{k_B T}{F L_p}}\right]. \tag{1.11}$$

An interesting connection can be found with the zero force case. As was mentioned above, in a circular DNA (equivalent to zero force) only 1/4 of the Lk is converted into Tw. Therefore effective torsional persistence length at zero force is $C(0) \approx C/4$.

Under sufficiently high torques DNA conformation and/or internal structure can be drastically altered. For example, under low tension both negative and positive supercoiling cause DNA to buckle and form plectonemes (Strick et al., 1996). At higher tension the symmetry breaks down, as negative torsion denatures DNA, while positive torque still results in buckling (Strick et al.,

1998). Finally, at high tension and positive torque DNA bases separate and flip on the outside (Allemand et al., 1998).

While several theoretical frameworks have been previously developed to describe structural transitions in DNA, here I will focus on the conceptually simple and general approach by Marko (Marko, 2007). Briefly, in this framework each DNA conformation is treated as a "state" possessing a certain free energy, dependent on the applied force F and degree of supercoiling σ (these two quantities are usually held constant in single-molecule experiments). DNA always adopts the conformation that minimizes its free energy. For example, let's consider the transition between stretched B-DNA (S state) and its plectonemic conformation (P state). The total free energy in the coexistence state (per unit length) G is written as:

$$G(\sigma) = x_s S(\sigma_s) + x_p P(\sigma_p), \qquad (1.12)$$

where x_s and x_p are fractions of DNA in states S and P, σ_s and σ_p are the boundaries of the transition, S and P are the free energies of the two states respectively. Equation (1.12) is minimized using the well-known Maxwell construction (Figure 1.2). Note that in the coexistence region free energy density changes linearly with the degree of supercoiling, which implies a constant torque.

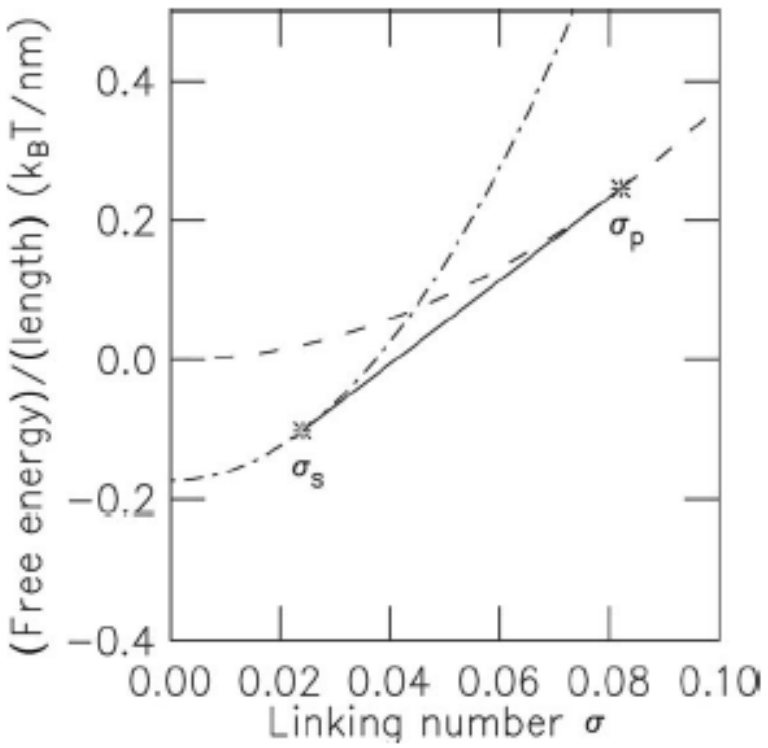

Figure 1.2: Maxwell construction for DNA phase transition analysis.

Depicted are free energies per unit length of the S state (dash-dot), P state (dash), and the coexistence state (solid line) as a function of the degree of supercoiling σ. Note that the line corresponding to the free energy coexistence state is tangential to the free energies of the pure states. Reproduced from (Marko, 2007) with the permission from the American Physical Society.

DNA Supercoiling *in vivo*

When describing the topological state of DNA *in* vivo, degree of supercoiling σ is the most widely used parameter. The typical value of the global degree of DNA supercoiling in both prokaryotes and eukaryotes is -0.06 (Roca, 2011), that is, cellular DNA is underwound. Importantly, the type of supercoiling differs between prokaryotes and eukaryotes. In the former, about 50% of supercoiling is unconstrained, and thus distributed between Tw and plectonemic Wr. The other 50% is constrained by various DNA-binding proteins, such as HU, HNS and RNA polymerase, and is thus predominantly solenoidal (Drlica, 1992). In contrast, the supercoiling of eukaryotic DNA is almost exclusively solenoidal, being constrained by the nucleosomes (Roca, 2011). Free linker DNA is on average relaxed, though localized unconstrained supercoiling can arise (Bermudez et al., 2010; Ljungman and Hanawalt, 1992), in particular due to transcription elongation (Kouzine et al., 2013; Matsumoto and Hirose, 2004).

The fact that cellular DNA is *a priori* underwound provides a remarkable connection between DNA mechanics and cell physiology. As was discussed above, since B-DNA is a right-handed helix, underwinding will loosen inter-strand interactions and has the potential to promote their complete separation. Incidentally, base separation is also required to initiate the formation of transcription and replication complexes on DNA (Kowalski and Eddy, 1989; Siebenlist, 1979). DNA supercoiling can therefore act as a sensitive regulator of these vital cellular processes. Moreover, strand-separated DNA is known to adopt special conformations, collectively known as non-B DNA structures, which are often stabilized by negative supercoiling (Palecek, 1991). Although initially these structures were considered a mere *in vitro* curiosity, research in the past

decades has demonstrated their existence *in vivo* and has provided examples of important regulatory roles they can play, particularly in transcription (Kouzine and Levens, 2007).

The presence of a well-defined DNA supercoiling *in vivo* immediately raises the question of how it is maintained and regulated. Major insight into this issue has been provided by James Wang's discovery of topoisomerases (Wang, 1971) – enzymes that are specifically adapted to manipulate DNA supercoiling (Figure 1.3). Two main groups of topoisomerases are currently known: type I and type II, classified depending on whether they cleave one or two DNA strands respectively (Koster et al., 2010; Vos et al., 2011). These groups are further divided into subclasses based on the structure and mechanism of action. The most important subclasses for single-strand operating topoisomerases are type IA and type IB. The former operate through a "strand passage" mechanism, in which one DNA strand is cleaved and the other is propagated through the gap, followed by the resealing of the nick (Vos et al., 2011). Type IB enzymes achieve supercoil relaxation by nicking the DNA and allowing the duplex to rotate to release excess torsion (Koster et al., 2005). On the other hand, all type II enzymes rely on strand passage mechanism, except that in this case a double-stranded break is formed and then sealed. Importantly, this process is also ATP-dependent (Vos et al., 2011). Specific topoisomerases differ in their preferences over positively or negatively supercoiled substrates, as well as the substrate conformation: for example, certain type II enzymes are very efficient in unknotting and decatenating DNA (Hsieh and Brutlag, 1980). Bacteria also possess a unique type II topoisomerase – DNA gyrase – that is able to not only relax, but also to introduce (negative) supercoils (Gellert et al., 1976). Gyrase activity is crucial for maintaining unconstrained negative supercoiling in prokaryotes (Hatfield and Benham, 2002).

Figure 1.3: Supercoil generation and processing *in vivo*.

(top) Transcription, the process of copying genomic DNA into RNA, involves the rotation of the RNA polymerase enzyme relative to its helical DNA track. Due to the size and typical confinement of the polymerase and associated machinery, the DNA is overtwisted (positive supercoiling) in front of the motor, and undertwisted (negative supercoiling) behind, in accordance with the "twin-supercoiled domain" model.

(bottom) During DNA replication, two identical copies are made of a single original DNA molecule. Just as during transcription, positive supercoiling is generated in front of the replisome complex as it progresses along the DNA track. Behind the replication fork, daughter DNA strands can be twisted and intertwined, forming positive precatenanes. Topoisomerases of various types act during both processes in order to relieve the torsional stress generated along the DNA. Adapted from (Forth et al., 2013) with permission from Annual Reviews.

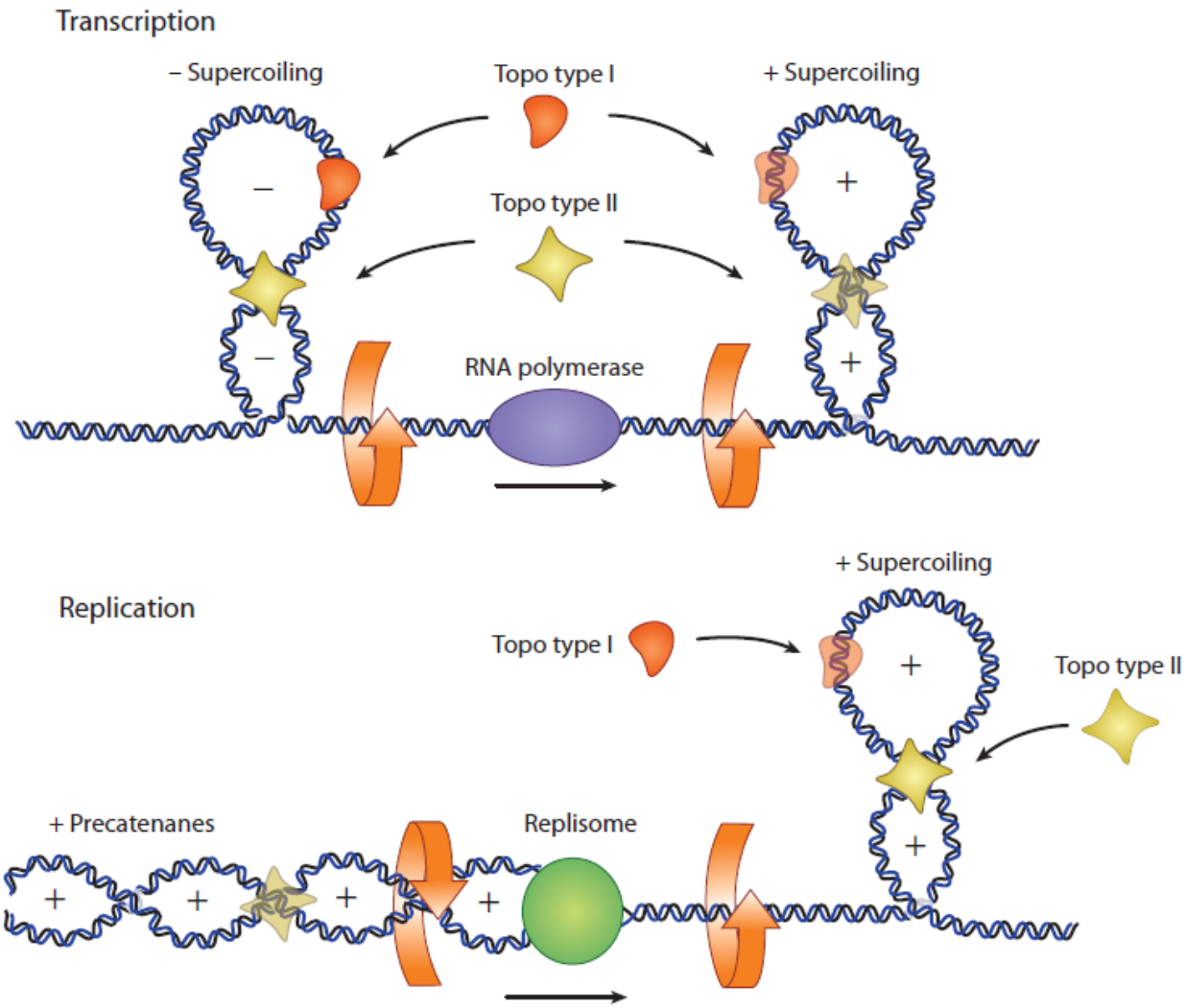
Transcription
– Supercoiling
Topo type I
+ Supercoiling
Topo type II
RNA polymerase
Replication
+ Supercoiling
Topo type I
Topo type II
+ Precatenanes
Replisome

While great strides have been made during the 1970s and 1980s regarding supercoiling-regulated activities of topoisomerases, in the late 1980s supercoiling-generating processes came to the fore, most notably transcription. During elongation, the RNAP machinery tracks the helical groove of DNA, which requires rotation of the enzyme relative to DNA. However, as suggested by Liu & Wang (Liu and Wang, 1987), polymerase can become immobilized, requiring DNA to rotate instead and thus generating positive supercoiling in front of, and negative supercoiling behind, the polymerase (Figure 1.3, top). The free rotation of polymerase can be prevented by a large viscous drag due to the RNA transcript and associated factors, such as ribosomes in prokaryotes and spliceosomes in eukaryotes, as well as tethering to the cell membrane and other cellular structures (Bermejo et al., 2012). This so-called "twin-supercoiled domain model" has been confirmed by numerous *in vitro* and *in vivo* experiments (Kouzine et al., 2008; Krasilnikov et al., 1999; Tsao et al., 1989; Wu et al., 1988). The vital importance of topoisomerases was now even more clear, as it was shown that polymerase elongation is impeded by excessive torsion (Garcia-Rubio and Aguilera, 2011; Harada et al., 2001)

Somewhat different topological problems are posed by another important cellular process: replication (Figure 1.3, bottom). Rapid movement of the replication fork, coupled with the unwinding of the parental DNA strands, generates positive supercoiling in the vicinity of the fork (Branzei and Foiani, 2010). If the replication machinery is immobilized, this supercoiling will produce plectonemic loops in front of the fork, in accordance with the twin-supercoiled domain model. Alternatively, the replisome may rotate, releasing the torsion upstream, but lead to the intertwining of the daughter strands (generating positive precatenanes) behind the fork (Branzei

and Foiani, 2010; Postow et al., 2001a). Failure to resolve the buildup of torsional stress can lead to fork reversal (Fierro-Fernandez et al., 2007) and genomic instability (Postow et al., 2001b).

Only now we are starting to understand the complex interrelation between supercoil-generating and supercoil-regulating processes and the structure of DNA and chromatin. Based on the previous discussion, several lines of inquiry can be identified: (i) topoisomerases need to relieve torsional stress generated by transcription and replication machineries; (ii) transcription-generated supercoiling can impact DNA stability and therefore regulate transcription initiation directly or through DNA-binding proteins; (iii) in eukaryotes, supercoiling and chromatin might be interrelated. Below I will elaborate on each of these points.

As was discussed above, different topoisomerases display partially overlapping activity, while maintaining a degree of specialization. For instance, consider the most abundant bacterial topoisomerases: topo I (type IA), gyrase (type IIB), and topo IV (type IIB). Topo I preferentially relaxes negative supercoils upstream of RNA polymerase (Roca, 2011). This is crucial to prevent formation of R-loops: instances when nascent mRNA chain displaces the non-template DNA strand upstream and forms an RNA-DNA hybrid (Figure 1.4a). This behavior is promoted by negative supercoiling (as it weakens DNA-DNA interactions) and has been found to inhibit cell growth (Drolet et al., 2003). Bacterial gyrase serves on the local scale to remove positive supercoils ahead of transcription and replication machinery (Roca, 2011). Importantly, due to its ability to introduce negative supercoils, gyrase can affect global levels of supercoiling. For example, extreme stress, such as salt shock or transfer to anaerobic growth, was found to change the global supercoiling of *E. coli* genome by up to 50% through the modulation of the gyrase

activity (Hatfield and Benham, 2002). Finally, topo IV is primarily involved in removing knots and catenanes formed during replication (Ullsperger and Cozzarelli, 1996).

Eukaryotes, in the absence of supercoil-generating activity of the bacterial gyrase, use topoisomerases, mainly type IB (topo I) and type II (topo II) solely to relax supercoiling (Roca, 2011). While early observations found their functions to be redundant (Kim and Wang, 1989), later on substrate preferences have been uncovered. Specifically, topo II was observed to relax supercoils in nucleosomal DNA much faster than topo I (Salceda et al., 2006). In yeast, topo I was found to alleviate negative supercoiling behind the elongating polymerase, while topo II was mostly associated with removal of positive supercoiling in front (French et al., 2011) to prevent transcription stalling (Figure 1.4b). Recent genome-wide mapping of dynamic supercoiling has discovered that topo I is broadly distributed upstream of the transcription start site (TSS), while topo II is localized at the TSS and enriched at highly transcribed genes (Kouzine et al., 2013). Taken together, these results are consistent with the mechanistic preferences of two types of topoisomerases. Since topo II naturally acts on the crossing of two DNA duplexes, it will be most efficient resolving complex 3D conformations induced by torsion, such as knots and plectonemes, as well as chromatin fibers. Topo I, on the other hand, is more suited to simpler geometries, with supercoiling predominantly in the form of Tw.

Figure 1.4: Examples of the regulatory roles of transcription-driven supercoiling.

(a) Excessive negative supercoiling upstream promotes formation of mRNA-DNA hybrids (R-loops).

(b) Excessive positive supercoiling downstream can lead to RNAP stalling.

(c) Negative supercoiling upstream can contribute to the melting of the promoter region and activate transcription.

(d) Negative supercoiling upstream can also promote formation of non-B DNA structures (e. g. G-quadruplexes, cruciform etc.) that can attract regulatory proteins.

Adapted from Ma, J. et al., manuscript in press.

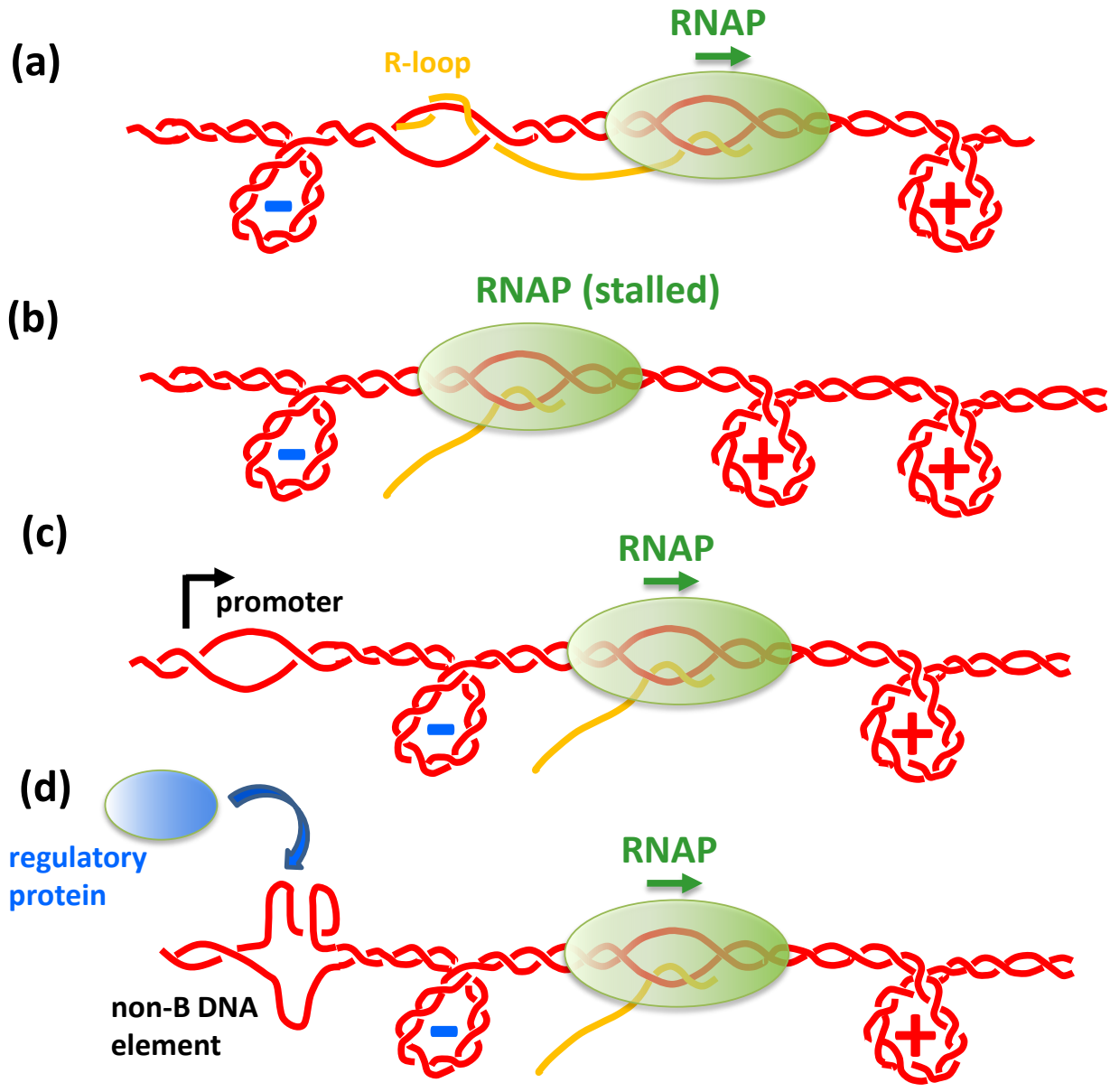
(a)
R-loop
RNAP
(b)
RNAP (stalled)
(c)
promoter
RNAP
(d)
regulatory protein
non-B DNA element
RNAP

While excess of transcription-generated torsion is deleterious to the cell, moderate amount of supercoiling can be necessary for proper gene expression. As was discussed above, architecture of the initiation complex requires DNA melting; therefore, negative supercoiling should favor initiation (Lim et al., 2003) (Figure 1.4c). Notably, an elongating polymerase will generate negative supercoiling behind, and can thus affect the rate of initiation from upstream promoters. Such coupling has been observed, e. g. in the case of divergent promoters of the ilvYC operon in *E. coli* (Rhee et al., 1999). A recent theoretical work has suggested, more generally, that bursts of transcription in bacteria can be explained by transient supercoiling affecting initiation (Mitarai et al., 2008). In a slightly different twist, negative supercoiling can promote formation of non-B DNA structures that can attract transcription factors (Kouzine and Levens, 2007) (Figure 1.4d). A well-studied example is the *c-myc* oncogene (Baranello et al., 2012). Two regulatory sequences, NHE III1 and FUSE, are found upstream of the *c-myc* promoter. FUSE element is AT-rich and thus easily melts upon experiencing torsional stress. Partially melted FUSE recruits FUSE-binding protein (FBP) that further activates transcription. The consequent increase in the level of supercoiling changes FUSE conformation further, which recruits FBP-interacting repressor (FIR) that inhibits transcription (Baranello et al., 2012). NHE III1 can also adopt alternative conformations, such as G-quadruplex and i-motif, that can regulate *c-myc* expression (Brooks and Hurley, 2009).

While impact on supercoiling on the structure of DNA has been studied extensively, much less is known about the interplay between supercoiling and chromatin. The basic unit of chromatin, the nucleosome, is a protein-DNA complex packaging ~1.7 turns of DNA in a negative supercoil (Luger et al., 1997) (Figure 1.5a). This negative writhe is partially compensated for by the

overtwisting of DNA on the nucleosomal surface (Luger et al., 1997), so that a linking number of −1 is associated with each nucleosome (Simpson et al., 1985). *In vitro* experiments have observed that nucleosomes preferentially form on negatively supercoiled DNA (Clark and Felsenfeld, 1991; Gupta et al., 2009) and are destabilized by positive torsion (Levchenko et al., 2005; Pfaffle et al., 1990). In the context of the twin-supercoiled domain model, this has led to proposals that transcription-dependent supercoiling will destabilize nucleosomes upstream and facilitate their reassembly downstream (Clark and Felsenfeld, 1991; Pfaffle et al., 1990). Torque could also affect higher-order chromatin structures, such as the 30-nm fiber (Figure 1.5b), which is believed to have a preferred chirality (Scheffer et al., 2011). However, *in vivo* data on the effects of supercoiling on chromatin is lacking. It is interesting to speculate whether nucleosome disassembly in eukaryotes can play a similar role to gyrase activity in prokaryotes (in both cases negative supercoiling is injected into DNA). For example, it has been observed that heat shock is followed by a rapid nucleosome loss in *Drosophila* (Petesch and Lis, 2008). In bacteria such shocks induce the increase in negative supercoiling (Higgins et al., 1988) – it remains to be seen if a similar change occurs in eukaryotes.

In summary, DNA supercoiling is ubiquitous *in vivo*, and nature has devised multiple mechanisms to precisely regulate the generation and relaxation of supercoiling. While the study of these processes *in vivo* is often exceedingly complicated, a lot can be learned from model *in vitro* systems.

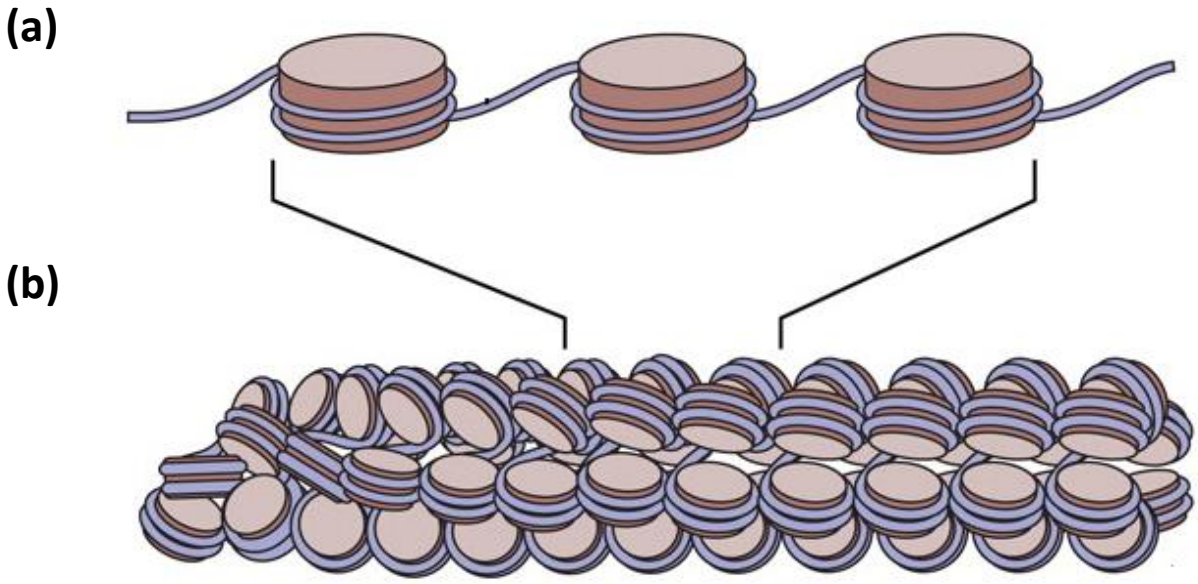

Figure 1.5: Chromatin structure and supercoiling.

(a) A nucleosomal array: DNA is wrapped around the core histones in a left-handed superhelix; individual nucleosomes are separated by regions of free linker DNA.

(b) Nucleosomal arrays are thought to form higher-order structures, e.g. 30 nm fiber, which can have a preferred chirality.

Adapted from (Jansen and Verstrepen, 2011) with permission from the American Society for Microbiology.

Single-Molecule Studies of DNA Supercoiling

While biochemical *in vitro* and *in vivo* experiments have greatly contributed to our understanding of supercoiling, single-molecule biophysics methods have gained increasing prominence over the last two decades. Novel instruments have been developed that allow precise control and measurement of the torsional state of DNA, something that is challenging to achieve by conventional means (Forth et al., 2013). Below I will give a brief overview of the advances in single-molecule studies of supercoiling, and provide motivation for the development of a novel tool, angular optical trapping.

Initial efforts in development of single-molecule techniques for the study of supercoiling focused on generating and measuring rotation of a torsionally constrained biological molecule. The experimental breakthrough was achieved by the magnetic tweezers (MTs) apparatus of Strick and co-workers (Strick et al., 1996). MTs utilize a pair of permanent magnets to exert force and torque on a paramagnetic bead attached to a single DNA molecule (Figure 1.6). A CCD camera captures images of the bead, which can be analyzed to extract force and extension information (Strick et al., 2003). The basic MTs are capable of exerting forces between several fN to ~100 pN and measure extension with a 10 nm accuracy (Strick et al., 2003). Recent advances have focused on improving resolution and acquisition speed using modern CMOS technology and performing parallel measurements on multiple DNA molecules (De Vlaminck and Dekker, 2012).

MTs have been first applied to study DNA behavior under tension and torque. Notable advances include first real time observation of plectoneme formation (Strick et al., 1996) and the study of base separation upon under- and over-winding, which identified a novel DNA phase, P-DNA, featuring a tightly interwound backbone with bases flipped on the outside (Allemand et al., 1998). Important elastic parameters, such as B-DNA torsional modulus and critical melting

torque, have been estimated (Strick et al., 1998). Subsequent experiments provided mechanistic insights into the formation of supercoil-stabilized secondary structures, such as Holliday junction (Dawid et al., 2006) and Z-DNA (Lee et al., 2010). MTs have been used in pioneering studies of nucleosome arrays under torsion, identifying them as extremely resilient structures capable of absorbing a significant amount of supercoiling (Bancaud et al., 2006). A follow-up study suggested an intriguing hypothesis of the formation of a right-handed nucleosome under large positive torsional stress (Bancaud et al., 2007).

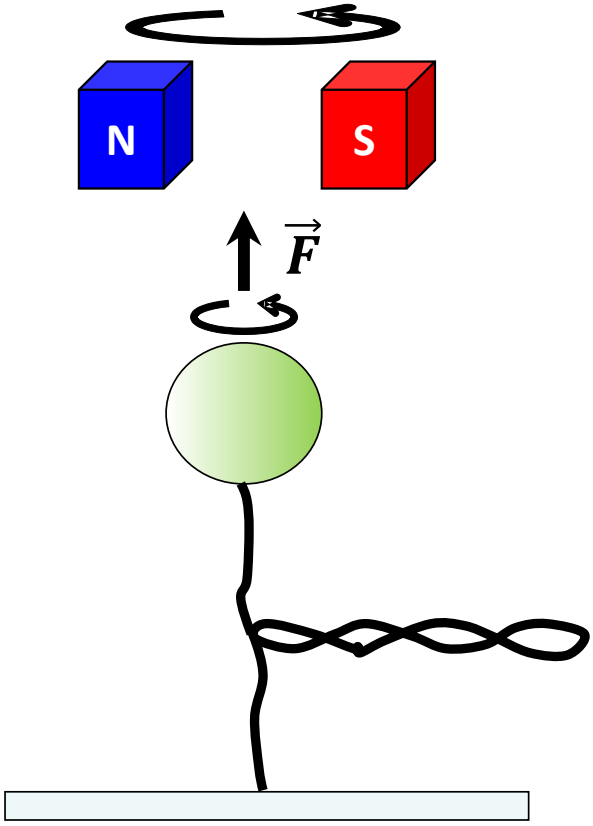

Figure 1.6: Magnetic tweezers configuration.

A pair of permanent magnets exerts a constant force on a paramagnetic bead. Rotation of the magnets induces rotation of the bead, which can introduce supercoils in the attached DNA molecule.

DNA supercoiling has also been successfully explored with MTs to study various DNA processing enzymes. By taking advantage of the linking number-extension conversion of the plectonemic DNA (Lk change by 1 induces about 50 nm extension change) Revyakin and co-workers have explored steps of *E. coli* RNA polymerase initiation (Revyakin et al., 2004; Revyakin et al., 2006). Chromatin remodeler RSC has been found to generate negatively supercoiled DNA loops upon translocation (Lia et al., 2006). MTs have been especially fruitfully applied to the study of topoisomerases: elucidating the mechanism of action of type IA (Dekker et al., 2002), type IB (Koster et al., 2005), and type IIA (Neuman et al., 2009; Strick et al., 2000) topoisomerases, as well as certain topoisomerase inhibitors (Koster et al., 2007).

While traditional MTs have significantly advanced our understanding of DNA supercoiling, they suffer from several drawbacks, most important being the inability to measure torque. Direct torque measurements are exceedingly important to precisely characterize the torsional properties of DNA. Major efforts have been therefore dedicated to developing single-molecule instruments able to measure torque. Currently, three major techniques exist: rotor bead tracking (RBT), torque-measuring magnetic tweezers, and angular optical trap (AOT). The reader is referred to a recent review (Forth et al., 2013) for an in-depth discussion of these methods. Below I will focus on my method of choice, the AOT.

Angular Optical Trapping

The technique of angular optical trapping, also called angular optical tweezers or optical torque wrench, was first developed in Michelle Wang's laboratory (La Porta and Wang, 2004). It represents an extension of the traditional optical tweezers (OTs) method: while OTs have been widely used to control and measure forces and extensions of biomolecules (Neuman and Block, 2004), AOT is supplemented with additional capabilities to control and measure torque and rotation.

In order to understand the principles of operation of the AOT, one has to first familiarize oneself with conventional OTs. Their story begins with the pioneering work by A. Ashkin in the 1970s and 80s, where he used laser beams to trap micron-sized inorganic particles (Ashkin, 1970; Ashkin and Dziedzic, 1971) and living organisms such as cells and bacteria (Ashkin and Dziedzic, 1987; Ashkin et al., 1987). The key requirement to create an optical trap with a laser is to focus the beam to a diffraction-limited spot, usually achieved with a high NA (>1.3) objective. A dielectric particle near the focus of a laser beam will experience a force due to the transfer of linear momentum by the incoming photons. This force has traditionally been decomposed into two components: scattering and gradient (Svoboda and Block, 1994). Scattering force acts in the direction of beam propagation, as scattering and absorption of incoming photons result in a net momentum transfer to the particle. While this force is usually dominant, in the case of a tightly focused beam gradient force, acting towards the beam center, becomes significant. This force arises from the interaction of induced dipoles in the dielectric particle with the inhomogeneous electric field of the laser beam (Neuman and Block, 2004). As the name suggests, this force is proportional to the gradient of the electric field. Thus, tightly focused beams are able to produce a gradient force that exceeds the scattering force and results in a stably trapped particle.

In an OTs apparatus, laser beam is used not only to manipulate, but also to measure the state of the trapped particle. This is usually accomplished using back focal plane detection scheme, which relies on the interference between forward-scattered light from the particle and the unscattered light (Neuman and Block, 2004; Rohrbach and Stelzer, 2002). The interference is detected by means of a quadrant photodiode (QPD). Lateral displacements of the particle result in a deviation of the beam position from the center of the QPD. Axial displacements result in the change of the overall light intensity at the QPD.

A typical experimental configuration for DNA-based experiments in a basic OTs setup (Figure 1.7) involves a dielectric bead (usually polystyrene, ~500 nm in diameter) trapped in the laser beam, with a single DNA molecule attached to it by one end, while its other end is coupled to a piezoelectric stage (Wang et al., 1997). Movement of the piezo stage stretches DNA, which pulls the bead away from the trap center, triggering a change in the back focal plane interference pattern as discussed above. In this manner sub-nanometer extension changes and force changes on the order of 0.1 pN can be measured (Neuman and Block, 2004).

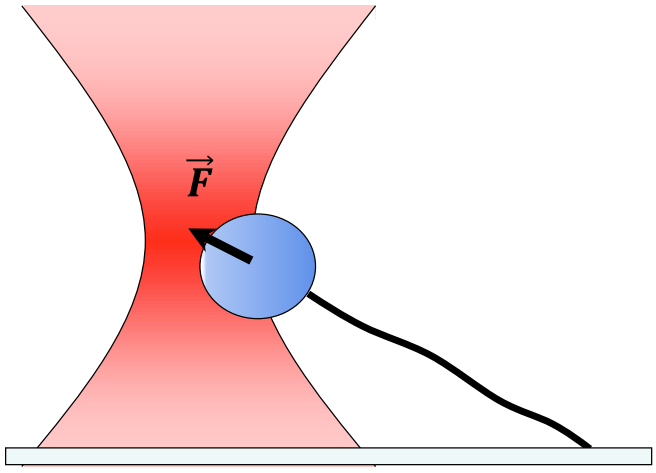

Figure 1.7: Optical tweezers configuration.

A DNA molecule is attached to the coverglass and a dielectric bead. The bead is trapped by a highly focused Gaussian beam.

The use of Gaussian beams and isotropic particles in conventional OTs precludes the possibility of angular manipulation. Therefore, many of the early demonstrations of rotation of the trapping particle relied on breaking the rotational symmetry of the particle and/or the input trapping beam (Bishop et al., 2003; Friese et al., 1998; Galajda and Ormos, 2003; O'Neil and Padgett, 2002). In a seminal work by Friese et al. (Friese et al., 1998), a calcite particle, which is optically birefringent, was rotated with both linear and circularly polarized light. This work provided the inspiration for a new instrument for single molecule studies – the AOT.

The angular trap operates based on the following principle. A dielectric particle in an electric field $\vec{E}$ generates polarization $\vec{P}$ such that $\vec{P} = \chi\vec{E}$, where χ is the electric susceptibility. If the particle is made of an anisotropic material (in other words, is optically birefringent), susceptibility is not a scalar, but a tensor. For a typical case of uniaxial birefringent materials, susceptibilities for the two axes are equal ($\chi_x = \chi_y \equiv \chi_o$ – ordinary), while the third is different ($\chi_z \equiv \chi_e$ – extraordinary). In materials such as quartz, the extraordinary axis is more easily polarizable than the ordinary ($\chi_e > \chi_o$). In this case a particle placed in a linear electric field will tend to align its polarization with the direction of the electric field, thus experiencing a restoring torque (Figure 1.8). Rotation of the electric field will induce the rotation of the particle (Friese et al., 1998; La Porta and Wang, 2004).

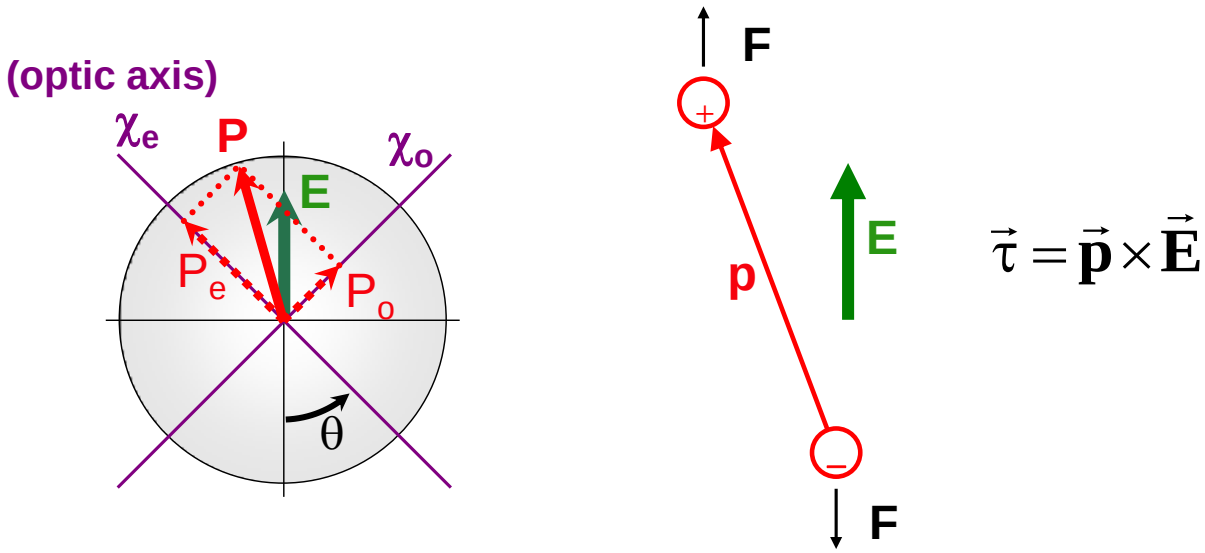

Figure 1.8: Operating principle of the AOT.

(left) In a birefringent material polarization $\vec{P}$ and electric field $\vec{E}$ in general are not aligned.

(right) In the case of a positive birefringent material, a restoring torque will be generated that will tend to align the extraordinary axis of the particle with the electric field. Adapted from (La Porta and Wang, 2004) with permission from the American Physical Society.

As in the case of OTs, the laser beam in an AOT is not only used to exert torque, but also to measure it. This is achieved on the basis of conservation of angular momentum. The upstream light (before it interacts with the particle) is linearly polarized. If, upon passing through the particle, a torque is exerted on the latter, this implies a change in the angular momentum of the particle and, therefore, an equal in magnitude but opposite in sign change in the angular momentum of the laser beam. For the measurement purpose, it is convenient to think of the state of the laser beam in terms of polarization. Incoming light is linearly polarized, or, equivalently, can be represented as a mixture of equal amounts of left- and right-circularly polarized light. Change of the angular momentum corresponds to the change of the relative amount of left- and right-handed polarization components, so that outgoing light is elliptically polarized (Nieminen et al., 2001). Change in the ellipticity of light therefore corresponds to the torque on the particle (La Porta and Wang, 2004; Nieminen et al., 2001).

While the first demonstration of an AOT utilized non-uniform quartz particles (La Porta and Wang, 2004), the precision required for biological experiments dictated the need for a more uniform handles. This was achieved in our lab by implementing the production of nanofabricated quartz cylinders (Deufel et al., 2007). By design, the extraordinary axis of these cylinders is radially oriented, thus enabling angular confinement, while the geometrical aspect ratio (lentgh≈2*diameter) guarantees stable three-dimensional trapping (Deufel et al., 2007). Additionally, one of the flat surfaces of each cylinder is functionalized with streptavidin for the attachment of biological molecules such as DNA. Finally, nanofabrication facilities are capable of producing billions of highly uniformed cylinders in a single batch.

The AOT in our lab has been successfully employed to study mechanical properties of DNA (Figure 1.9). For the first time critical torque during the plectonemic transition has been measured (Forth et al., 2008) and found to agree with a recently developed physical model (Marko, 2007). That work also observed fast dynamics of the first plectonemic loop formation,

which has escaped MTs observations, underscoring the advantage of high spatial and temporal resolution offered by the AOT (Forth et al., 2008). Subsequent work investigated the formation of a Holliday junction and directly measured its torque-force relationship (Forth et al., 2011).

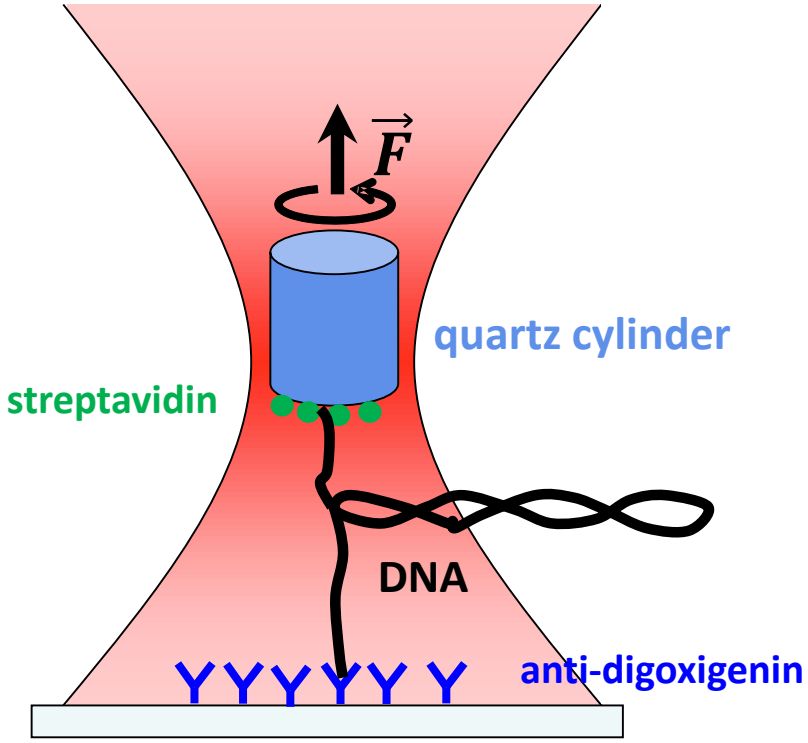

Figure 1.9: Typical AOT configuration.

A nanofabricated quartz cylinder is trapped in the laser beam. Rotation of the input polarization induces the rotation of the cylinder. A DNA molecule is attached to the cylinder via biotin / streptavidin linkage, and to the coverglass via digoxigenin / anti-digoxigenin linkage.

Summary of the Dissertation Research

At this point the reader should have gained a solid understanding of the importance of DNA supercoiling, and of the single-molecule methods used to study it, most notably angular optical trapping (AOT). The remainder of the dissertation is devoted to the original research.

It is instructive to note that the torque-measuring capability of the AOT was crucial for the advances reported below. Direct measurement of the torque signal has enabled me to clearly distinguish the boundaries of DNA phase transitions (as discussed above in **DNA Topology and Mechanics**) and thus resolve several existing controversies in the field. I will begin by discussing the signature of B-DNA extension in the presence of torsion and how it can be used to determine DNA twist-stretch coupling modulus. I will specifically contrast the AOT experiment with an earlier study (Lionnet et al., 2006) performed with MTs and point out the crucial role of the torque signal in the correct interpretation of the data.

Next, I will describe the study of DNA melting under torsion. By using the torque signal to identify the boundaries of the melting transition, we were able to demonstrate that torsionally-melted DNA is a left-handed structure, unlike the open bubble configuration arising during thermal melting. In addition, these experiments provided a complete description of the elasticity of torsionally-melted DNA and identified complex sequence-dependent behavior at low forces.

Finally, we shall examine a more complex system: DNA with a single assembled nucleosome – the first time AOT has been used to analyze the behavior of a protein-DNA complex. I will demonstrate how precise control over torque and force in an angular trap has enabled us to characterize nucleosome unwrapping on supercoiled DNA. We have also observed that positive torque leads to a dramatic loss of some of the nucleosomal histones - H2A/H2B dimers. I will

discuss the importance of this finding in light of the *in vivo* observations of histone dynamics during transcription.

References

Allemand, J.F., Bensimon, D., Lavery, R., and Croquette, V. (1998). Stretched and overwound DNA forms a Pauling-like structure with exposed bases. Proc Natl Acad Sci U S A *95*, 14152-14157.

Ashkin, A. (1970). Acceleration and Trapping of Particles by Radiation Pressure. Physical Review Letters *24*, 156-159.

Ashkin, A., and Dziedzic, J.M. (1971). Optical Levitation by Radiation Pressure. Applied Physics Letters *19*, 283-285.

Ashkin, A., and Dziedzic, J.M. (1987). Optical trapping and manipulation of viruses and bacteria. Science *235*, 1517-1520.

Ashkin, A., Dziedzic, J.M., and Yamane, T. (1987). Optical trapping and manipulation of single cells using infrared laser beams. Nature *330*, 769-771.

Bancaud, A., Conde e Silva, N., Barbi, M., Wagner, G., Allemand, J.F., Mozziconacci, J., Lavelle, C., Croquette, V., Victor, J.M., Prunell, A.*, et al.* (2006). Structural plasticity of single chromatin fibers revealed by torsional manipulation. Nat Struct Mol Biol *13*, 444-450.

Bancaud, A., Wagner, G., Conde, E.S.N., Lavelle, C., Wong, H., Mozziconacci, J., Barbi, M., Sivolob, A., Le Cam, E., Mouawad, L.*, et al.* (2007). Nucleosome chiral transition under positive torsional stress in single chromatin fibers. Mol Cell *27*, 135-147.

Baranello, L., Levens, D., Gupta, A., and Kouzine, F. (2012). The importance of being supercoiled: How DNA mechanics regulate dynamic processes. Biochim Biophys Acta *1819*, 632-638.

Bermejo, R., Lai, M.S., and Foiani, M. (2012). Preventing replication stress to maintain genome stability: resolving conflicts between replication and transcription. Mol Cell *45*, 710-718.

Bermudez, I., Garcia-Martinez, J., Perez-Ortin, J.E., and Roca, J. (2010). A method for genome-wide analysis of DNA helical tension by means of psoralen-DNA photobinding. Nucleic Acids Res *38*, e182.

Bishop, A.I., Nieminen, T.A., Heckenberg, N.R., and Rubinsztein-Dunlop, H. (2003). Optical application and measurement of torque on microparticles of isotropic nonabsorbing material. Physical Review A *68*, 8.

Branzei, D., and Foiani, M. (2010). Maintaining genome stability at the replication fork. Nat Rev Mol Cell Biol *11*, 208-219.

Brooks, T.A., and Hurley, L.H. (2009). The role of supercoiling in transcriptional control of MYC and its importance in molecular therapeutics. Nat Rev Cancer *9*, 849-861.

Bryant, Z., Stone, M.D., Gore, J., Smith, S.B., Cozzarelli, N.R., and Bustamante, C. (2003). Structural transitions and elasticity from torque measurements on DNA. Nature *424*, 338-341.

Bustamante, C., Macosko, J.C., and Wuite, G.J. (2000). Grabbing the cat by the tail: manipulating molecules one by one. Nat Rev Mol Cell Biol *1*, 130-136.

Bustamante, C., Marko, J.F., Siggia, E.D., and Smith, S. (1994). Entropic elasticity of lambda-phage DNA. Science *265*, 1599-1600.

Clark, D.J., and Felsenfeld, G. (1991). Formation of nucleosomes on positively supercoiled DNA. EMBO J *10*, 387-395.

Dawid, A., Guillemot, F., Breme, C., Croquette, V., and Heslot, F. (2006). Mechanically controlled DNA extrusion from a palindromic sequence by single molecule micromanipulation. Phys Rev Lett *96*, 188102.

De Vlaminck, I., and Dekker, C. (2012). Recent advances in magnetic tweezers. Annu Rev Biophys *41*, 453-472.

Dekker, N.H., Rybenkov, V.V., Duguet, M., Crisona, N.J., Cozzarelli, N.R., Bensimon, D., and Croquette, V. (2002). The mechanism of type IA topoisomerases. Proc Natl Acad Sci U S A *99*, 12126-12131.

Deufel, C., Forth, S., Simmons, C.R., Dejgosha, S., and Wang, M.D. (2007). Nanofabricated quartz cylinders for angular trapping: DNA supercoiling torque detection. Nat Methods *4*, 223-225.

Drlica, K. (1992). Control of bacterial DNA supercoiling. Mol Microbiol *6*, 425-433.

Drolet, M., Broccoli, S., Rallu, F., Hraiky, C., Fortin, C., Masse, E., and Baaklini, I. (2003). The problem of hypernegative supercoiling and R-loop formation in transcription. Front Biosci *8*, d210-221.

Dulbecco, R., and Vogt, M. (1963). Evidence for a Ring Structure of Polyoma Virus DNA. Proc Natl Acad Sci U S A *50*, 236-243.

Fierro-Fernandez, M., Hernandez, P., Krimer, D.B., Stasiak, A., and Schvartzman, J.B. (2007). Topological locking restrains replication fork reversal. Proc Natl Acad Sci U S A *104*, 1500-1505.

Forth, S., Deufel, C., Patel, S.S., and Wang, M.D. (2011). Direct measurements of torque during Holliday junction migration. Biophys J *101*, L5-7.

Forth, S., Deufel, C., Sheinin, M.Y., Daniels, B., Sethna, J.P., and Wang, M.D. (2008). Abrupt buckling transition observed during the plectoneme formation of individual DNA molecules. Phys Rev Lett *100*, 148301.

Forth, S., Sheinin, M.Y., Inman, J., and Wang, M.D. (2013). Torque measurement at the single molecule level. Annual Review of Biophysics.

French, S.L., Sikes, M.L., Hontz, R.D., Osheim, Y.N., Lambert, T.E., El Hage, A., Smith, M.M., Tollervey, D., Smith, J.S., and Beyer, A.L. (2011). Distinguishing the roles of Topoisomerases I and II in relief of transcription-induced torsional stress in yeast rRNA genes. Mol Cell Biol *31*, 482-494.

Friese, M.E.J., Nieminen, T.A., Heckenberg, N.R., and Rubinsztein-Dunlop, H. (1998). Optical alignment and spinning of laser-trapped microscopic particles. Nature *394*, 348-350.

Galajda, P., and Ormos, P. (2003). Orientation of flat particles in optical tweezers by linearly polarized light. Optics Express *11*, 446-451.

Garcia-Rubio, M.L., and Aguilera, A. (2011). Topological constraints impair RNA polymerase II transcription and causes instability of plasmid-borne convergent genes. Nucleic Acids Res *40*, 1050-1064.

Garcia, H.G., Grayson, P., Han, L., Inamdar, M., Kondev, J., Nelson, P.C., Phillips, R., Widom, J., and Wiggins, P.A. (2007). Biological consequences of tightly bent DNA: the other life of a macromolecular celebrity. Biopolymers *85*, 115-130.

Gellert, M., Mizuuchi, K., O'Dea, M.H., and Nash, H.A. (1976). DNA gyrase: an enzyme that introduces superhelical turns into DNA. Proc Natl Acad Sci U S A *73*, 3872-3876.

Gupta, P., Zlatanova, J., and Tomschik, M. (2009). Nucleosome assembly depends on the torsion in the DNA molecule: a magnetic tweezers study. Biophys J *97*, 3150-3157.

Harada, Y., Ohara, O., Takatsuki, A., Itoh, H., Shimamoto, N., and Kinosita, K., Jr. (2001). Direct observation of DNA rotation during transcription by Escherichia coli RNA polymerase. Nature *409*, 113-115.

Hatfield, G.W., and Benham, C.J. (2002). DNA topology-mediated control of global gene expression in Escherichia coli. Annu Rev Genet *36*, 175-203.

Higgins, C.F., Dorman, C.J., Stirling, D.A., Waddell, L., Booth, I.R., May, G., and Bremer, E. (1988). A physiological role for DNA supercoiling in the osmotic regulation of gene expression in S. typhimurium and E. coli. Cell *52*, 569-584.

Hsieh, T., and Brutlag, D. (1980). ATP-dependent DNA topoisonmerase from D. melanogaster reversibly catenates duplex DNA rings. Cell *21*, 115-125.

Jansen, A., and Verstrepen, K.J. (2011). Nucleosome positioning in Saccharomyces cerevisiae. Microbiol Mol Biol Rev *75*, 301-320.

Kanaar, R., and Cozzarelli, N.R. (1992). Roles of supercoiled DNA structure in DNA transsactions. Current Opinion in Structural Biology *2*, 369-379.

Kim, R.A., and Wang, J.C. (1989). Function of DNA topoisomerases as replication swivels in Saccharomyces cerevisiae. J Mol Biol *208*, 257-267.

King, G.A., Gross, P., Bockelmann, U., Modesti, M., Wuite, G.J., and Peterman, E.J. (2013). Revealing the competition between peeled ssDNA, melting bubbles, and S-DNA during DNA overstretching using fluorescence microscopy. Proc Natl Acad Sci U S A *110*, 3859-3864.

Koster, D.A., Croquette, V., Dekker, C., Shuman, S., and Dekker, N.H. (2005). Friction and torque govern the relaxation of DNA supercoils by eukaryotic topoisomerase IB. Nature *434*, 671-674.

Koster, D.A., Crut, A., Shuman, S., Bjornsti, M.A., and Dekker, N.H. (2010). Cellular strategies for regulating DNA supercoiling: a single-molecule perspective. Cell *142*, 519-530.

Koster, D.A., Palle, K., Bot, E.S., Bjornsti, M.A., and Dekker, N.H. (2007). Antitumour drugs impede DNA uncoiling by topoisomerase I. Nature *448*, 213-217.

Kouzine, F., Gupta, A., Baranello, L., Wojtowicz, D., Ben-Aissa, K., Liu, J., Przytycka, T.M., and Levens, D. (2013). Transcription-dependent dynamic supercoiling is a short-range genomic force. Nat Struct Mol Biol *20*, 396-403.

Kouzine, F., and Levens, D. (2007). Supercoil-driven DNA structures regulate genetic transactions. Front Biosci *12*, 4409-4423.

Kouzine, F., Sanford, S., Elisha-Feil, Z., and Levens, D. (2008). The functional response of upstream DNA to dynamic supercoiling in vivo. Nat Struct Mol Biol *15*, 146-154.

Kowalski, D., and Eddy, M.J. (1989). The DNA unwinding element: a novel, cis-acting component that facilitates opening of the Escherichia coli replication origin. EMBO J *8*, 4335-4344.

Krasilnikov, A.S., Podtelezhnikov, A., Vologodskii, A., and Mirkin, S.M. (1999). Large-scale effects of transcriptional DNA supercoiling in vivo. J Mol Biol *292*, 1149-1160.

La Porta, A., and Wang, M.D. (2004). Optical torque wrench: angular trapping, rotation, and torque detection of quartz microparticles. Phys Rev Lett *92*, 190801.

Lee, M., Kim, S.H., and Hong, S.C. (2010). Minute negative superhelicity is sufficient to induce the B-Z transition in the presence of low tension. Proc Natl Acad Sci U S A *107*, 4985-4990.

Levchenko, V., Jackson, B., and Jackson, V. (2005). Histone release during transcription: displacement of the two H2A-H2B dimers in the nucleosome is dependent on different levels of transcription-induced positive stress. Biochemistry *44*, 5357-5372.

Lia, G., Praly, E., Ferreira, H., Stockdale, C., Tse-Dinh, Y.C., Dunlap, D., Croquette, V., Bensimon, D., and Owen-Hughes, T. (2006). Direct observation of DNA distortion by the RSC complex. Mol Cell *21*, 417-425.

Lim, H.M., Lewis, D.E., Lee, H.J., Liu, M., and Adhya, S. (2003). Effect of varying the supercoiling of DNA on transcription and its regulation. Biochemistry *42*, 10718-10725.

Lionnet, T., Joubaud, S., Lavery, R., Bensimon, D., and Croquette, V. (2006). Wringing out DNA. Phys Rev Lett *96*, 178102.

Liu, L.F., and Wang, J.C. (1987). Supercoiling of the DNA template during transcription. Proc Natl Acad Sci U S A *84*, 7024-7027.

Ljungman, M., and Hanawalt, P.C. (1992). Localized torsional tension in the DNA of human cells. Proc Natl Acad Sci U S A *89*, 6055-6059.

Luger, K., Mader, A.W., Richmond, R.K., Sargent, D.F., and Richmond, T.J. (1997). Crystal structure of the nucleosome core particle at 2.8 A resolution. Nature *389*, 251-260.

Marko, J.F. (2007). Torque and dynamics of linking number relaxation in stretched supercoiled DNA. Phys Rev E Stat Nonlin Soft Matter Phys *76*, 021926.

Marko, J.F., and Siggia, E.D. (1995). Stretching DNA. Macromolecules *28*, 8759-8770.

Matsumoto, K., and Hirose, S. (2004). Visualization of unconstrained negative supercoils of DNA on polytene chromosomes of Drosophila. J Cell Sci *117*, 3797-3805.

Mitarai, N., Dodd, I.B., Crooks, M.T., and Sneppen, K. (2008). The generation of promoter-mediated transcriptional noise in bacteria. PLoS Comput Biol *4*, e1000109.

Moroz, J.D., and Nelson, P. (1997). Torsional directed walks, entropic elasticity, and DNA twist stiffness. Proc Natl Acad Sci U S A *94*, 14418-14422.

Nelson, D.L., and Cox, M.M. (2005). Lehninger Principles of Biochemistry (New York, W. H. Freeman and Company).

Neuman, K.C., and Block, S.M. (2004). Optical trapping. Rev Sci Instrum *75*, 2787-2809.

Neuman, K.C., Charvin, G., Bensimon, D., and Croquette, V. (2009). Mechanisms of chiral discrimination by topoisomerase IV. Proc Natl Acad Sci U S A *106*, 6986-6991.

Nieminen, T.A., Heckenberg, N.R., and Rubinsztein-Dunlop, H. (2001). Optical measurement of microscopic torques. Journal of Modern Optics *48*, 405-413.

O'Neil, A.T., and Padgett, M.J. (2002). Rotational control within optical tweezers by use of a rotating aperture. Optics Letters *27*, 743-745.

Odijk, T. (1995). Stiff Chains and Filaments under Tension. Macromolecules *28*, 7016-7018.

Palecek, E. (1991). Local supercoil-stabilized DNA structures. Crit Rev Biochem Mol Biol *26*, 151-226.

Petesch, S.J., and Lis, J.T. (2008). Rapid, transcription-independent loss of nucleosomes over a large chromatin domain at Hsp70 loci. Cell *134*, 74-84.

Pfaffle, P., Gerlach, V., Bunzel, L., and Jackson, V. (1990). In vitro evidence that transcription-induced stress causes nucleosome dissolution and regeneration. J Biol Chem *265*, 16830-16840.

Postow, L., Crisona, N.J., Peter, B.J., Hardy, C.D., and Cozzarelli, N.R. (2001a). Topological challenges to DNA replication: conformations at the fork. Proc Natl Acad Sci U S A *98*, 8219-8226.

Postow, L., Ullsperger, C., Keller, R.W., Bustamante, C., Vologodskii, A.V., and Cozzarelli, N.R. (2001b). Positive torsional strain causes the formation of a four-way junction at replication forks. J Biol Chem *276*, 2790-2796.

Revyakin, A., Ebright, R.H., and Strick, T.R. (2004). Promoter unwinding and promoter clearance by RNA polymerase: detection by single-molecule DNA nanomanipulation. Proc Natl Acad Sci U S A *101*, 4776-4780.

Revyakin, A., Liu, C., Ebright, R.H., and Strick, T.R. (2006). Abortive initiation and productive initiation by RNA polymerase involve DNA scrunching. Science *314*, 1139-1143.

Rhee, K.Y., Opel, M., Ito, E., Hung, S., Arfin, S.M., and Hatfield, G.W. (1999). Transcriptional coupling between the divergent promoters of a prototypic LysR-type regulatory system, the ilvYC operon of Escherichia coli. Proc Natl Acad Sci U S A *96*, 14294-14299.

Roca, J. (2011). The torsional state of DNA within the chromosome. Chromosoma *120*, 323-334.

Rohrbach, A., and Stelzer, E.H.K. (2002). Three-dimensional position detection of optically trapped dielectric particles. Journal of Applied Physics *91*, 5474-5488.

Salceda, J., Fernandez, X., and Roca, J. (2006). Topoisomerase II, not topoisomerase I, is the proficient relaxase of nucleosomal DNA. EMBO J *25*, 2575-2583.

Scheffer, M.P., Eltsov, M., and Frangakis, A.S. (2011). Evidence for short-range helical order in the 30-nm chromatin fibers of erythrocyte nuclei. Proc Natl Acad Sci U S A *108*, 16992-16997.

Siebenlist, U. (1979). RNA polymerase unwinds an 11-base pair segment of a phage T7 promoter. Nature *279*, 651-652.

Simpson, R.T., Thoma, F., and Brubaker, J.M. (1985). Chromatin reconstituted from tandemly repeated cloned DNA fragments and core histones: a model system for study of higher order structure. Cell *42*, 799-808.

Smith, S.B., Cui, Y., and Bustamante, C. (1996). Overstretching B-DNA: the elastic response of individual double-stranded and single-stranded DNA molecules. Science *271*, 795-799.

Strick, T.R., Allemand, J.F., Bensimon, D., Bensimon, A., and Croquette, V. (1996). The elasticity of a single supercoiled DNA molecule. Science *271*, 1835-1837.

Strick, T.R., Allemand, J.F., Bensimon, D., and Croquette, V. (1998). Behavior of supercoiled DNA. Biophys J *74*, 2016-2028.

Strick, T.R., Croquette, V., and Bensimon, D. (2000). Single-molecule analysis of DNA uncoiling by a type II topoisomerase. Nature *404*, 901-904.

Strick, T.R., Dessinges, M.N., Charvin, G., Dekker, N.H., Allemand, J.F., Bensimon, D., and Croquette, V. (2003). Stretching of macromolecules and proteins. Reports on Progress in Physics *66*, 1-45.

Svoboda, K., and Block, S.M. (1994). Biological applications of optical forces. Annu Rev Biophys Biomol Struct *23*, 247-285.

Travers, A., and Muskhelishvili, G. (2007). A common topology for bacterial and eukaryotic transcription initiation? EMBO Rep *8*, 147-151.

Tsao, Y.P., Wu, H.Y., and Liu, L.F. (1989). Transcription-driven supercoiling of DNA: direct biochemical evidence from in vitro studies. Cell *56*, 111-118.

Ullsperger, C., and Cozzarelli, N.R. (1996). Contrasting enzymatic activities of topoisomerase IV and DNA gyrase from Escherichia coli. J Biol Chem *271*, 31549-31555.

Vinograd, J., Lebowitz, J., Radloff, R., Watson, R., and Laipis, P. (1965). The twisted circular form of polyoma viral DNA. Proc Natl Acad Sci U S A *53*, 1104-1111.

Vologodskii, A.V., and Cozzarelli, N.R. (1994). Conformational and thermodynamic properties of supercoiled DNA. Annu Rev Biophys Biomol Struct *23*, 609-643.

Vos, S.M., Tretter, E.M., Schmidt, B.H., and Berger, J.M. (2011). All tangled up: how cells direct, manage and exploit topoisomerase function. Nat Rev Mol Cell Biol *12*, 827-841.

Wang, J.C. (1971). Interaction between DNA and an Escherichia coli protein omega. J Mol Biol *55*, 523-533.

Wang, J.C. (1985). DNA topoisomerases. Annu Rev Biochem *54*, 665-697.

Wang, M.D., Yin, H., Landick, R., Gelles, J., and Block, S.M. (1997). Stretching DNA with optical tweezers. Biophys J *72*, 1335-1346.

Watson, J.D., and Crick, F.H. (1953a). Genetical implications of the structure of deoxyribonucleic acid. Nature *171*, 964-967.

Watson, J.D., and Crick, F.H. (1953b). Molecular structure of nucleic acids; a structure for deoxyribose nucleic acid. Nature *171*, 737-738.

Wu, H.Y., Shyy, S.H., Wang, J.C., and Liu, L.F. (1988). Transcription generates positively and negatively supercoiled domains in the template. Cell *53*, 433-440.

Zhang, X., Chen, H., Le, S., Rouzina, I., Doyle, P.S., and Yan, J. (2013). Revealing the competition between peeled ssDNA, melting bubbles, and S-DNA during DNA overstretching by single-molecule calorimetry. Proc Natl Acad Sci U S A *110*, 3865-3870.

CHAPTER 2

TWIST-STRETCH COUPLING AND PHASE TRANSITION DURING DNA SUPERCOILING

*Physical Chemistry Chemical Physics, 2009, Volume 11, pp. 4800-4803. Sheinin, M. Y. and Wang, M. D. *Twist-stretch Coupling and Phase Transition during DNA Supercoiling.* Adapted by permission from the PCCP Owner Societies.

Introduction

During various cellular processes DNA molecules often experience moderate tension and torque. These perturbations may be generated by motor enzymes and provide a mechanism for the regulation of DNA replication, DNA repair, transcription, and DNA recombination (Cozzarelli et al., 2006; Koster et al., 2005; Liu and Wang, 1987; Travers and Thompson, 2004). Therefore, understanding tensile and torsional responses of DNA is essential to understanding how mechanical perturbations may regulate cellular activities.

A single DNA molecule can be extended under force and rotated under torque, as has been investigated using optical and magnetic tweezers and micropipettes during the past two decades (Allemand et al., 1998; Bryant et al., 2003; Deufel et al., 2007; Forth et al., 2008; Smith et al., 1996; Strick et al., 1996; Strick et al., 1998; Wang et al., 1997). In particular, some of these studies revealed that the tensile and torsional responses of DNA are coupled. Initial analyses suggested that DNA undertwists when extended, indicating a positive twist-stretch coupling coefficient (Marko, 1998; Moroz and Nelson, 1997). More recent studies by Gore et al. (Gore et al., 2006) and Lionnet et al. (Lionnet et al., 2006) using magnetic tweezers, as well as our own work using angular optical trapping (Deufel et al., 2007) provide compelling evidence to the contrary: DNA overtwists when extended and, conversely, DNA extends when overtwisted. However, there remains some ambiguity in identifying the signatures of twist-stretch coupling in the extension curves when the DNA was overtwisted under constant force. While Lionnet et al. (Lionnet et al., 2006) interpreted a peak in this curve to be indicative of the onset of a phase transition from B- to supercoiled P- (scP-) DNA, our earlier work indicated that the peak of the curve and the phase transition did not coincide at the particular force examined (Deufel et al.,

2007). In general, there was a lack of understanding of the nature of the extension peak location and its relation to both twist-stretch coupling and phase transitions.

The goals of this work are to differentiate between the signatures of twist-stretch coupling and those of phase transitions, and to provide an explanation for the existence of the maximum in the extension signal. To this end, we carried out DNA torsional experiments using an angular optical trap in conjunction with nanofabricated quartz cylinders so that torque, angle, force, and extension of a DNA molecule were simultaneously measured during DNA supercoiling, using previously described methods (Deufel et al., 2007; Forth et al., 2008). An important advantage of this approach is the direct detection of the torque signal, allowing unambiguous identification of the onset of the phase transition where torque plateaus.

Materials and Methods

The DNA template used in this study was constructed using previously described protocols (Forth et al., 2008). In brief, a 4218-bp piece of DNA was ligated at one end to a short (60-bp) oligonucleotide labeled with multiple digoxygenin (dig) tags and at the other end to an oligonucleotide of the same length labeled with multiple biotin tags.

The experimental configurations and procedures were similar to those described previously (Deufel et al., 2007; Forth et al., 2008). In brief, prior to a measurement, DNA molecules were torsionally constrained at one end to streptavidin-coated nanofabricated quartz cylinders (Deufel et al., 2007) and at the other end to an anti-dig coated coverslip. All experiments were performed in phosphate-buffered saline (157 mM Na^+, 4 mM K^+, 12 mM PO_4^{3-}, 140 mM Cl^-,

pH=7.4) at 23±1 ºC. The experiment began with a torsion-free DNA molecule which was held under constant tension. The DNA was first slightly undertwisted and then overwound via a steady rotation of the input laser polarization at 5 Hz, so as to explore a range of DNA supercoiling. During this time, torque, angular orientation, position, and force of the cylinder as well as the location of the coverglass were simultaneously recorded. The torque exerted on the DNA was measured from the torque exerted on the cylinder by the optical trap after subtracting the viscous drag torque of the rotating cylinder.

Results and Discussion

Figure 2.1 shows representative single traces of extension and the corresponding torque as a function of number of turns added to the DNA at three different applied forces (1.9, 7.7, and 9.6 pN). The number of turns was also converted to the degree of supercoiling σ, defined as the number of turns added to dsDNA divided by the number of naturally occurring helical turns in the given dsDNA. The DNA extension is also shown as the relative extension, defined as the extension normalized to the contour length of DNA template in its B-form.

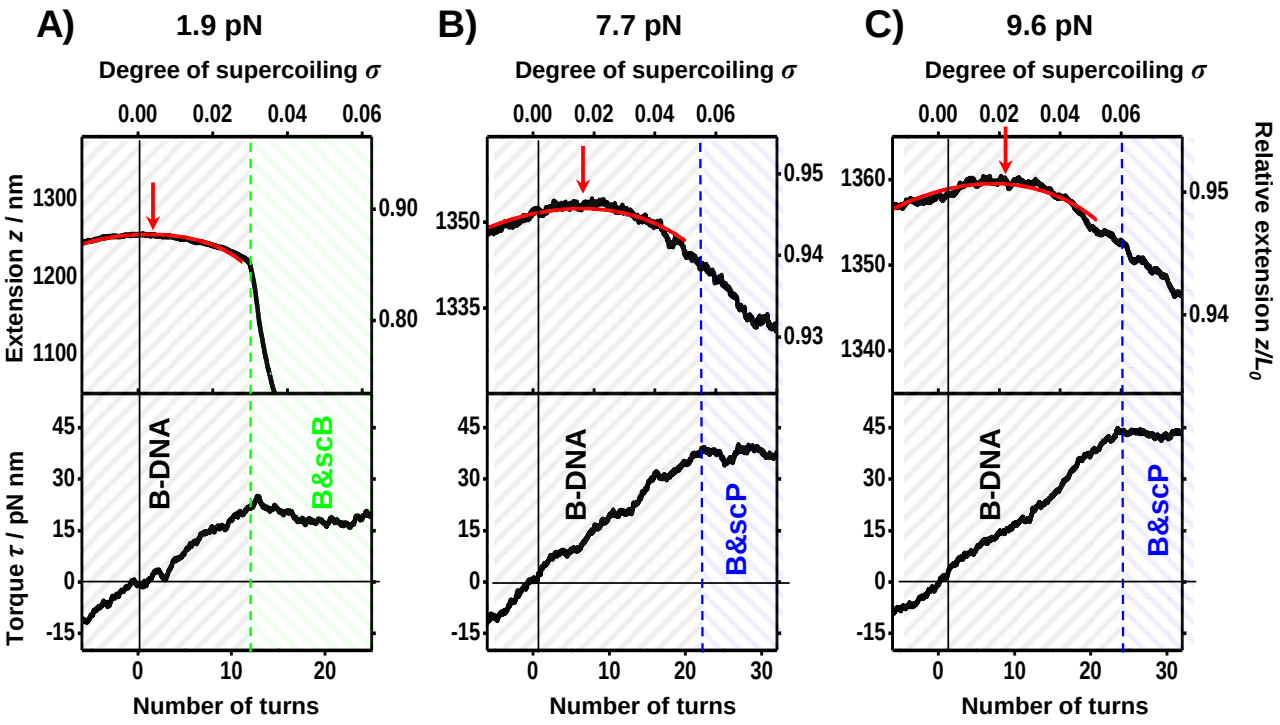

Figure 2.1: Examples of extension and torque versus turn number during DNA supercoiling.

DNA molecules of 4.2 kbp in length were wound at 5 Hz under constant forces: A) 1.9 pN; B) 7.7 pN; C) 9.6 pN. Data were collected at 2 kHz and averaged with a sliding box window of 2.0 s for torque and 0.2 s for extension. The torque signal had more Brownian noise relative to signal and was subjected to more filtering. Red curves are fits to Equation (2.2) for B-DNA. Extension maxima are indicated with red arrows. A plateau in the torque reflects a phase transition, and the onset of each transition is indicated by a dashed line.

Some overall features of these data are summarized below. At the beginning of each trace ($\sigma \sim -0.02$) DNA was in its B-form. As the DNA was twisted, torque increased linearly while extension remained approximately constant. At lower forces (< 6 pN) this continued until the DNA buckled to form a plectoneme, evidenced by a sudden decrease in extension and a concurrent plateau in torque, whose value was force-dependent (Forth et al., 2008). Under this low force range, the signatures for the onset of the buckling transition may be recognized in either extension or torque. At higher forces we used (6 pN < F < 10 pN), as the molecule was overtwisted, DNA underwent a scP-DNA transition instead, as previously observed (Allemand et al., 1998) The onset of this transition was only evidenced by a sudden torque plateau around 40 pN nm (Bryant et al., 2003; Deufel et al., 2007). These phase transitions may be thought of as first-order-like phase transitions since two separate phases may coexist and can be transformed from one to another by simply changing the twist in the DNA (Marko and Siggia, 1995). Because there were no concurrent distinct features in the extension signal, the ability to monitor torque signal was essential in unambiguously locating the onset of this transition. In addition, the buckling torque showed a strong force-dependence as previously observed (Forth et al., 2008); whereas the scP transition torque showed little force-dependence.

Several features relevant to twist-stretch coupling were also immediately evident. First, near $\sigma = 0$, the extension curve had a small but positive slope, which implied a negative twist-stretch coupling coefficient, i.e., DNA was extended when overtwisted. This observation was in accordance with previous studies (Deufel et al., 2007; Gore et al., 2006; Lionnet et al., 2006). Second, upon overtwisting, extension reached a maximum (indicated by an arrow in Figure 2.1) at σ_{z_max}, as has also been previously observed (Deufel et al., 2007; Lionnet et al., 2006). In

addition, as the force increased, σ_{z_max} increased while the magnitude in the curvature of the extension at σ_{z_max} gradually decreased. Third, the location of the extension maximum σ_{z_max} clearly did not coincide with the onset of the phase transition (indicated by a dashed line on the right) where torque began to plateau. This was the case for the range of forces we examined. Therefore the location of the maximum is not indicative of an onset of a phase transition, contrary to what has been previously reported with the magnetic tweezers experiments, where the lack of torque signal might have complicated the interpretation of the results (Lionnet et al., 2006).

To understand the nature of the extension signal for the B-form DNA, we performed a detailed analysis of both the extension and torque signals to gain insights in the twist-stretch coupling coefficient and the location of the extension maximum. We followed the analysis developed by Marko (Marko, 1998). This theory also takes into account the contribution from bending fluctuations to DNA extension, using a treatment similar to that of Moroz and Nelson (Moroz and Nelson, 1997). For a DNA molecule held under constant σ and force F, the free energy G includes contributions from bending, stretching, twisting, and twist-stretch coupling, and can be expressed as:

$$\frac{G}{k_B T L_0} = \frac{1}{L_p}\sqrt{\frac{L_p F}{k_B T} - \frac{1}{4}\left(C_0\omega_0\sigma + \frac{gF}{K_0}\right)^2} + \frac{C_0}{2}{\omega_0}^2\sigma^2 - \frac{F}{k_B T} - \frac{k_B T}{2K_0}\left(\frac{F}{k_B T} - g\omega_0\sigma\right)^2, \qquad (2.1)$$

where L_p is the bending persistence length, K_0 the stretch modulus, C_0 the twist persistence length, g the twist-stretch coupling modulus (unitless), $k_B T$ the thermal energy, L_0 the contour

length, and $\omega_0 = 2\pi/3.57$ nm^{-1} the natural twist rate. This theory predicts DNA extension z as a function of σ and applied force F:

$$\frac{z}{L_0} = -\frac{1}{L_0}\frac{\partial G}{\partial F}|_\sigma = 1 + \frac{F}{K_0} - \frac{k_B T g \omega_0 \sigma}{K_0} - \sqrt{\frac{k_B T}{4 L_p F}} \cdot \frac{1 - \frac{g C_0 \omega_0 \sigma + \frac{g^2 F}{K_0}}{2 L_p K_0} k_B T}{\sqrt{1 - \frac{k_B T}{4 L_p F}\left(C_0 \omega_0 \sigma - \frac{g F}{K_0}\right)^2}}. \quad (2.2)$$

We used Equation (2.1) to obtain a prediction of torque τ as a function of σ and applied force F:

$$\tau = \frac{1}{\omega_0 L_0}\frac{\partial G}{\partial F}|_F = k_B T g \omega_0 \sigma \left(C_0 - \frac{k_B T g^2}{K_0}\right) + \frac{k_B T g F}{K_0} - \frac{\frac{k_B T C_0}{4 L_p}\left(C_0 \omega_0 \sigma + \frac{g F}{K_0}\right)}{\sqrt{\frac{L_p F}{k_B T} - \frac{\left(C_0 \omega_0 \sigma + \frac{g F}{K_0}\right)^2}{4}}}. \quad (2.3)$$

Thus, Equations (2.2) and (2.3) form a complete set of relations that fully describe force, extension, torque, and twist for a B-form DNA.

Below, we will focus on the analysis of the extension signal. Equation (2.2) contains several terms and its last term is due to the contribution of DNA bending fluctuations in the presence of the twist-stretch coupling. We found that Equation. (2.2) predicts the existence of a maximum in the extension curve, reflecting an interplay between twist-stretch coupling and bending fluctuations. In the absence of any twist-stretch coupling, the maximum is centrally located, i.e., if $g = 0$, $\sigma_{z\_max} = 0$. Twist-stretch coupling shifts the location of the maximum away from the center (Figure 2.2). If $g > 0$, then $\sigma_{z\_max} < 0$; and if $g < 0$, then $\sigma_{z\_max} > 0$. The absolute value of σ_{z_max} increases with an increase in force.

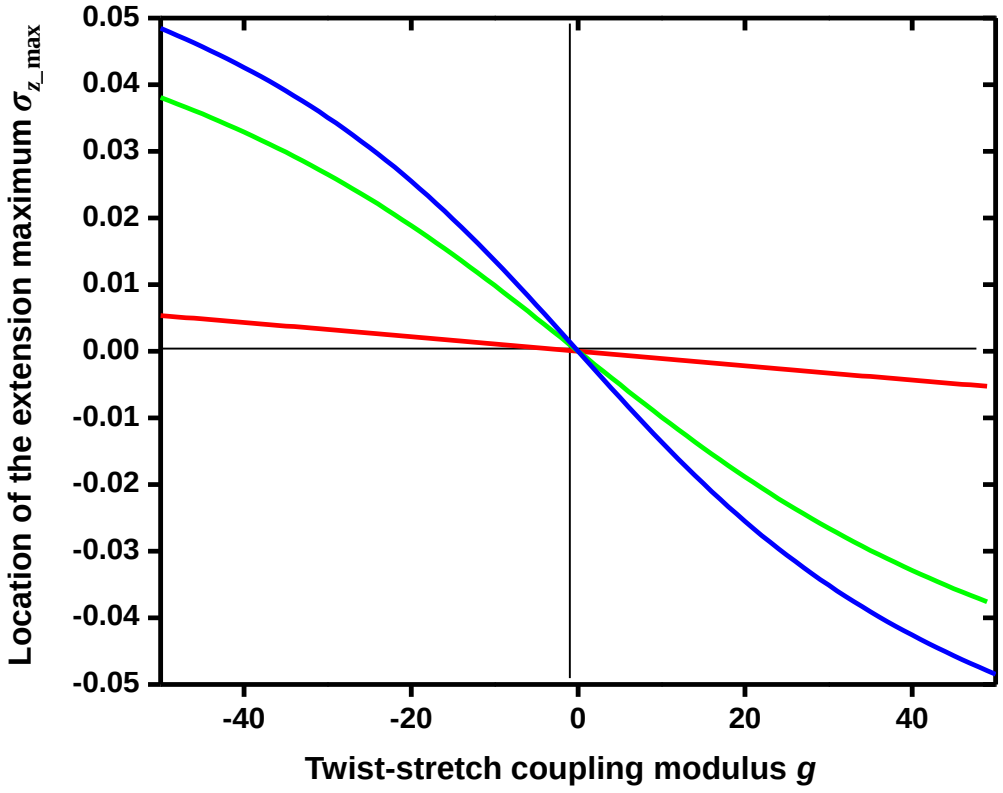

Figure 2.2: Effect of twist-stretch coupling on the location of the extension maximum σ_{z_max}.

Values of σ_{z_max} have been numerically calculated from Equation (2.2) at three different forces: 1.9 pN (red), 7.7 pN (green) and 9.6 pN (blue).

Notice that if bending fluctuations are neglected, Equation (2.2) is then simplified to:

$$\frac{z}{L_0} = 1 + \frac{F}{K_0} - \frac{k_B T g \omega_0 \sigma}{K_0}, \tag{2.4}$$

In contrast to Equation (2.2), Equation (2.4) predicts a linear relation between extension and the degree of supercoiling: if $g > 0$, then slope < 0; and if $g < 0$, then slope > 0. It does not predict a maximum in the extension curve.

We performed a fit of Equation (2.2) to our extension data for the B-form DNA with g as the only fit parameter. Other parameters were taken from previous measurements obtained under similar experimental conditions: K_0 = 1200 pN (Smith et al., 1996; Wang et al., 1997), C_0 = 100 nm (Bryant et al., 2003; Forth et al., 2008), and L_p = 43 nm (Forth et al., 2008; Smith et al., 1996; Wang et al., 1997). Our data were well fit by Equation (2.2) and some examples are shown in Figure 2.1 (red). In particular, the experimental observations that $\sigma_{z\_max} > 0$ and increases with increasing force were indicative of a negative value for the twist-stretch coupling modulus g. Figure 2.3 shows g values obtained from the fits under various forces. Over the force range examined, g was essentially independent of the force: $g = -21 \pm 1$ (mean ± sem, N = 41). The g value is sensitive to the value used for C_0. For example, a ±10% uncertainty in C_0 will result in a ±15% uncertainty in g.

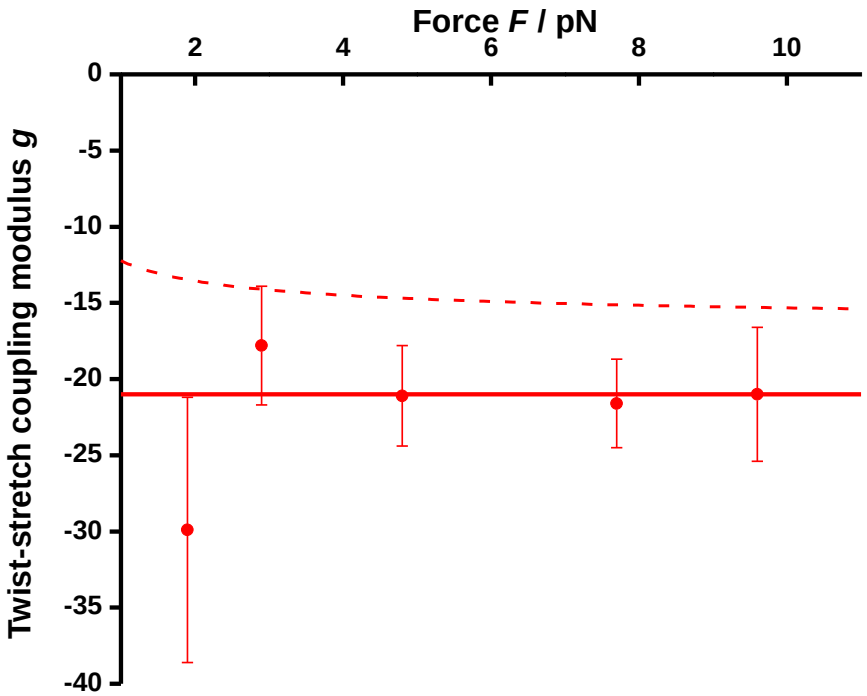

Figure 2.3: Measurement of the twist-stretch coupling modulus *g*.

For each force, the twist-stretch coupling modulus was determined using Equation (2.2) from 7-11 traces of data. The mean of the modulus *g* is shown as the solid horizontal line. For comparison, the magnitude of *g* would have been underestimated by ~ 20% if Equation (2.4) were to be used instead (dashed line).

If Equation (2.4) is used to obtain a g value instead, the magnitude of g is underestimated by ~ 20% over the range of forces examined (dashed line in Figure 2.3). This difference does not vanish even with an increase in force, since the geometric coupling between bending and writhe fluctuations leads to a decrease in extension (Marko, 1998). Interestingly, Lionnet et al. (Lionnet et al., 2006) used Equation (2.4) to fit their extension data and obtained $g = -16 \pm 7$ (mean ± sd, N > 36), whose magnitude is ~ 20% lower than our measured value. On the other hand, Gore et al. (Gore et al., 2006) made a measurement of twist angle as a function of extension change when the DNA was not torsionally constrained and obtained $g = -22 \pm 5$ (mean ± sem, N = 4), more in accord with our measured value. In the analysis by Gore et al. (Gore et al., 2006), the bending fluctuations were also neglected resulting in a similar linear approximation. Thus one might expect that the magnitude of g was similarly underestimated. Careful analysis using Equations (2.2) and (2.4) reveals that this effect was almost completely canceled by another linear approximation made to convert force to extension change. Taking together all these results (summarized in Table 2.1), the twist-stretch coupling modulus g should be about -21.

	g (unitless)	*Bending fluctuations*
This work	**−21±1** (mean±SEM, N=41)	Considered
Lionnet et al. (2006)	**−16±7** (mean±SD, N>36)	Neglected
Gore et al. (2006)	**−22±5** (mean±SEM, N=4)	Neglected, but the effect of this approximation is canceled by another approximation (extension calculated as proportional to force)

Table 2.1: Summary of the values of the twist-stretch coupling modulus obtained in recent single-molecule experiments. Considerations pertaining to bending fluctuations are specifically indicated.

The extension maximum, however, can only be explained using Equation (2.2) and not Equation (2.4). Figure 2.4 plots σ_{z_max} obtained as a function of force. For comparison, we also plotted the critical σ_c values for phase transitions to plectoneme (scB-) or scP-DNA. As this figure indicates, when DNA is positively supercoiled under moderate forces (2 pN < F < 20 pN), the DNA extension reaches a maximum long before DNA buckling or a transition to scP-DNA. At even higher forces (F > 20 pN), the scP-DNA transition is reached before the extension reaches a maximum. This figure clearly indicates that σ_{z_max} and σ_c do not coincide, except at ~ 20 pN. Therefore, the maximum in the extension in general is not indicative of a phase transition, in contrast to the interpretation of Lionnet et al. (Lionnet et al., 2006)

Twist-stretch coupling should also alter the torque signal. We found that consideration of the twist-stretch coupling as in Equation (2.3) will lower the expected torque value at most by ~ 1 pN nm (Figure 2.5). This is below the uncertainty of our experimental determination of torque.

The analysis described in this work may not be valid at forces significantly higher than those used in the current work. In the absence of torsional constraints, Equation (2.3) predicts a monotonic increase in overtwisting angle with an increase in force. However, Gore et al. (Gore et al., 2006) found that the twist angle starts to decrease with force above ~ 30 pN.

It is also worth mentioning that we do not consider sequence-dependent effects on twist-stretch coupling or phase transitions here. Prior simulation work (Lionnet et al., 2006; Lionnet and Lankas, 2007) suggests that DNA sequence may modulate the twist-stretch coupling. Future experiments with more refined measurements may help verify this prediction.

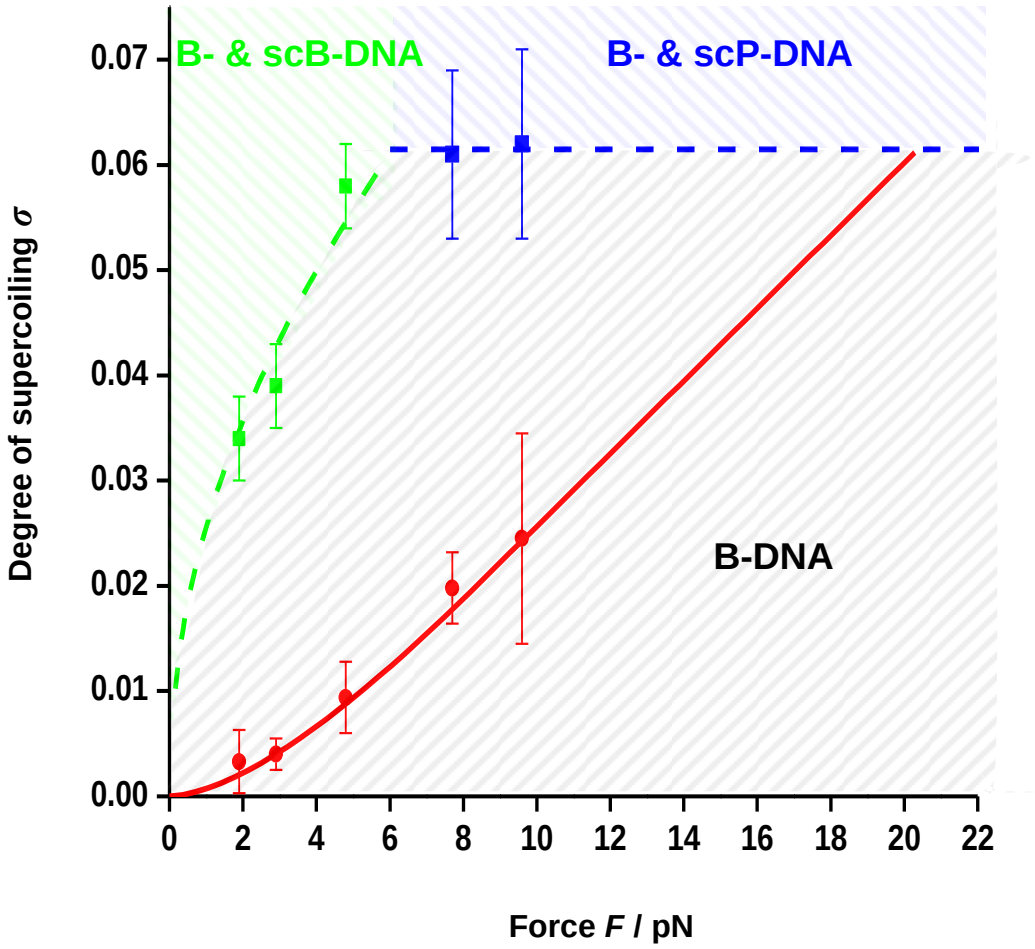

Figure 2.4: The degree of supercoiling at extension maximum σ_{z_max} and at the onsets of phase transitions.

The measured values of σ_{z_max} (red circles) are plotted together with σ_{z_max} calculated using the mean value of g from Fig. 2.3 (red line). For comparison, also shown are the measured degree of supercoiling at the buckling transition and its fit using a Marko theory (Marko, 2007) (green), as well as the measured degree of supercoiling at the onset to the scP transition with a constant fit (blue).

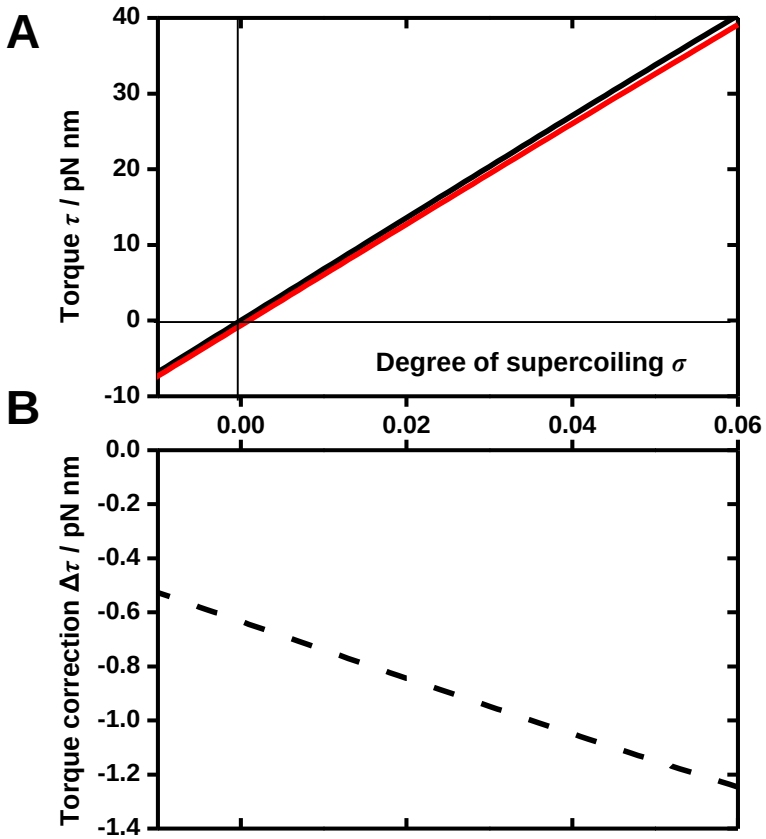

Figure 2.5: Effect of twist-stretch coupling on torque.

a) The figure represents torque calculated using Equation (2.3) with same parameters as used elsewhere for 9.6 pN of force (highest force used in our experiments) and $g = 0$ (black) and our measured value of $g = -21$ (red).

b) Calculated difference between torques expected in the presence and absence of twist-stretch coupling (i.e., the difference between the red and black curves in a).

References

Allemand, J.F., Bensimon, D., Lavery, R., and Croquette, V. (1998). Stretched and overwound DNA forms a Pauling-like structure with exposed bases. Proc Natl Acad Sci U S A *95*, 14152-14157.

Bryant, Z., Stone, M.D., Gore, J., Smith, S.B., Cozzarelli, N.R., and Bustamante, C. (2003). Structural transitions and elasticity from torque measurements on DNA. Nature *424*, 338-341.

Cozzarelli, N.R., Cost, G.J., Nollmann, M., Viard, T., and Stray, J.E. (2006). Giant proteins that move DNA: bullies of the genomic playground. Nat Rev Mol Cell Biol *7*, 580-588.

Deufel, C., Forth, S., Simmons, C.R., Dejgosha, S., and Wang, M.D. (2007). Nanofabricated quartz cylinders for angular trapping: DNA supercoiling torque detection. Nat Methods *4*, 223-225.

Forth, S., Deufel, C., Sheinin, M.Y., Daniels, B., Sethna, J.P., and Wang, M.D. (2008). Abrupt buckling transition observed during the plectoneme formation of individual DNA molecules. Phys Rev Lett *100*, 148301.

Gore, J., Bryant, Z., Nollmann, M., Le, M.U., Cozzarelli, N.R., and Bustamante, C. (2006). DNA overwinds when stretched. Nature *442*, 836-839.

Koster, D.A., Croquette, V., Dekker, C., Shuman, S., and Dekker, N.H. (2005). Friction and torque govern the relaxation of DNA supercoils by eukaryotic topoisomerase IB. Nature *434*, 671-674.

Lionnet, T., Joubaud, S., Lavery, R., Bensimon, D., and Croquette, V. (2006). Wringing out DNA. Phys Rev Lett *96*, 178102.

Lionnet, T., and Lankas, F. (2007). Sequence-dependent twist-stretch coupling in DNA. Biophys J *92*, L30-32.

Liu, L.F., and Wang, J.C. (1987). Supercoiling of the DNA template during transcription. Proc Natl Acad Sci U S A *84*, 7024-7027.

Marko, J.F. (1998). DNA under high tension: Overstretching, undertwisting, and relaxation dynamics. Physical Review E *57*, 2134-2149.

Marko, J.F. (2007). Torque and dynamics of linking number relaxation in stretched supercoiled DNA. Phys Rev E Stat Nonlin Soft Matter Phys *76*, 021926.

Marko, J.F., and Siggia, E.D. (1995). Statistical-Mechanics of Supercoiled DNA. Physical Review E *52*, 2912-2938.

Moroz, J.D., and Nelson, P. (1997). Torsional directed walks, entropic elasticity, and DNA twist stiffness. Proc Natl Acad Sci U S A *94*, 14418-14422.

Smith, S.B., Cui, Y., and Bustamante, C. (1996). Overstretching B-DNA: the elastic response of individual double-stranded and single-stranded DNA molecules. Science *271*, 795-799.

Strick, T.R., Allemand, J.F., Bensimon, D., Bensimon, A., and Croquette, V. (1996). The elasticity of a single supercoiled DNA molecule. Science *271*, 1835-1837.

Strick, T.R., Allemand, J.F., Bensimon, D., and Croquette, V. (1998). Behavior of supercoiled DNA. Biophys J *74*, 2016-2028.

Travers, A.A., and Thompson, J.M. (2004). An introduction to the mechanics of DNA. Philos Transact A Math Phys Eng Sci *362*, 1265-1279.

Wang, M.D., Yin, H., Landick, R., Gelles, J., and Block, S.M. (1997). Stretching DNA with optical tweezers. Biophys J *72*, 1335-1346.

CHAPTER 3

UNDERWOUND DNA UNDER TENSION: STRUCTURE, ELASTICITY, AND SEQUENCE-DEPENDENT BEHAVIORS

Introduction

Negative DNA supercoiling is known to play an important role throughout the cell cycle. Circular DNA, as seen in plasmids and genomic DNA of prokaryotes, is maintained in an underwound state (Nelson and Cox, 2005), while negative supercoiling in eukaryotic genomes is predominantly constrained within nucleosomes (Kouzine and Levens, 2007). Negative torsion affects cellular processes through changes in DNA conformation, such as plectoneme formation (Vinograd et al., 1965), cruciform extrusion from palindromic sequences (Liu and West, 2004), and conversion of B-DNA regions into unusual structures such as Z- or H-DNA (Kouzine and Levens, 2007). Most importantly, underwinding can promote local melting of the DNA (Jacob et al., 1974) which is a requirement for the initiation of replication (Baker et al., 1986) and transcription (Siebenlist, 1979). A common feature of many prokaryotic and eukaryotic replication origins is the so called DNA unwinding element (DUE), an easily denaturing segment of DNA (Umek and Kowalski, 1988). Since the sequences of DUEs are generally not conserved, it is believed that proteins may recognize general structural features of the unpaired DNA strands, rather than a particular sequence (DePamphilis, 1996).

In order to better understand the regulatory mechanisms of torsionally-melted DNA, it is important to know its structural and elastic properties. Early insights were provided by experiments on circular plasmid DNA (Kahn et al., 1994) which yielded estimates of persistence length and torsional modulus of small regions of strand-separated DNA. In the last two decades, single-molecule manipulation techniques have become powerful tools to study DNA mechanics (Allemand et al., 1998; Bryant et al., 2003; Celedon et al., 2009; Forth et al., 2008; Leger et al., 1999; Sheinin and Wang, 2009; Strick et al., 1996; Wang et al., 1997). Although these methods

have provided insights for B-DNA, torsionally-melted DNA has not yet been fully examined and is still poorly understood. Even the structure of melted DNA is controversial as it is unclear whether a melted DNA takes on the form of two parallel single-strands (Allemand et al., 1998) or a left-handed helix (Bryant et al., 2003; Leger et al., 1999). Elastic parameters of melted DNA have only been roughly estimated by examining the coexistence state of B-DNA and melted DNA (Sarkar et al., 2001). To date, there has been no direct and complete description of the tensile and torsional elasticity of melted DNA, and even less is known about the sequence-dependence of the elastic properties of melted DNA.

In the current work, we employed our angular optical trap (Deufel et al., 2007; Forth et al., 2008; Inman et al., 2010; La Porta and Wang, 2004; Sheinin and Wang, 2009) to carry out a comprehensive study of torsionally underwound DNA. Direct torque detection is essential to our approach, as it allows unambiguous identification of the phase boundaries (Marko, 2007; Sheinin and Wang, 2009) as well as direct measurements of torsional elastic parameters. Our experiments allow for the full characterization of both the torsional and tensile properties of melted DNA.

Materials and Methods

Experiments were performed with one of three constructs. Initial experiments were done using a 2.2 kbp DNA construct (Sequence A) as described previously (Forth et al., 2008). Briefly, a 2154-bp fragment (51% GC content) was produced *via* PCR, cut with BsaI, and the ends were ligated to two 62-bp linker arms. The linker arms contained six equally spaced dT-biotin or dT-digoxigenin modified bases. The DNA molecules were incubated with custom nanofabricated

quartz cylinders (Deufel et al., 2007), which were coated with streptavidin on the bottom surface. A microscope coverslip was coated with anti-digoxigenin (40 μg/ml in PBS) for specific attachment to the DNA, and casein (4 mg/ml in PBS) to prevent non-specific interactions. For each force, 7-15 individual DNA molecules were investigated. Experiments were performed in PBS (137 mM NaCl, 2.7 mM KCl, 4.3 mM Na_2HPO_4, 1.4 mM K_2HPO_4, pH 7.4) at 23±1 ˚C.

To determine the effect of sequence during underwinding, two additional constructs were generated. The first was generated from a plasmid incorporating an ~ 75% GC-rich 1 kb sequence of the PepA protein from *M. paratuberculosis*. From this plasmid, a 1573 bp PCR fragment was produced and a rotationally constrained construct (Sequence C) was created with an overall GC-content of 64%. From a second plasmid, pBR322 (New England Biolabs, Inc., Ipswich, Mass.), a 1720 bp PCR fragment (52% GC content) was generated (Sequence B). Although Sequence B and Sequence A have similar GC-content, the linear sequence is different.

It is known that certain DNA sequences are prone to forming non-B-DNA structures, the most notable of which is Z-DNA (Ho et al., 1986). We have investigated whether Z-DNA was likely to form in our templates using freely available software (http://gac-web.cgrb.oregonstate.edu/zDNA/, (Ho et al., 1986)). The analysis of all sequences used in this study revealed that only a few short regions (<1.5 % of the total template length) were identified as being capable of Z-DNA formation.

Angular optical trapping was carried out as described previously (La Porta and Wang, 2004). Briefly, linearly polarized light was used to trap and rotate a nanofabricated quartz cylinder

(Deufel et al., 2007) with a DNA molecule attached. Torque measurement was achieved by monitoring the change in the ellipticity of light after it had interacted with the cylinder (Friese et al., 1998; La Porta and Wang, 2004; Nieminen et al., 2001). DNA was either under- or overwound at a constant force (maintained *via* feedback on the position of the piezoelectric stage). The particle was rotated at 10-20 Hz, so as to minimize experimental time and, consequently, drift in torque signal (about 1-2 pN·nm/min).

Experimental Results

We first carried out experiments on Sequence A under a range of constant forces (Figure 3.1). As DNA was continuously twisted, both the torque and the extension were directly monitored. The degree of supercoiling σ is defined as the number of turns added to dsDNA divided by the number of naturally occurring helical turns in the given molecule. The experiment began with the DNA in a slightly overwound state, as evidenced by a torque plateau (Bryant et al., 2003; Forth et al., 2008; Lipfert et al., 2010; Sheinin and Wang, 2009) at the far right of the Figure 3.1. Rotation of the DNA in the underwinding direction resulted first in the disappearance of non-B form structures such as plectonemic loops or supercoiled P-DNA, and the subsequent twisting of B-DNA where torque was proportional to the number of turns (Bryant et al., 2003; Forth et al., 2008). The onset of a DNA torsional melting transition occurred when the torque reached approximately −10 pN nm, a value that compares well with previous work (Bryant et al., 2003; Lipfert et al., 2010; Strick et al., 1998a). A large number of turns had to be applied before the molecule completed the transition to a fully melted state. The end of the torsional melting transition was signaled by a decrease in the torque (corresponding to an increase in magnitude)

and a concomitant shortening in extension. Interestingly, upon further unwinding, the torque plateaued again, indicating another phase transition, while the extension continued to decrease, albeit at a slower rate.

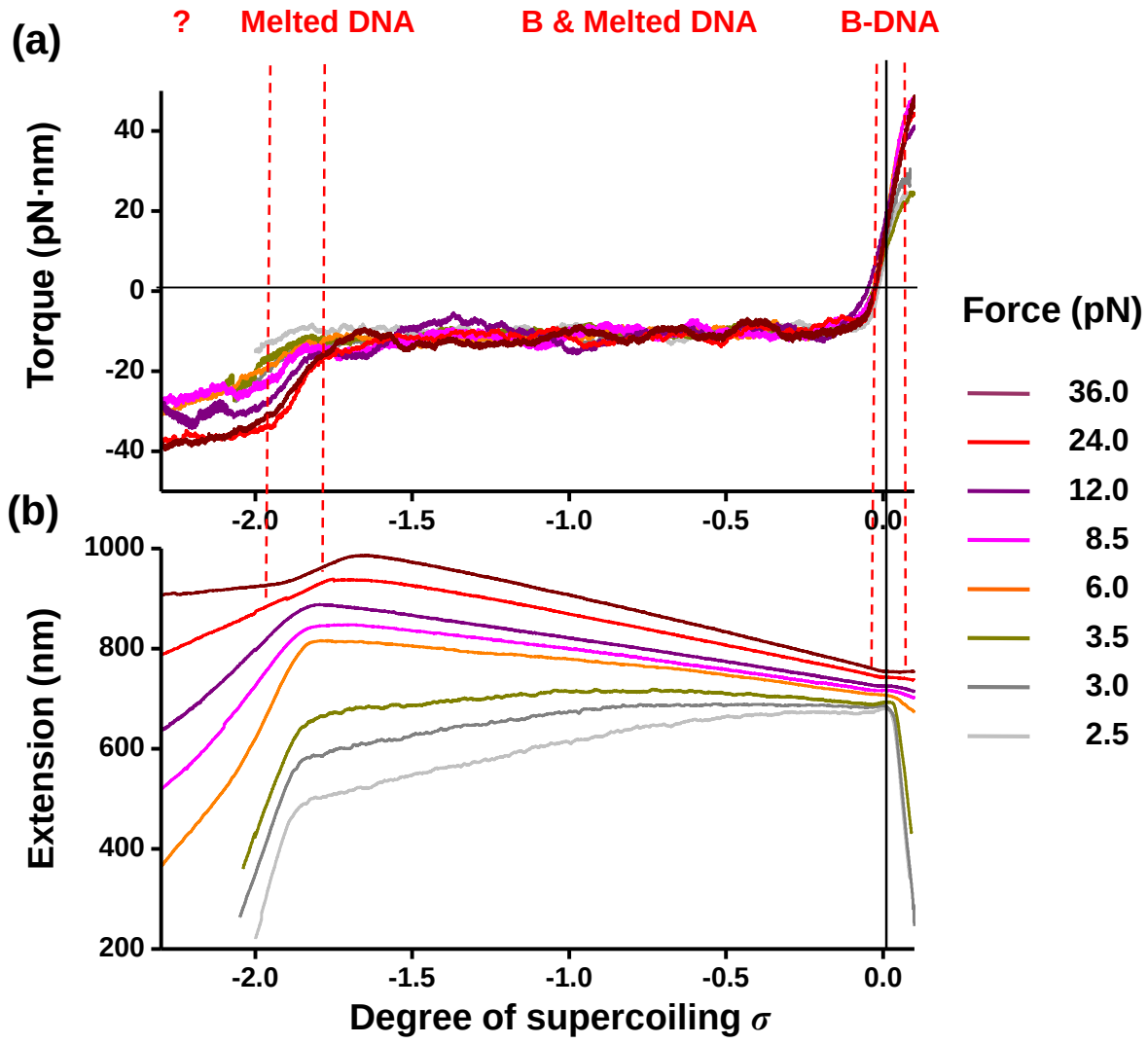

Figure 3.1: Torque (a) and extension (b) traces for sequence A, averaged over multiple single molecule experiments. Dashed lines indicate phase boundaries for measurements at 24 pN.

Several parameters can be determined from the data taken in the fully melted state. First is the natural twist of torsionally-melted DNA. The degree of supercoiling at the end of the melting transition σ_{end} was slightly force-dependent (Figure 3.2a), with an average value of approximately −1.8; the corresponding twist is therefore ≈ −13 bp/turn, comparable to but larger in magnitude than previous indirect estimates of −9 bp/turn (Leger et al., 1999; Sarkar et al., 2001). This negative helicity indicates that the melted DNA takes on a left-handed structure, and we will therefore follow the notation of Bryant et al. (Bryant et al., 2003) to designate such a form of torsionally-melted DNA as L-DNA. A previous single-molecule study (Allemand et al., 1998) employed glyoxal, which chemically reacts with unpaired DNA bases, to infer $\sigma_{end} \sim -1$. The discrepancy may lie in the difference in experimental conditions, such as the significantly lower salt concentration in the previous study (Allemand et al., 1998) which may have disfavored the left-handed wrapping that we observe.

In addition to helicity, several key elastic parameters of L-DNA may also be determined. For this analysis, data below 5 pN were excluded, since secondary structures within L-DNA likely existed at low forces (see below). A fit of L-DNA extension at the end of the melting transition versus force to the WLC model (Figure 3.2b) yielded a persistence length of ~ 3 nm, much smaller than that of B-DNA, and a contour length of 0.48 nm/bp, 40% longer than B-DNA. Due to significant interdependence of the parameters from the full fit we were not able to reliably determine the L-DNA stretch modulus. The torsional modulus *C* was calculated from the slope of the torque versus linking number data: $C = \frac{\partial \tau}{\partial \sigma} \frac{L_L}{2\pi k_B T \cdot Lk_0}$, where L_L is the contour length of L-DNA and Lk_0 is the linking number in relaxed B-DNA, calculated as number of basepairs / helical pitch (Figure 3.2c). The torsional modulus for L-DNA was found to be ~ 20 nm at high

force, much smaller than that of B-DNA (~ 100 nm) (Bryant et al., 2003; Forth et al., 2008; Lipfert et al., 2010).

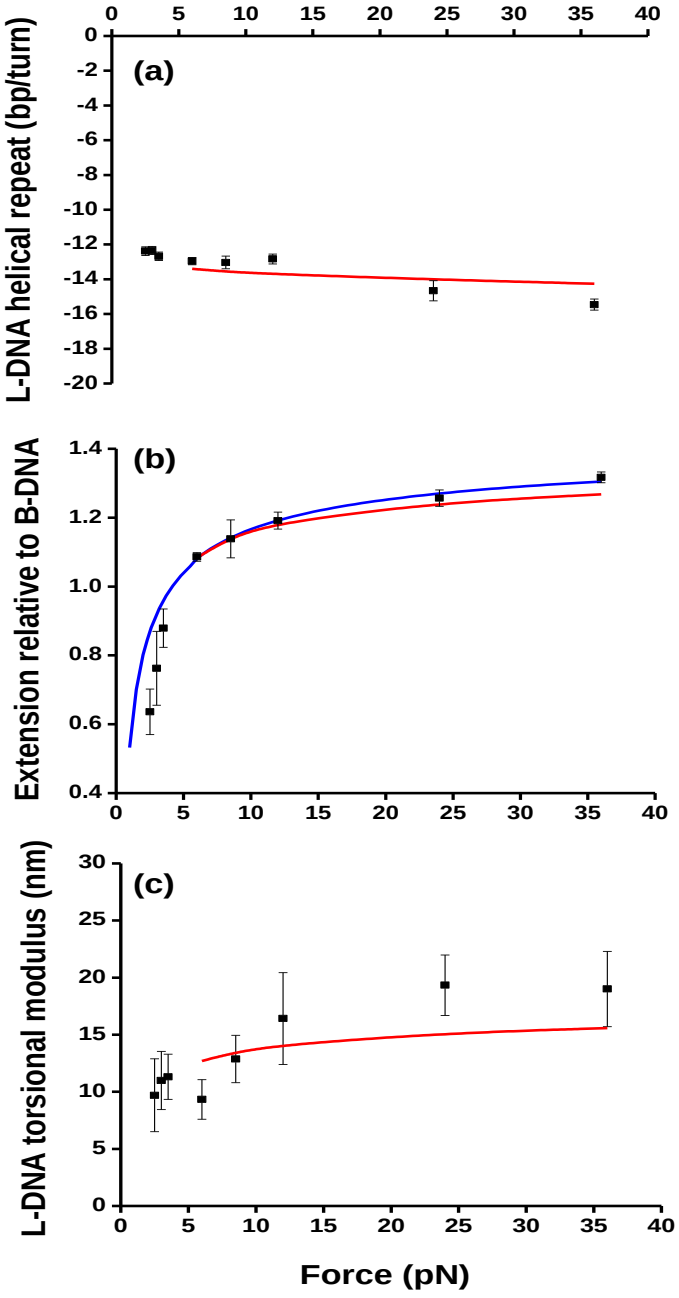

Figure 3.2: Force-dependence of elastic parameters of L-DNA.
Measurements (black squares) are compared with theory discussed in the main text (red lines). The extension data were also fit by the worm-like chain model (blue).

It is informative to compare our measured elastic parameters of torsionally-melted DNA with those of alternate structures that can form upon negative supercoiling (Table 3.1). Unlike a simple "DNA bubble", L-DNA possesses a well-defined helicity and is significantly torsionally stiffer. On the other hand, it is easily bent, in contrast to highly rigid base-paired Z-DNA. In addition, based on recent data (Lee et al., 2010), the torque during the B- to Z-DNA transition is estimated to be –5 pN nm, a factor of two smaller in magnitude from the measured average melting torque (–10 pN nm). Based on these differences, we conclude that torsionally-melted DNA under substantial tension (> 5 pN) likely consists predominantly of a single form (L-DNA), while other sequence-dependent structures (such as Z-DNA) make only a minor contribution to the overall content of underwound DNA.

	B-DNA	L-DNA (this work)	DNA "bubble" (Kahn et al., 1994)	Z-DNA (Thomas and Bloomfield, 1983)
Handedness	**right**	**left**	**none**	**left**
Helical repeat (bp/turn)	**10.5**	**−12 to −15**	**∞**	**-12**
Contour length (nm/bp)	**0.34**	**0.48**	**0.54**	**0.37**
Persistence length (nm)	**43**	**3**	**2-3**	**200**
Torsional modulus (nm)	**100**	**10 to 20**	**1**	**?**

Table 3.1: Comparison of main elastic parameters of L-DNA with those of B-DNA, DNA "bubble", and Z-DNA.

Theoretical Modeling

Recently a phenomenological model of DNA phase transitions under force and torque has been proposed (Marko, 2007), specifically focusing on supercoiling and melting transitions. The theory has been shown to agree well with our previous experiments on positively supercoiled DNA (Forth et al., 2008). Here we examine the applicability of the theory to the melting transition, using a similar framework with small modifications, as described below.

For a pure state (i) of DNA structure, the free energy may be expressed using a harmonic approximation:

$$G_i = \varepsilon_i - g_i(F) + \frac{c_i(F)\left(\sigma - \sigma_{0,i}\right)^2}{2}, \tag{3.1}$$

where ε_i is an energy offset and $\sigma_{0,i}$ is the relaxed degree of supercoiling for the state. Assuming the DNA in each state behaves as a semiflexible polymer with twist compliance, stretching energies $g_i(F)$ and torsional coefficients $c_i(F)$ as a function of force F can be approximated (Marko, 2007; Moroz and Nelson, 1997):

$$g_i(F) = b_i\left(F - \sqrt{\frac{k_B T F}{L_{\boldsymbol{p,i}}}} + \frac{F^2}{2K_i}\right), \tag{3.2}$$

$$c_i(F) = k_B T C_i {\omega_0}^2\left[1 - \frac{C}{4L_{\boldsymbol{p,i}}}\sqrt{\frac{k_B T}{L_{\boldsymbol{p,i}} F}}\right], \tag{3.3}$$

where $L_{p,i}$ is persistence length, C_i is torsional modulus, K_i is stretch modulus (assumed to be infinity for L-DNA), b_i is contour length ratio to that of B-DNA, and ω_0 is the natural twist of B-DNA. Following Marko (Marko, 2007), we analytically expressed the linking numbers at the onset and the end of a transition to a new phase as well as the extension and torque throughout this process:

$$\sigma_{start} = \frac{c_L}{c_L - c_B}\left(-\sigma_{0,L} - \sqrt{{\sigma_{0,L}}^2 + \frac{2(c_B - c_L)}{c_L c_B}(g_B + \varepsilon_L - g_L)}\right), \tag{3.4}$$

$$\sigma_{end} = \sigma_{0,L} + \frac{c_B}{c_L - c_B}\left(-\sigma_{0,L} - \sqrt{{\sigma_{0,L}}^2 + \frac{2(c_B - c_L)}{c_L c_B}(g_B + \varepsilon_L - g_L)}\right), \tag{3.5}$$

where $c_L(F)$, $c_B(F)$, $g_L(F)$, and $g_B(F)$ are force-dependent parameters given by Equations (3.2) and (3.3). Note that $\sigma_{0,B} = 0$ and $\varepsilon_B = 0$ in this formulation. As B-DNA is gradually underwound, DNA initially remains in the B-form ($\sigma > \sigma_{start}$), then undergoes a transition to L-DNA where B- and L- DNA co-exist ($\sigma_{end} < \sigma < \sigma_{start}$), and finally converts fully to L-DNA ($\sigma < \sigma_{end}$). For a pure state, torque and extension can be calculated as appropriate derivatives of the free energy:

$$\tau_i(F) = \frac{1}{\omega_0}\frac{\partial G_i}{\partial \sigma}, \tag{3.6}$$

$$\frac{z_i}{L_i} = -\frac{\partial G_i}{\partial F}, \tag{3.7}$$

In the coexistence state, torque is constant, while extension is a linear combination of the two states (Marko, 2007).

We obtained analytical expressions for extension and torque for all three regions and performed a global fit to the data. Since there was considerably more noise in the torque signal compared to extension signal, the global fit was limited to the extension data surrounding the region of σ_{end}. There were five fit parameters: $L_{\boldsymbol{p,L}}$ C_L, b_L, $\sigma_{0,L}$, and ε_L, with ε_L mostly determining the melting torque. We have set the L-DNA stretch modulus K_L to infinity, as it could not be determined accurately over the range of forces explored. We also note that the WLC fit of the L-DNA extension, at the end of the melting transition, is an approximation in that it neglects L-DNA shortening due to writhe fluctuations (Moroz and Nelson, 1997). Fitting agreed reasonably well with the experimental data (red lines in Figure 3.2 and black lines in Figure 3.3), yielding elastic parameters of L-DNA in good agreement with those obtained above, as shown in Table 3.2.

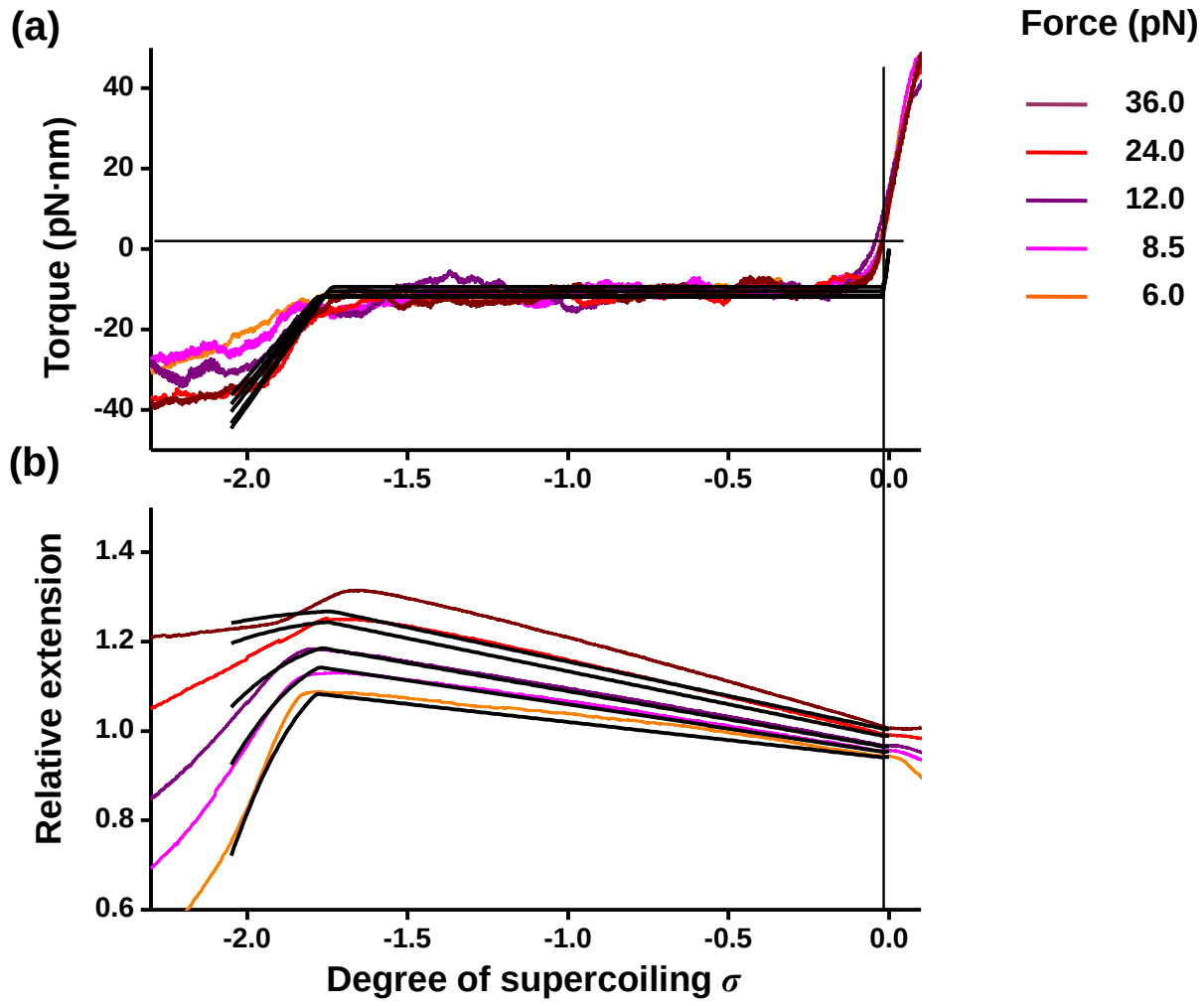

Figure 3.3: Results of the global fit (black lines) to the high force data from Figure 3.1.

	Phase transition theory	Worm-like-chain model
$L_{p,L}$ (nm)	5.5±1.0	3.3±0.7
C_L (nm)	17±7	18±3
b_L	1.37±0.03	1.42±0.07
$\sigma_{0,L}$	-1.6±0.1	not applicable
ε_L (kT/bp)	3	not applicable

Table 3.2: L-DNA parameters obtained using two methods: a global fit to the phase transition theory, and a fit of the L-DNA data to a worm-like-chain model.

Sequence-Dependent Behavior

Both thermal- and torsion-induced DNA melting transitions have been shown to occur in a sequence-dependent manner (Kowalski and Eddy, 1989; Strick et al., 1998b; Yakovchuk et al., 2006). However, little is known about the effects of DNA sequence on the elasticity of melted DNA. We investigated this on the single-molecule level by repeating the experiments described above using two additional constructs, Sequence B and Sequence C, that were derived from two entirely different plasmids and differ from the original Sequence A in GC content and overall sequence.

Surprisingly, while the torque signal during the melting transition was only marginally affected by sequence or GC content (data not shown), the extension change varied considerably in a force-dependent manner. Figure 3.4a depicts individual traces for each construct at a low (3.5 pN) and a high (12 pN) force for the three sequences. Figure 3.4b presents the reversibility data for Sequence B. Extension traces for the different sequences coincide at high forces, and unwinding and re-winding traces are fully reversible, indicating quasi-equilibrium measurements. In contrast, significant differences in extension traces were found at low forces, even for sequences with nearly identical overall GC-content. In addition, the extension traces for unwinding and rewinding no longer coincided and thus the process was no longer reversible, indicating the breakdown of the quasi-equilibrium condition. This trend became more prominent as force decreased. Based on these observations, we speculate that this sequence-dependent behavior at low forces may be attributable to the formation of secondary structures in L-DNA.

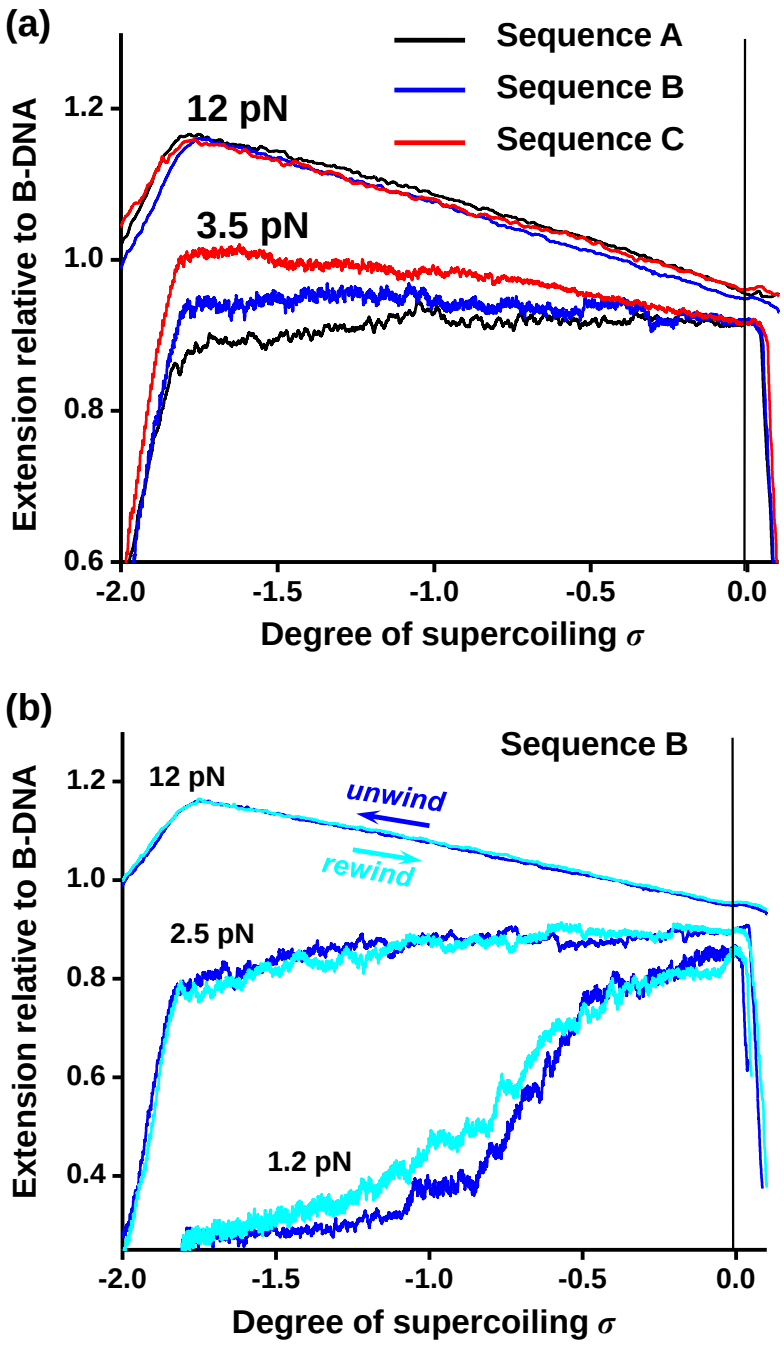

Figure 3.4: Sequence-dependence of melted DNA.
Representative extension traces of single DNA molecules are shown for different DNA sequences.
(a) Sequence-dependence. Extension behavior is identical for all three sequences at 12 pN (upper traces) and differs at 3.5 pN (lower traces).
(b) Reversibility illustrated using sequence B. Extension behavior is reversible at high force, and shows hysteresis at low force.

Conclusions

In summary, our single molecule experiments suggest a structural and mechanical model of torsionally-melted DNA under physiological salt conditions and tension > 5 pN. It is a left-handed structure (L-DNA) with a helicity of ~ −13 bp/turn. Its contour length is ~40% longer than B-DNA. L-DNA is quite flexible in response to bending, with a persistence length of ~3 nm, but has a relatively large effective torsional modulus of ~20 nm (at high force). We find that the B-DNA to L-DNA transition and L-DNA unwinding can be well described by a simple phase-transition model. At lower forces (< 5 pN), L-DNA adopts a more compacted configuration whose properties depend strongly on the DNA sequence. This behavior could be attributed to the formation of secondary structures in L-DNA. Indeed, the plateau-like force-extension curves (Figure 3.5) are reminiscent of those for ssDNA (Dessinges et al., 2002) and P-DNA (Allemand et al., 1998), which form hairpins and supercoiled P-DNA respectively.

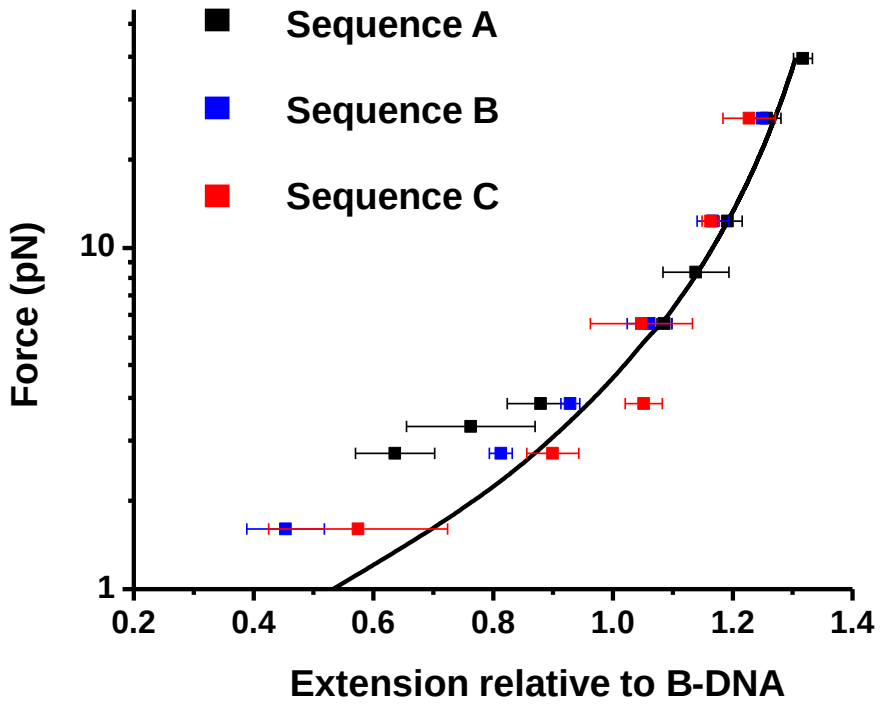

Figure 3.5: Effects of DNA sequence on the elasticity of torsionally-melted DNA. Force-extension curves for all three sequences coincide above 5 pN, but diverge below this force. Black line – WLC fit to the data for Sequence A.

Our data on phase transitions in underwound DNA are summarized in Figure 3.6, and present a complexity exceeding that found by earlier studies (Bryant et al., 2003; Leger et al., 1999). The range of forces explored here is well within that exerted by DNA-based motor proteins (Smith et al., 2001; Wang et al., 1998), some of which are also known to generate negative supercoiling. It is therefore possible for L-DNA to occur *in vivo*, where it may serve as a recognition target for regulatory factors. In addition to a detailed study of L-DNA, we have also discovered another DNA phase which appears upon further underwinding of L-DNA. The nature of this phase transition is outside the scope of the present work and requires further investigation. The data may be interpreted as the formation of supercoiled L-DNA (by analogy with supercoiled B-DNA). However, the rate of extension decrease during that phase transition is slower than during L-DNA twisting, and opposite to expectations based on existing data for supercoil formation. An alternative hypothesis can be formulated, based on an early work on DNA torsional melting (Allemand et al., 1998), where it was found that upon overwinding at sufficiently high force DNA bases flip to the outside of the phosphate backbone, forming a new structure named P-DNA. Molecular simulations by the same group have shown that a similar structure can be formed upon underwinding. It might thus be possible that the new phase we observed is akin to left-handed P-DNA - "LP-DNA". More conclusive evidence might be obtained by further molecular modeling that will be able to distinguish between two phases of torsionally underwound DNA.

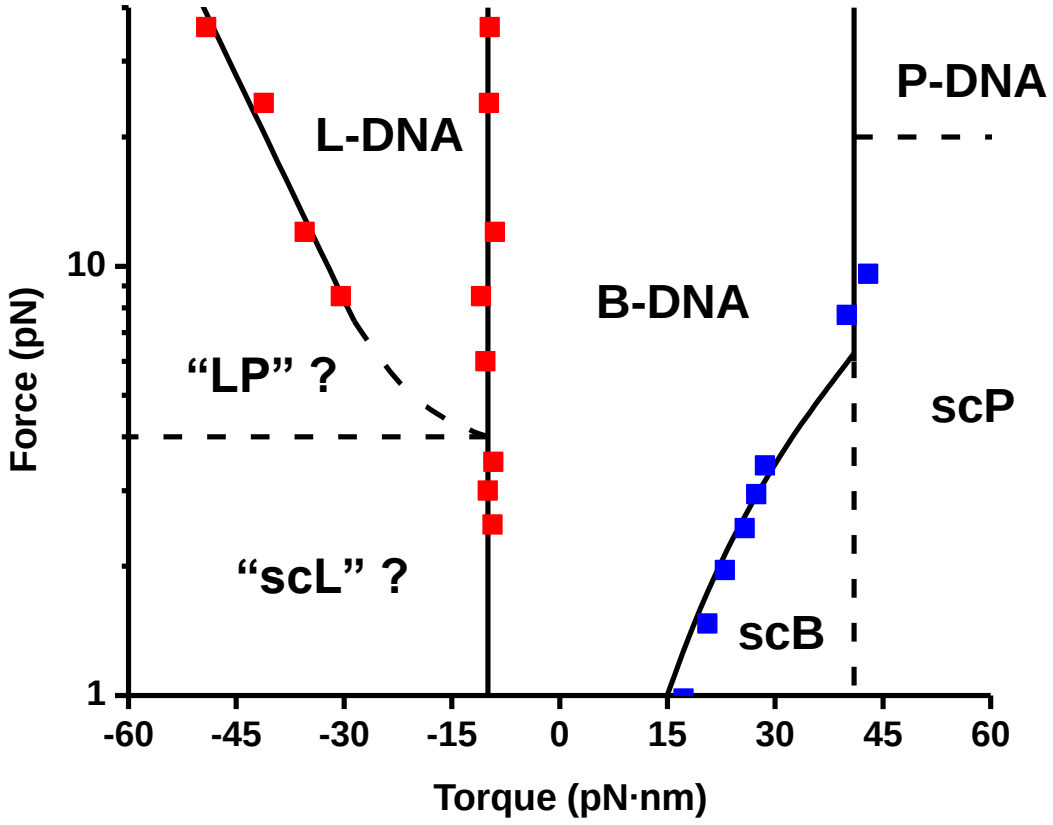

Figure 3.6: DNA force-torque phase diagram.

Note that the B-scB, B-P, and B-L transitions along the solid lines have been predicted theoretically (Marko, 2007) and verified by our previous (blue squares) and current (red squares) experimental measurements (Deufel et al., 2007; Forth et al., 2008; Sheinin and Wang, 2009). Dashed lines indicate putative phase transitions.

Our current work also extends theoretical understanding of torsionally-melted DNA, from previous analytical (Benham, 1979; Marko, 2007) and computational (Randall et al., 2009; Wereszczynski and Andricioaei, 2006) studies. Further research is needed to elucidate the precise effect sequence has on the structure and properties of L-DNA, as torsionally induced *in vivo* melting tends to be localized to specific sequences. Additionally, a comparative study between P-DNA and "LP-DNA" can undoubtedly add more colors to the rich palette of the physics of DNA phase transitions.

References

Allemand, J.F., Bensimon, D., Lavery, R., and Croquette, V. (1998). Stretched and overwound DNA forms a Pauling-like structure with exposed bases. Proc Natl Acad Sci U S A *95*, 14152-14157.

Baker, T.A., Sekimizu, K., Funnell, B.E., and Kornberg, A. (1986). Extensive unwinding of the plasmid template during staged enzymatic initiation of DNA replication from the origin of the Escherichia coli chromosome. Cell *45*, 53-64.

Benham, C.J. (1979). Torsional stress and local denaturation in supercoiled DNA. Proc Natl Acad Sci U S A *76*, 3870-3874.

Bryant, Z., Stone, M.D., Gore, J., Smith, S.B., Cozzarelli, N.R., and Bustamante, C. (2003). Structural transitions and elasticity from torque measurements on DNA. Nature *424*, 338-341.

Celedon, A., Nodelman, I.M., Wildt, B., Dewan, R., Searson, P., Wirtz, D., Bowman, G.D., and Sun, S.X. (2009). Magnetic tweezers measurement of single molecule torque. Nano Lett *9*, 1720-1725.

DePamphilis, M.L., ed. (1996). DNA Replication in Eukaryotic Cells (Cold Springs Harbor Press).

Dessinges, M.N., Maier, B., Zhang, Y., Peliti, M., Bensimon, D., and Croquette, V. (2002). Stretching single stranded DNA, a model polyelectrolyte. Phys Rev Lett *89*, 248102.

Deufel, C., Forth, S., Simmons, C.R., Dejgosha, S., and Wang, M.D. (2007). Nanofabricated quartz cylinders for angular trapping: DNA supercoiling torque detection. Nat Methods *4*, 223-225.

Forth, S., Deufel, C., Sheinin, M.Y., Daniels, B., Sethna, J.P., and Wang, M.D. (2008). Abrupt buckling transition observed during the plectoneme formation of individual DNA molecules. Phys Rev Lett *100*, 148301.

Friese, M.E.J., Nieminen, T.A., Heckenberg, N.R., and Rubinsztein-Dunlop, H. (1998). Optical alignment and spinning of laser-trapped microscopic particles. Nature *394*, 348-350.

Ho, P.S., Ellison, M.J., Quigley, G.J., and Rich, A. (1986). A computer aided thermodynamic approach for predicting the formation of Z-DNA in naturally occurring sequences. EMBO J *5*, 2737-2744.

Inman, J., Forth, S., and Wang, M.D. (2010). Passive torque wrench and angular position detection using a single-beam optical trap. Opt Lett *35*, 2949-2951.

Jacob, R.J., Lebowitz, J., and Printz, M.P. (1974). Unpaired bases in superhelical DNA: kinetic evidence. Nucleic Acids Res *1*, 549-558.

Kahn, J.D., Yun, E., and Crothers, D.M. (1994). Detection of localized DNA flexibility. Nature *368*, 163-166.

Kouzine, F., and Levens, D. (2007). Supercoil-driven DNA structures regulate genetic transactions. Front Biosci *12*, 4409-4423.

Kowalski, D., and Eddy, M.J. (1989). The DNA unwinding element: a novel, cis-acting component that facilitates opening of the Escherichia coli replication origin. EMBO J *8*, 4335-4344.

La Porta, A., and Wang, M.D. (2004). Optical torque wrench: angular trapping, rotation, and torque detection of quartz microparticles. Phys Rev Lett *92*, 190801.

Lee, M., Kim, S.H., and Hong, S.C. (2010). Minute negative superhelicity is sufficient to induce the B-Z transition in the presence of low tension. Proc Natl Acad Sci U S A *107*, 4985-4990.

Leger, J.F., Romano, G., Sarkar, A., Robert, J., Bourdieu, L., Chatenay, D., and Marko, J.F. (1999). Structural transitions of a twisted and stretched DNA molecule. Physical Review Letters *83*, 1066-1069.

Lipfert, J., Kerssemakers, J.W., Jager, T., and Dekker, N.H. (2010). Magnetic torque tweezers: measuring torsional stiffness in DNA and RecA-DNA filaments. Nat Methods *7*, 977-980.

Liu, Y., and West, S.C. (2004). Happy Hollidays: 40th anniversary of the Holliday junction. Nat Rev Mol Cell Biol *5*, 937-944.

Marko, J.F. (2007). Torque and dynamics of linking number relaxation in stretched supercoiled DNA. Physical Review E *76*, 021926.

Moroz, J.D., and Nelson, P. (1997). Torsional directed walks, entropic elasticity, and DNA twist stiffness. Proc Natl Acad Sci U S A *94*, 14418-14422.

Nelson, D.L., and Cox, M.M. (2005). Lehninger Principles of Biochemistry (New York, W. H. Freeman and Company).

Nieminen, T.A., Heckenberg, N.R., and Rubinsztein-Dunlop, H. (2001). Optical measurement of microscopic torques. Journal of Modern Optics *48*, 405-413.

Randall, G.L., Zechiedrich, L., and Pettitt, B.M. (2009). In the absence of writhe, DNA relieves torsional stress with localized, sequence-dependent structural failure to preserve B-form. Nucleic Acids Res. *37*, 5568-5577.

Sarkar, A., Leger, J.F., Chatenay, D., and Marko, J.F. (2001). Structural transitions in DNA driven by external force and torque. Phys Rev E Stat Nonlin Soft Matter Phys *63*, 051903.

Sheinin, M.Y., and Wang, M.D. (2009). Twist-stretch coupling and phase transition during DNA supercoiling. Phys Chem Chem Phys *11*, 4800-4803.

Siebenlist, U. (1979). RNA polymerase unwinds an 11-base pair segment of a phage T7 promoter. Nature *279*, 651-652.

Smith, D.E., Tans, S.J., Smith, S.B., Grimes, S., Anderson, D.L., and Bustamante, C. (2001). The bacteriophage straight phi29 portal motor can package DNA against a large internal force. Nature *413*, 748-752.

Strick, T.R., Allemand, J.F., Bensimon, D., Bensimon, A., and Croquette, V. (1996). The elasticity of a single supercoiled DNA molecule. Science *271*, 1835-1837.

Strick, T.R., Allemand, J.F., Bensimon, D., and Croquette, V. (1998a). Behavior of supercoiled DNA. Biophys J *74*, 2016-2028.

Strick, T.R., Croquette, V., and Bensimon, D. (1998b). Homologous pairing in stretched supercoiled DNA. Proc Natl Acad Sci U S A *95*, 10579-10583.

Thomas, T.J., and Bloomfield, V.A. (1983). Chain flexibility and hydrodynamics of the B and Z forms of poly(dG-dC).poly(dG-dC). Nucleic Acids Res *11*, 1919-1930.

Umek, R.M., and Kowalski, D. (1988). The ease of DNA unwinding as a determinant of initiation at yeast replication origins. Cell *52*, 559-567.

Vinograd, J., Lebowitz, J., Radloff, R., Watson, R., and Laipis, P. (1965). The twisted circular form of polyoma viral DNA. Proc Natl Acad Sci U S A *53*, 1104-1111.

Wang, M.D., Schnitzer, M.J., Yin, H., Landick, R., Gelles, J., and Block, S.M. (1998). Force and velocity measured for single molecules of RNA polymerase. Science *282*, 902-907.

Wang, M.D., Yin, H., Landick, R., Gelles, J., and Block, S.M. (1997). Stretching DNA with optical tweezers. Biophys J *72*, 1335-1346.

Wereszczynski, J., and Andricioaei, I. (2006). On structural transitions, thermodynamic equilibrium, and the phase diagram of DNA and RNA duplexes under torque and tension. Proc Natl Acad Sci U S A *103*, 16200-16205.

Yakovchuk, P., Protozanova, E., and Frank-Kamenetskii, M.D. (2006). Base-stacking and base-pairing contributions into thermal stability of the DNA double helix. Nucleic Acids Res *34*, 564-574.

CHAPTER 4

NUCLEOSOME STABILITY UNDER TENSION AND TORQUE

Introduction

Nucleosome, the fundamental unit of chromatin, consists of 147 bp of DNA wrapped around a complex of histone proteins – $(H3/H4)_2$ tetramer and a pair of H2A/H2B dimers (Luger et al., 1997) (Figure 4.1). Nucleosomes are crucial for maintaining the genome in a compacted state, which is reflected in the large binding affinity of the histone octamer to DNA (on the order of 40 k_BT (Brower-Toland et al., 2002; Ranjith et al., 2007)). On the other hand, nucleosomes need to provide a controlled access to DNA during vital cellular processes such as transcription and replication (Alabert and Groth, 2012; Li et al., 2007). This is accomplished via a plethora of mechanisms, including "breathing" – partial unwrapping of the DNA from the histone core, nucleosome sliding, and histone loss and deposition (Andrews and Luger, 2011; Bell et al., 2011). Whole protein families, such as histone chaperones, chromatin remodelers, and transcription factors, have been implicated in facilitating these transactions (Bell et al., 2011). Recent experimental advances have also brought attention to the role mechanistic effects can play in regulating nucleosome structure and stability (Brower-Toland et al., 2002; Hall et al., 2009; Lavelle, 2009). However, the relative importance of the contribution of these factors is not clear.

One of the most striking features of the nucleosome is the well-defined helical path of the DNA: about 1.65 turns is wrapped around the histone octamer in a left-handed (negative) superhelix (Luger et al., 1997). This negative supercoiling, first discovered almost 40 years ago (Germond et al., 1975), has been associated with nucleosome preference of negatively over positively supercoiled DNA during *in vitro* assembly (Clark and Felsenfeld, 1991; Pfaffle and Jackson, 1990). It has also been suggested that positive supercoiling can promote nucleosome disassembly (Levchenko et al., 2005; Pfaffle et al., 1990). However, *in vivo* relevance of these observation was for a long time questioned due to the absence of evidence for unconstrained supercoiling in eukaryotes (Sinden et al., 1980). Only recently *in vivo* studies have convincingly demonstrated

that unconstrained supercoiling is ubiquitous in eukaryotic cells, even in the presence of a full complement of topoisomerases (Kouzine et al., 2013; Kouzine et al., 2008; Matsumoto and Hirose, 2004). This supercoiling was found to be transcription-dependent, in agreement with the "twin-supercoiled domain" model, which states that immobilized groove-tracking enzymes such as RNA polymerase will generate DNA supercoiling during elongation (Liu and Wang, 1987). It is therefore established that cellular chromatin can experience transient torsional stress.

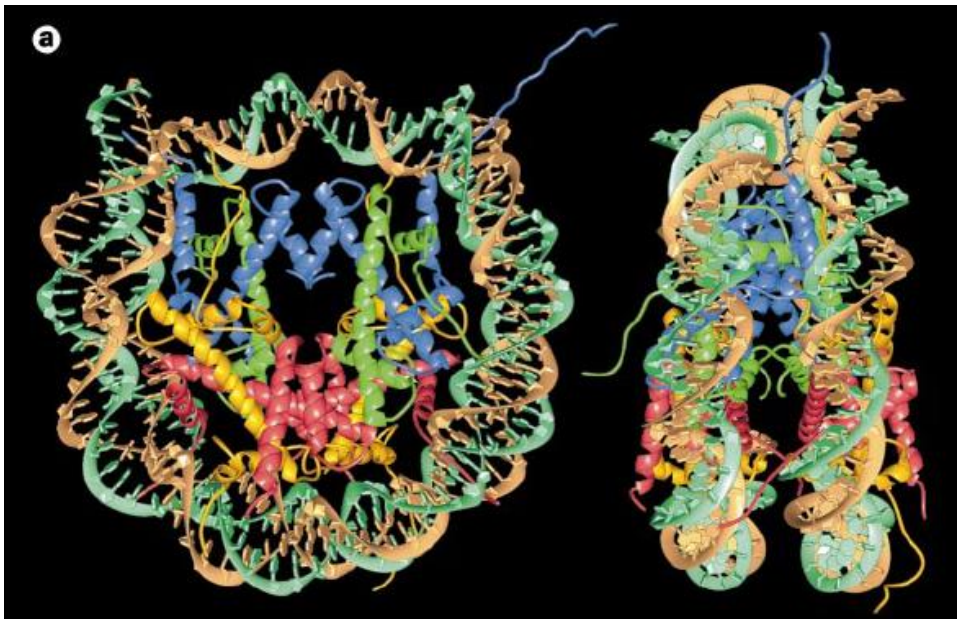

Figure 4.1: Nucleosome crystal structure.

Ribbon traces of 146-bp DNA (brown and turquoise) and eight histone proteins main chains (blue: H3, green: H4, yellow: H2A, red: H2B). The views are down the DNA superhelix axis (left) and perpendicular to it (right). Adapted from (Luger et al., 1997) with permission from Nature Publishing Group.

Recent single-molecule experiments have investigated the behavior of supercoiled chromatin, finding evidence for a flexible structure capable of accommodating a significant amount of supercoiling (Bancaud et al., 2006; Bancaud et al., 2007). However, low tension employed in the previous studies precluded the investigation of the effect of torque on nucleosome disruption. This problem is very pertinent in the context of transcription, as RNA polymerase is known to exert large forces (Galburt et al., 2007; Wang et al., 1998), which are in principle sufficient to disrupt the nucleosome (Brower-Toland et al., 2002; Mihardja et al., 2006). Could torque play a supportive role in this process?

During RNA polymerase elongation through chromatin nucleosomes are displaced downstream and reformed upstream; however, reformation is often accompanied by a partial or total histone loss (Hodges et al., 2009; Kireeva et al., 2002; Kulaeva et al., 2009). It has been shown *in vitro* that various factors, such as transcription speed (Bintu et al., 2012b), histone modifications (Bintu et al., 2012a; Hsieh et al., 2010), and polymerase cooperation (Jin et al., 2010; Kulaeva et al., 2010) can affect the frequency and type of histone loss. Since, as discussed above, torsion is intimately associated with transcription and has already been found to regulate nucleosome assembly, could it also influence the fate of histones upon transcription?

In order to address these questions, we have carried out a comprehensive investigation of the response of a single nucleosome to force and torque. Such investigation requires full experimental control of a nucleosome under torsion – specifying a desired degree of DNA supercoiling at will, direct measurements of torque in the DNA, and access to a large range of forces. We have achieved these capabilities using an angular optical trap (AOT), a technique that we recently developed for single-molecule torsional studies (Deufel et al., 2007; Forth et al., 2008; La Porta and Wang, 2004; Sheinin et al., 2011). By investigating nucleosome disruption under different levels of torque, we have found that torque differentially affects stability of the outer and inner turns of the nucleosome. We have also observed that positive torque induced

dramatic H2A/H2B dimer loss, suggesting that this can be a mechanism to regulate histone turnover during transcription.

Materials and Methods

The DNA construct used for all experiments consisted of 4 pieces: two middle segments and two linker segments (Figure 4.2). Linkers were made by performing PCR on the pLB601 plasmid (Forth et al., 2008) with a mix of 0.2 mM unmodified dNTP (Roche Applied Science) and 0.08 mM biotin-16-dCTP (Chemcyte Inc.) or 0.04 mM digoxigenin-11-dUTP (Roche Applied Science). Resulting 535 bp DNA fragments with multiple tags were digested with BsaI (New England Biolabs) to create single 4-bp overhangs and purified. Middle segments (1058 and 1720 bp) were created by PCR from, respectively, pLB601 and pBR322 plasmids (New England Biolabs), digested with BsaI to create two 4-bp overhangs and purified. The shorter (1 kb) segment contained the 601 positioning element (Lowary and Widom, 1998) in the middle and was used for nucleosome assembly (see below). All the BsaI cut sites were introduced via PCR primers.

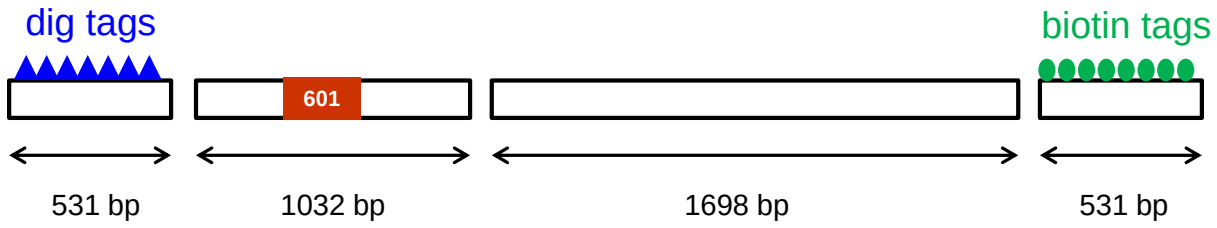

Figure 4.2: DNA template schematic. Digoxigenin tags are blue triangles, biotin tags are green ovals. Segment lengths indicated are those after BsaI digest. The 601 positioning element is red.

For most of the experiments, we used purified HeLa histones, which were assembled into nucleosomes using a well-established salt-dialysis method (Dyer et al., 2004). Nucleosomes were stored at 4 ºC for several weeks. For tetrasome experiments recombinant *Xenopus* $(H3/H4)_2$ tetramers (purchased from CSU Protein Purification and Characterization Facility and obtained from Dr. Karolin Luger's lab) were used. To control for potential differences between different types of histones, we also assembled nucleosomes using recombinant *Xenopus* octamers (CSU Protein Purification and Characterization Facility) and performed experiments using these nucleosomes.

On the day of the experiment, the four DNA pieces (including 1 kb fragment with a single assembled nucleosome or tetrasome) were mixed in equal ratios at 5-10 nM concentration (25 nM for tetrasome experiments) and ligated at 16ºC for 1 hour. Experiments were conducted in a climate-controlled room at a temperature of 23±1ºC in a nucleosome buffer containing 10 mM Tris-Cl (pH 8.0), 100 mM NaCl, 1.5 mM $MgCl_2$, 1 mM EDTA, 1 mM DTT, 0.02% Tween and 2 mg/ml acBSA. Casein from bovine milk (Sigma) at 4 mg/ml was used to passivate the surface.

Nucleosomal DNA stretching experiments were performed with the constraint of a fixed linking number: –0.019, 0, +0.015, +0.028, +0.041, +0.056. While DNA torsional modulus is force-dependent, at high forces (>2 pN) relevant in our experiments this force-dependence is negligible (Moroz and Nelson, 1997), so that stretching process can be approximated as occurring under a nearly constant torque.

Data were anti-alias filtered at 1 kHz, acquired at 2 kHz, and decimated with averaging to 200 Hz. All data were acquired and analyzed using custom written LabView software. Detection of sudden nucleosomal DNA releases was performed by cross-correlating a step function with the extension time series. Cross-correlation time series exhibited a sharp peak at the sudden DNA release point. The force at this time point was called the disruption force. Basepair release was found by calculating extension difference right after and right before the release and then converting it to number of basepairs using WLC model of torsionally constrained DNA (Marko, 1998, 2007).

Error bar σ for the probability of outer turn release p was calculated as the standard error of a binomial distribution $\sigma = \sqrt{\frac{p(1-p)}{n}}$, where n is the number of trials. Error bar for the normalized sudden outer turn release probability upon second stretch was calculated by defining the 66% confidence interval of the ratio of two proportions: $\frac{p_1}{p_2} = exp\left[ln\left(\frac{p_1}{p_2}\right) \pm \sqrt{\frac{n_1-x_1}{n_1 x_1} + \frac{n_2-x_2}{n_2 x_2}}\right]$, where p_1 is the sudden outer turn release probability upon second stretch at +38 pN·nm, p_2 is the sudden outer turn release probability upon control stretch +38 pN·nm, n_1 and n_2 are the respective number of trials, and x_1 and x_2 are the respective number of sudden outer turn releases (Koopman, 1984). The standard error for some of the force and basepair release measurements of the sudden outer turn release has been corrected using the t-statistic to account for small number of observations (N<10).

Results

In order to probe nucleosome stability under torsion, we twisted a nucleosomal DNA molecule to generate a desired degree of supercoiling and torque, and then stretched the DNA in order to disrupt the nucleosome (Figure 4.3a). The ranges of forces (1-30 pN) and torques (−10 to +40 pN·nm) used were chosen so as to maintain DNA in its native B-form conformation (Deufel et al., 2007; Forth et al., 2008; Marko, 2007; Sheinin et al., 2011) and are comparable to those measured or estimated for molecular motors such as RNA polymerase (Galburt et al., 2007; Wang et al., 1998). Figure 4.3b shows examples of the resulting force-extension curves. We found that DNA was released in two stages during stretching: a sudden release or gradual peeling at low force (< 6 pN); and a sudden release at high force (≥ 6 pN). These features resemble those of previous single molecule studies of torsionally unconstrained nucleosomes (Brower-Toland et al., 2005; Brower-Toland et al., 2002; Mihardja et al., 2006; Simon et al., 2011) which interpreted these two stages as the unwrapping of the outer turn DNA (low force) followed by the inner turn DNA (high force). Inner turn unwrapping always manifests itself as a sudden high-force transition (Brower-Toland et al., 2005; Brower-Toland et al., 2002; Mihardja et al., 2006; Simon et al., 2011). In contrast, the unwrapping process of the outer turn reflects a delicate energy balance between weaker histone-DNA interactions (Hall et al., 2009) and linker DNA bending (Mihardja et al., 2006; Sudhanshu et al., 2011) and was previously observed to proceed in either a gradual (Brower-Toland et al., 2002; Mihardja et al., 2006) or an abrupt (Kruithof and van Noort, 2009; Mihardja et al., 2006) manner, depending on the buffer conditions and type of histones used.

Figure 4.3: Experimental configuration and representative traces.

a) Configuration of the nucleosome stretching assay. DNA with a single nucleosome was torsionally constrained between a nanofabricated quartz cylinder and a coverglass, and was placed under desired torsion by adding twist via the cylinder. The angle of the cylinder, α, was then fixed, while the force, F, was increased at a rate of 2 pN/s to disrupt the nucleosome. This allowed the outer and inner turns of the nucleosomal DNA to be successively unwrapped.

b) Examples of individual force-extension curves of nucleosomes under approximately +19 pN·nm of torque. Red and blue curves correspond to traces with sudden and gradual outer turn DNA releases respectively, and the black curve corresponds to a naked DNA trace.

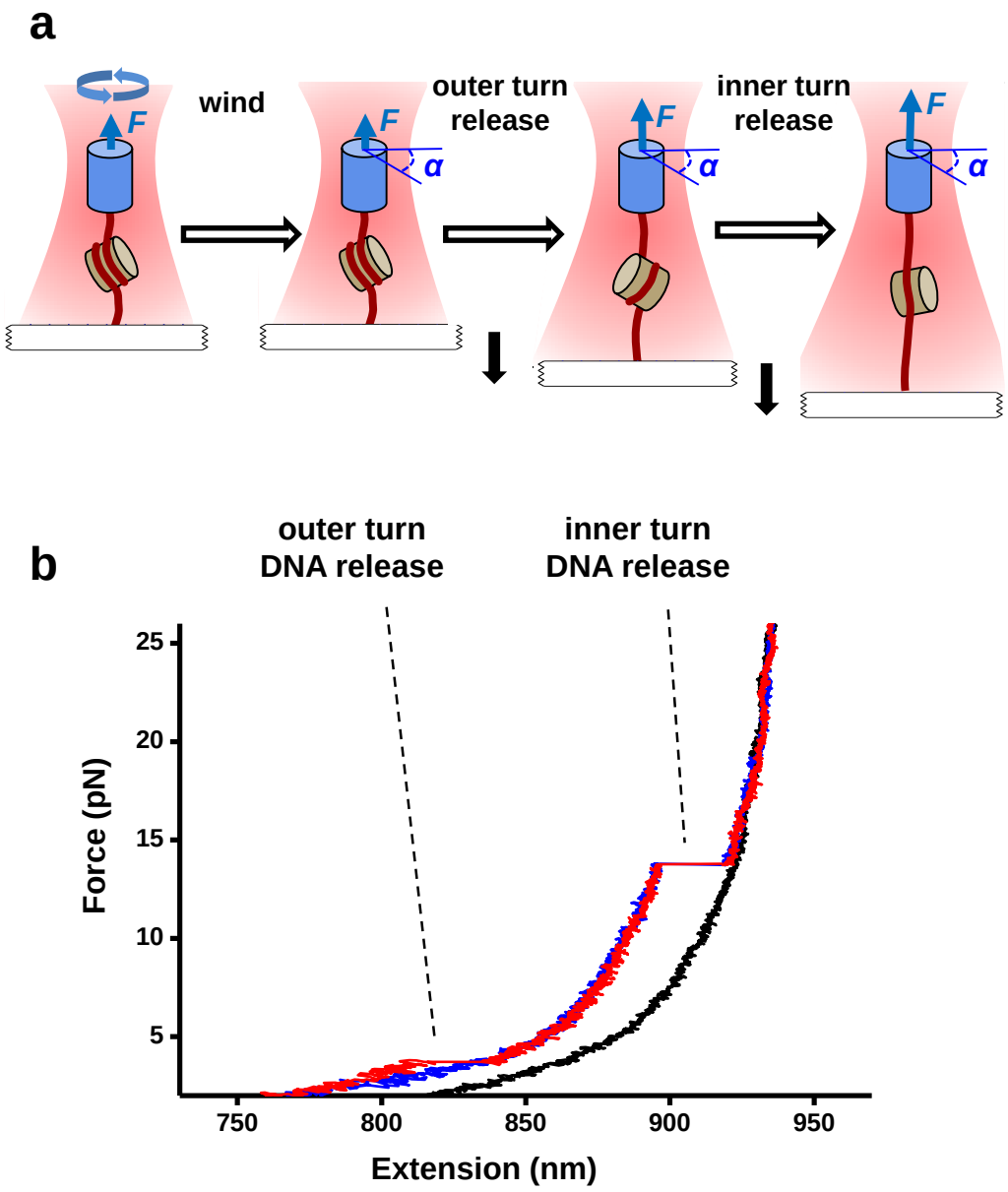
a
wind
outer turn
release
inner turn
release
F
α
b
outer turn
DNA release
inner turn
DNA release
Force (pN)
25
20
15
10
5
750
800
850
900
950
Extension (nm)

We then proceeded to analyze the characteristic parameters of the unwrapping process as a function of torque. First, we quantified sudden outer and inner turn DNA release of a nucleosome and found that approximately the same amount of DNA was released in both cases, independent of torque (Figure 4.4a). This indicates that at the start of the stretching, ~140-150 bp were associated with a nucleosome on either relaxed or supercoiled DNA, and the initial force (~ 1 pN) did not release DNA from a nucleosome.

In contrast, torque did have a significant impact on the disruption forces. Interestingly, the trends observed were different for outer and inner turns: torsion was found to stabilize the outer turn, but destabilize the inner turn (Figure 4.4b). The increased stability of the outer turn is consistent with the model of nucleosome under torsion proposed by Prunell and co-workers (Bancaud et al., 2006; De Lucia et al., 1999; Sivolob and Prunell, 2004): both negative and positive torque promote tighter wrapping of the linker DNA around the histone core, thus resisting unwrapping. This tightening can disfavor DNA breathing and restrict the access of transcription factors to the nucleosomal DNA (Li and Widom, 2004). It is the inner turn interactions, however, that form the key impediment to the progression of transcription machinery through a nucleosome (Hall et al., 2009; Hodges et al., 2009). Large positive torque reduces the force of the inner turn disruption by over 30%, and low to moderate torques by over 10%. Interestingly, the latter number is similar to the effect of extensive histone tail acetylation (Brower-Toland et al., 2005). Acetylation is known to be a hallmark of transcriptionally active chromatin (Campos and Reinberg, 2009); it is therefore tempting to speculate that moderate torque is also capable of assisting transcription.

Figure 4.4: Characterizing nucleosome disruption under force and torque.

a) Sudden release of the inner (filled squares) and outer (open circles) turns of DNA in a nucleosome. Error bars are SEM.

b) Mean disruption forces of the inner (filled squares) and outer (open circles) turns of DNA in a nucleosome. Error bars are SEM.

c) Fraction of traces that displayed a sudden outer turn release as a function of torque.

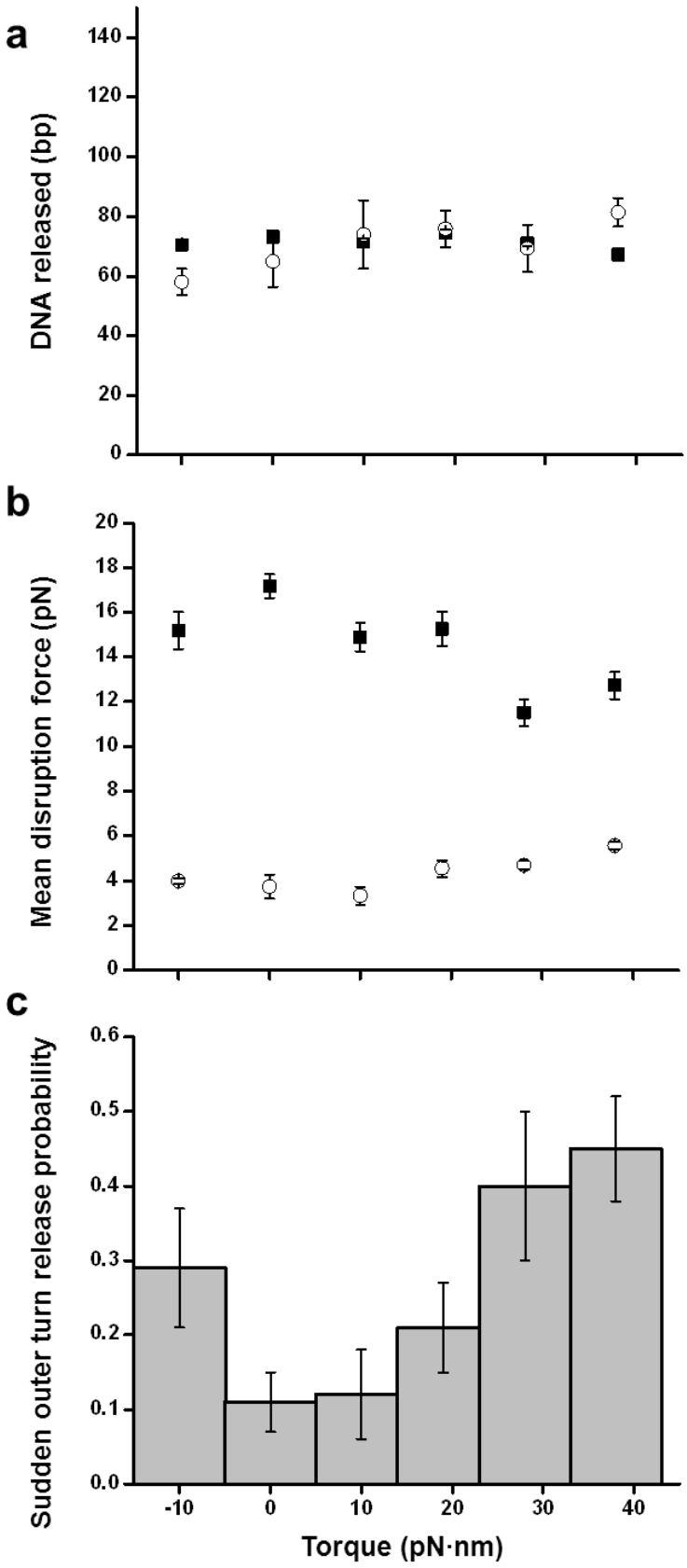
a
DNA released (bp)
0
20
40
60
80
100
120
140
b
Mean disruption force (pN)
0
2
4
6
8
10
12
14
16
18
20
c
Sudden outer turn release probability
0.0
0.1
0.2
0.3
0.4
0.5
0.6
-10
0
10
20
30
40
Torque (pN·nm)

We also examined the probability of observing a sudden outer turn transition as a function of torque (Figure 4.4c). The probability exhibited a strong torque-dependence which agreed with the trends in outer turn disruption force (Figure 4.4b). While only ~10% of traces exhibited a sudden low force transition for unconstrained DNA, this number went up to 30% for DNA under −10 pN·nm and to almost 50% under +38 pN·nm of torque.

Which histone-DNA interactions are correlated with the outer turn unwrapping? While examination of the crystal structure indicates that H2A/H2B-DNA contacts form the bulk of those interactions (Luger et al., 1997), no direct proof currently exists. To test this hypothesis we performed stretching experiments at several values of torque on tetrasomes – particles containing solely an $(H3/H4)_2$ tetramer. We have compared the behavior of recombinant *Xenopus* tetramers with their octameric counterparts, as well as purified HeLa octamers (Figure 4.5). Even at +38 pN·nm of torque no sudden outer turn disruption was observed (Figure 4.5c), which led us to conclude that the presence of H2A/H2B dimers is indeed required for this transition. Notably, high force transition for tetramers exhibited the same characteristics as that of the octamers, indicating that it is predominantly governed by H3/H4-DNA interactions (at least under our experimental conditions) (Figure 4.5a and 4.5b).

Figure 4.5: Characterizing tetrasome disruption under force and torque. Red color refers to *Xenopus* recombinant tetrasome, blue - *Xenopus* recombinant nucleosome, black – HeLa purified nucleosome. Note that no outer turn release is observed in a tetrasome.

a) Sudden release of the inner (filled squares) and outer (open circles) turns of DNA in a tetrasome and a nucleosome. Error bars are SEM.

b) Mean disruption forces of the inner (filled squares) and outer (open circles) turns of DNA in a tetrasome and a nucleosome. Error bars are SEM.

c) Fraction of traces that displayed a sudden outer turn release as a function of torque.

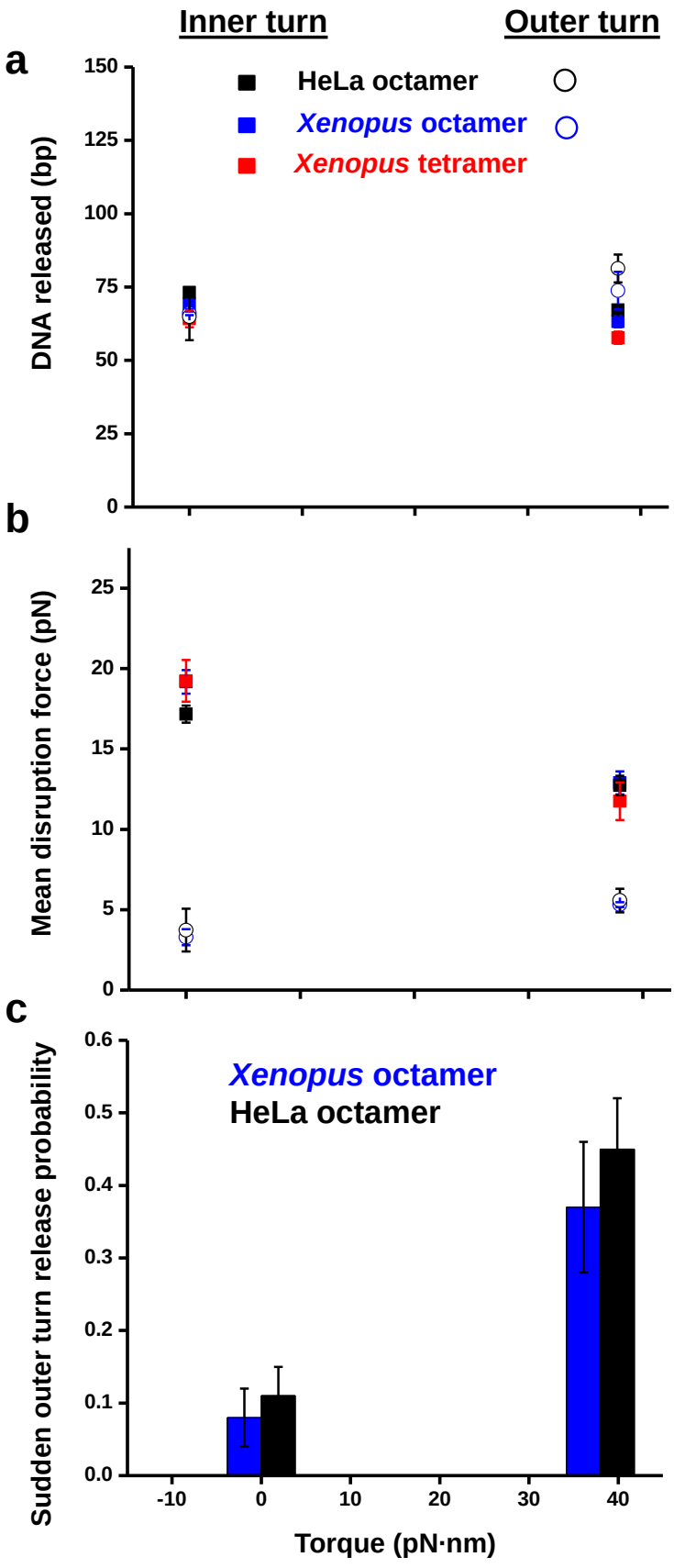
Inner turn
Outer turn
a
HeLa octamer
Xenopus octamer
Xenopus tetramer
DNA released (bp)
150
125
100
75
50
25
0
b
Mean disruption force (pN)
25
20
15
10
5
0
c
Xenopus octamer
HeLa octamer
Sudden outer turn release probability
0.6
0.5
0.4
0.3
0.2
0.1
0.0
-10
0
10
20
30
40
Torque (pN·nm)

Having established that outer turn unwrapping serves as an indicator of the H2A/H2B presence, we employed this observation to study the fate of histones upon nucleosome disruption. In the experiment designed to mimic effects of transcription through chromatin under torque, we first stretched the DNA under a certain torque, then relaxed the molecule, wound it to reach +38 pN·nm of torque and stretched again (Figure 4.6a). This 'checking' assay was based on the following two observations. First, the occurrence of the sudden low force, outer turn disruption requires the presence of a full octamer with both a $(H3/H4)_2$ tetramer and H2A/H2B dimers (Figure 4.5c). This sudden disruption occurs at a well-defined probability for a given torque value (Figure 4.4c) and is always followed by a high-force sudden disruption of the inner turn DNA. Second, the occurrence of a sudden high-force disruption requires the presence of $(H3/H4)_2$ tetramer only (Figure 4.5), and represents either the sudden unwrapping of the inner-turn DNA for a nucleosome or the sudden unwrapping of a single turn of a tetrasome. This always occurs as long as a $(H3/H4)_2$ tetramer is present. The torque for the control stretch (+38 pN·nm) was chosen because it had the largest chance of observing a sudden low force transition (Figure 4.4c).

Interestingly, we found that torsion differentially affected the stability of the $(H3/H4)_2$ tetramer and the H2A/H2B dimers in a nucleosome. High-force unwrapping upon the second stretch was observed in ~70 ± 10% of the traces, irrespective of torsion, which signifies that the $(H3/H4)_2$ tetramer was efficiently retained on both relaxed and supercoiled DNA (Figure 4.6b middle). This lack of torque dependence can be explained by the flexible chirality of the tetramer, which can readily flip between left- and right-handed conformations (Hamiche et al., 1996). For a nucleosome on a relaxed or a negatively supercoiled DNA, the sudden low force disruption upon

the second stretch was observed at ~60 ± 15% of that expected for a full complement of histones, indicating that under these conditions a full nucleosome is retained on the DNA with ~60% probability. In contrast, the disruption of a nucleosome under positive torque caused a significant loss of H2A/H2B dimers, so that only 10-15% of the nucleosomes retained a full complement of histones (Figure 4.6b top). This observation suggests that transcription-generated positive supercoiling may result in preferential expulsion of H2A/H2B dimers (Figure 4.6b bottom).

Figure 4.6: Histone fate upon disruption under torque.

a) Experimental strategy to examine the nucleosome stability under torque. A nucleosomal DNA molecule was supercoiled to a desired torsion, stretched at 2 pN/s up to 30 pN to disrupt the nucleosome before being relaxed over 1 s to 0.7 pN. It was then wound to +38 pN·nm and stretched again to determine which histones remained on the DNA. The time between relaxation and the second stretching was always kept at 30 s.

b) (Top) The probability of observing a sudden disruption at low force during the second stretch (right inset) was normalized to the corresponding value of the control stretch at +38 pN·nm of torque. Normalized probability of observing a sudden low force disruption is equivalent to the probability of retaining H2A/H2B after the initial stretch. (Middle) The probability of observing a sudden high force disruption (right inset) signifies the probability of retaining $(H3/H4)_2$ after the initial stretch. Insets show a representative trace of the force-extension curve resulting from a second stretch. (Bottom) Cartoons of predominant histones remaining on the DNA after disruption.

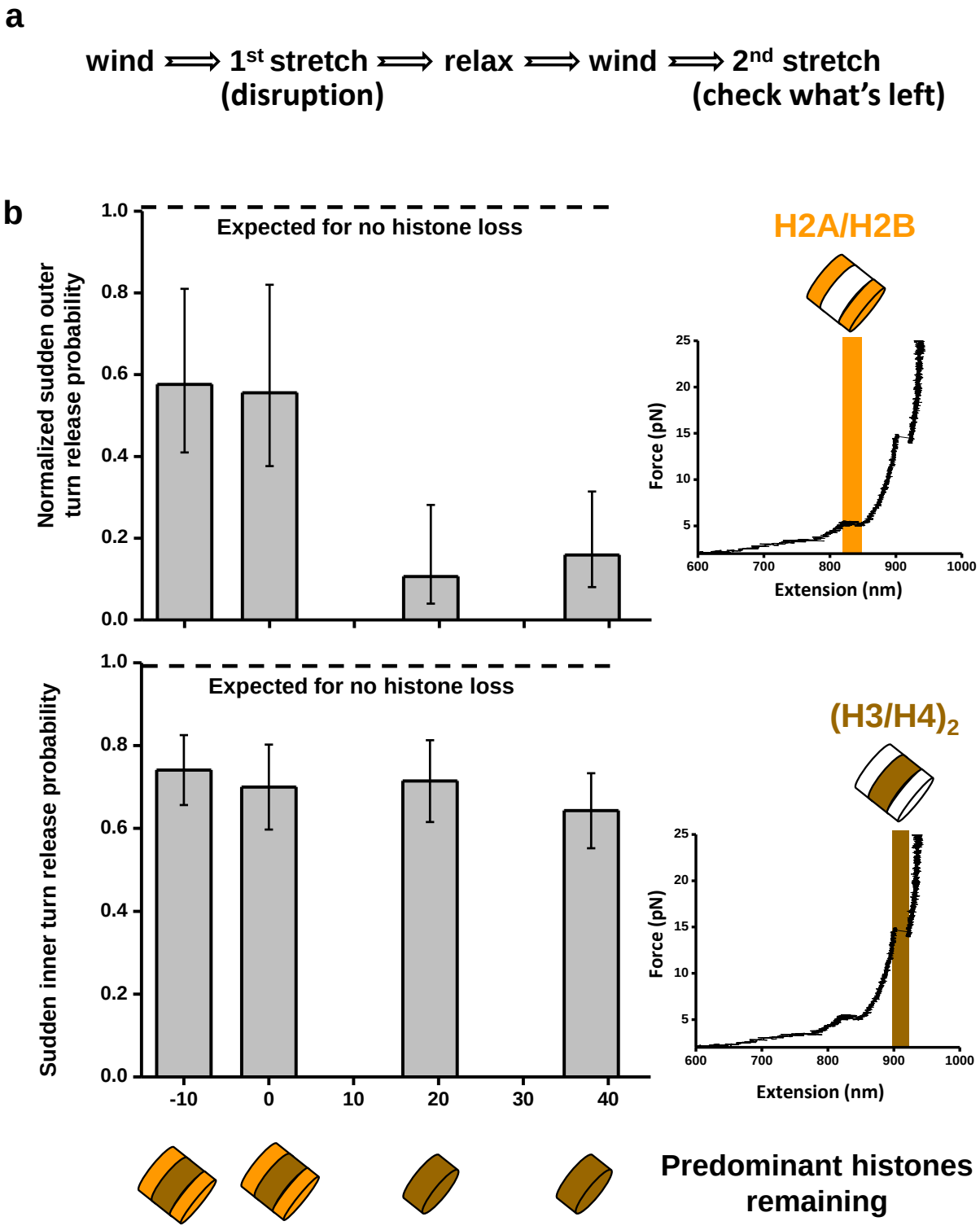
a
wind ⟹ 1st stretch ⟹ relax ⟹ wind ⟹ 2nd stretch
(disruption)
(check what's left)
b
Expected for no histone loss
Normalized sudden outer turn release probability
1.0
0.8
0.6
0.4
0.2
0.0
H2A/H2B
Force (pN)
25
20
15
10
5
600
700
800
900
1000
Extension (nm)
Expected for no histone loss
Sudden inner turn release probability
(H3/H4)2
-10
0
10
20
30
40
Predominant histones remaining

Discussion

In this work we present the first comprehensive investigation of single nucleosome response to torsion, examining its impact on the nucleosome stability and the histone fate. We find that nucleosomes under torque and force behave qualitatively similar to the nucleosomes under force alone. However, important quantitative differences suggest ways in which torque can act as a regulatory mechanism *in vivo*. First, torque was found to stabilize the outer turn of the nucleosome. It is known that DNA at the entry/exit sites is prone to spontaneous unwrapping (Li et al., 2005; Li and Widom, 2004), which may facilitate transcription factor binding (Bell et al., 2011). In this scenario the torque appears to play a repressing role. The effect is expected to be subtle, and careful *in vivo* studies are required to evaluate its significance. On the other hand, the destabilizing effect of torque (especially positive torque) on the highly stable interactions of the nucleosome inner turn should favor transcription elongation through chromatin. We found that moderate positive torque of 10-20 pN·nm, the range accessible to RNA polymerase (Ma, J., manuscript in press), destabilized the inner turn interactions by over 10%, an effect comparable to that of histone tail acetylation (Brower-Toland et al., 2005).

While the effect of torque on nucleosome stability is relatively modest, its impact on the fate of histones upon nucleosome disruption is profound. We discovered that torsion differentially influences tetramer and dimer reformation. In our experiments $(H3/H4)_2$ tetramer was efficiently retained on the DNA irrespective of torsion (~70% of the time), and H2A/H2B dimers displayed a similar retention rate for relaxed and negatively supercoiled DNA. In contrast, moderate and high positive torsion led to almost complete (~80%) dimer loss. /Moderate torque used in our

experiments is within the range accessible to RNA polymerase (Ma, J., manuscript in press), which suggests that torsion can provide an efficient mechanism for dimer eviction during transcription, in agreement with a previous *in vitro* study (Levchenko et al., 2005). While transcription on a linear template has also been observed to cause dimer loss (Kireeva et al., 2002), the eviction efficiency has been found not to exceed 30% even at an elevated salt concentration (Bintu et al., 2012b).

Previous *in vivo* studies found that H2A/H2B dimers are quickly exchanged at the sites of active transcription (Kimura and Cook, 2001). This may have functional significance for the deposition of histone variants (such as H2A.Z) that are known to regulate transcription (Petesch and Lis, 2012). While many factors, such as NAP-1, FACT, RSC and others, have been implicated in assisting H2A/H2B disassembly (Petesch and Lis, 2012), our study points out a purely mechanistic way of efficient dimer removal. The plausibility of such a mechanism is supported by recent observations of association between active transcription and DNA supercoiling *in vivo* (Kouzine et al., 2013; Matsumoto and Hirose, 2004). Importantly, the observed stability of tetramers in our study is also in agreement with *in vivo* observations of the slow exchange of H3/H4 histones (Kimura and Cook, 2001).

By analyzing the behavior of single nucleosomes under torque, our experiments pave the way to future investigation of nucleosome arrays and chromatin fibers under tension and torque. The high spatial and temporal resolution and direct torque measurements provided by the angular optical trap will undoubtedly be beneficial for such studies. It will be interesting to examine the effects of torsion on histones bearing specific post-translational modifications, as well as the

action of histone chaperones and chromatin remodelers. Future experiments should also attempt to reconstruct RNA polymerase elongation along a torsionally constrained chromatin template, building up on previous work performed on unconstrained templates (Bintu et al., 2012a; Hodges et al., 2009).

References

Alabert, C., and Groth, A. (2012). Chromatin replication and epigenome maintenance. Nat Rev Mol Cell Biol *13*, 153-167.

Andrews, A.J., and Luger, K. (2011). Nucleosome structure(s) and stability: variations on a theme. Annu Rev Biophys *40*, 99-117.

Bancaud, A., Conde e Silva, N., Barbi, M., Wagner, G., Allemand, J.F., Mozziconacci, J., Lavelle, C., Croquette, V., Victor, J.M., Prunell, A.*, et al.* (2006). Structural plasticity of single chromatin fibers revealed by torsional manipulation. Nat Struct Mol Biol *13*, 444-450.

Bancaud, A., Wagner, G., Conde, E.S.N., Lavelle, C., Wong, H., Mozziconacci, J., Barbi, M., Sivolob, A., Le Cam, E., Mouawad, L.*, et al.* (2007). Nucleosome chiral transition under positive torsional stress in single chromatin fibers. Mol Cell *27*, 135-147.

Bell, O., Tiwari, V.K., Thoma, N.H., and Schubeler, D. (2011). Determinants and dynamics of genome accessibility. Nat Rev Genet *12*, 554-564.

Bintu, L., Ishibashi, T., Dangkulwanich, M., Wu, Y.Y., Lubkowska, L., Kashlev, M., and Bustamante, C. (2012a). Nucleosomal elements that control the topography of the barrier to transcription. Cell *151*, 738-749.

Bintu, L., Kopaczynska, M., Hodges, C., Lubkowska, L., Kashlev, M., and Bustamante, C. (2012b). The elongation rate of RNA polymerase determines the fate of transcribed nucleosomes. Nat Struct Mol Biol *18*, 1394-1399.

Brower-Toland, B., Wacker, D.A., Fulbright, R.M., Lis, J.T., Kraus, W.L., and Wang, M.D. (2005). Specific contributions of histone tails and their acetylation to the mechanical stability of nucleosomes. J Mol Biol *346*, 135-146.

Brower-Toland, B.D., Smith, C.L., Yeh, R.C., Lis, J.T., Peterson, C.L., and Wang, M.D. (2002). Mechanical disruption of individual nucleosomes reveals a reversible multistage release of DNA. Proc Natl Acad Sci U S A *99*, 1960-1965.

Campos, E.I., and Reinberg, D. (2009). Histones: annotating chromatin. Annu Rev Genet *43*, 559-599.

Clark, D.J., and Felsenfeld, G. (1991). Formation of nucleosomes on positively supercoiled DNA. EMBO J *10*, 387-395.

De Lucia, F., Alilat, M., Sivolob, A., and Prunell, A. (1999). Nucleosome dynamics. III. Histone tail-dependent fluctuation of nucleosomes between open and closed DNA conformations. Implications for chromatin dynamics and the linking number paradox. A relaxation study of mononucleosomes on DNA minicircles. J Mol Biol *285*, 1101-1119.

Deufel, C., Forth, S., Simmons, C.R., Dejgosha, S., and Wang, M.D. (2007). Nanofabricated quartz cylinders for angular trapping: DNA supercoiling torque detection. Nat Methods *4*, 223-225.

Dyer, P.N., Edayathumangalam, R.S., White, C.L., Bao, Y., Chakravarthy, S., Muthurajan, U.M., and Luger, K. (2004). Reconstitution of nucleosome core particles from recombinant histones and DNA. Methods Enzymol *375*, 23-44.

Forth, S., Deufel, C., Sheinin, M.Y., Daniels, B., Sethna, J.P., and Wang, M.D. (2008). Abrupt buckling transition observed during the plectoneme formation of individual DNA molecules. Phys Rev Lett *100*, 148301.

Galburt, E.A., Grill, S.W., Wiedmann, A., Lubkowska, L., Choy, J., Nogales, E., Kashlev, M., and Bustamante, C. (2007). Backtracking determines the force sensitivity of RNAP II in a factor-dependent manner. Nature *446*, 820-823.

Germond, J.E., Hirt, B., Oudet, P., Gross-Bellark, M., and Chambon, P. (1975). Folding of the DNA double helix in chromatin-like structures from simian virus 40. Proc Natl Acad Sci U S A *72*, 1843-1847.

Hall, M.A., Shundrovsky, A., Bai, L., Fulbright, R.M., Lis, J.T., and Wang, M.D. (2009). High-resolution dynamic mapping of histone-DNA interactions in a nucleosome. Nat Struct Mol Biol *16*, 124-129.

Hamiche, A., Carot, V., Alilat, M., De Lucia, F., O'Donohue, M.F., Revet, B., and Prunell, A. (1996). Interaction of the histone (H3-H4)2 tetramer of the nucleosome with positively supercoiled DNA minicircles: Potential flipping of the protein from a left- to a right-handed superhelical form. Proc Natl Acad Sci U S A *93*, 7588-7593.

Hodges, C., Bintu, L., Lubkowska, L., Kashlev, M., and Bustamante, C. (2009). Nucleosomal fluctuations govern the transcription dynamics of RNA polymerase II. Science *325*, 626-628.

Hsieh, F.K., Fisher, M., Ujvari, A., Studitsky, V.M., and Luse, D.S. (2010). Histone Sin mutations promote nucleosome traversal and histone displacement by RNA polymerase II. EMBO Rep *11*, 705-710.

Jin, J., Bai, L., Johnson, D.S., Fulbright, R.M., Kireeva, M.L., Kashlev, M., and Wang, M.D. (2010). Synergistic action of RNA polymerases in overcoming the nucleosomal barrier. Nat Struct Mol Biol *17*, 745-752.

Kimura, H., and Cook, P.R. (2001). Kinetics of core histones in living human cells: little exchange of H3 and H4 and some rapid exchange of H2B. J Cell Biol *153*, 1341-1353.

Kireeva, M.L., Walter, W., Tchernajenko, V., Bondarenko, V., Kashlev, M., and Studitsky, V.M. (2002). Nucleosome remodeling induced by RNA polymerase II: loss of the H2A/H2B dimer during transcription. Mol Cell *9*, 541-552.

Koopman, P.A.R. (1984). Confidence-Intervals for the Ratio of 2 Binomial Proportions. Biometrics *40*, 513-517.

Kouzine, F., Gupta, A., Baranello, L., Wojtowicz, D., Ben-Aissa, K., Liu, J., Przytycka, T.M., and Levens, D. (2013). Transcription-dependent dynamic supercoiling is a short-range genomic force. Nat Struct Mol Biol *20*, 396-403.

Kouzine, F., Sanford, S., Elisha-Feil, Z., and Levens, D. (2008). The functional response of upstream DNA to dynamic supercoiling in vivo. Nat Struct Mol Biol *15*, 146-154.

Kruithof, M., and van Noort, J. (2009). Hidden Markov analysis of nucleosome unwrapping under force. Biophys J *96*, 3708-3715.

Kulaeva, O.I., Gaykalova, D.A., Pestov, N.A., Golovastov, V.V., Vassylyev, D.G., Artsimovitch, I., and Studitsky, V.M. (2009). Mechanism of chromatin remodeling and recovery during passage of RNA polymerase II. Nat Struct Mol Biol *16*, 1272-1278.

Kulaeva, O.I., Hsieh, F.K., and Studitsky, V.M. (2010). RNA polymerase complexes cooperate to relieve the nucleosomal barrier and evict histones. Proc Natl Acad Sci U S A *107*, 11325-11330.

La Porta, A., and Wang, M.D. (2004). Optical torque wrench: angular trapping, rotation, and torque detection of quartz microparticles. Phys Rev Lett *92*, 190801.

Lavelle, C. (2009). Forces and torques in the nucleus: chromatin under mechanical constraints. Biochem Cell Biol *87*, 307-322.

Levchenko, V., Jackson, B., and Jackson, V. (2005). Histone release during transcription: displacement of the two H2A-H2B dimers in the nucleosome is dependent on different levels of transcription-induced positive stress. Biochemistry *44*, 5357-5372.

Li, B., Carey, M., and Workman, J.L. (2007). The role of chromatin during transcription. Cell *128*, 707-719.

Li, G., Levitus, M., Bustamante, C., and Widom, J. (2005). Rapid spontaneous accessibility of nucleosomal DNA. Nat Struct Mol Biol *12*, 46-53.

Li, G., and Widom, J. (2004). Nucleosomes facilitate their own invasion. Nat Struct Mol Biol *11*, 763-769.

Liu, L.F., and Wang, J.C. (1987). Supercoiling of the DNA template during transcription. Proc Natl Acad Sci U S A *84*, 7024-7027.

Lowary, P.T., and Widom, J. (1998). New DNA sequence rules for high affinity binding to histone octamer and sequence-directed nucleosome positioning. J Mol Biol *276*, 19-42.

Luger, K., Mader, A.W., Richmond, R.K., Sargent, D.F., and Richmond, T.J. (1997). Crystal structure of the nucleosome core particle at 2.8 A resolution. Nature *389*, 251-260.

Marko, J.F. (1998). DNA under high tension: Overstretching, undertwisting, and relaxation dynamics. Physical Review E *57*, 2134-2149.

Marko, J.F. (2007). Torque and dynamics of linking number relaxation in stretched supercoiled DNA. Phys Rev E Stat Nonlin Soft Matter Phys *76*, 021926.

Matsumoto, K., and Hirose, S. (2004). Visualization of unconstrained negative supercoils of DNA on polytene chromosomes of Drosophila. J Cell Sci *117*, 3797-3805.

Mihardja, S., Spakowitz, A.J., Zhang, Y., and Bustamante, C. (2006). Effect of force on mononucleosomal dynamics. Proc Natl Acad Sci U S A *103*, 15871-15876.

Moroz, J.D., and Nelson, P. (1997). Torsional directed walks, entropic elasticity, and DNA twist stiffness. Proc Natl Acad Sci U S A *94*, 14418-14422.

Petesch, S.J., and Lis, J.T. (2012). Overcoming the nucleosome barrier during transcript elongation. Trends Genet *28*, 285-294.

Pfaffle, P., Gerlach, V., Bunzel, L., and Jackson, V. (1990). In vitro evidence that transcription-induced stress causes nucleosome dissolution and regeneration. J Biol Chem *265*, 16830-16840.

Pfaffle, P., and Jackson, V. (1990). Studies on rates of nucleosome formation with DNA under stress. J Biol Chem *265*, 16821-16829.

Ranjith, P., Yan, J., and Marko, J.F. (2007). Nucleosome hopping and sliding kinetics determined from dynamics of single chromatin fibers in Xenopus egg extracts. Proc Natl Acad Sci U S A *104*, 13649-13654.

Sheinin, M.Y., Forth, S., Marko, J.F., and Wang, M.D. (2011). Underwound DNA under tension: structure, elasticity, and sequence-dependent behaviors. Phys Rev Lett *107*, 108102.

Simon, M., North, J.A., Shimko, J.C., Forties, R.A., Ferdinand, M.B., Manohar, M., Zhang, M., Fishel, R., Ottesen, J.J., and Poirier, M.G. (2011). Histone fold modifications control nucleosome unwrapping and disassembly. Proc Natl Acad Sci U S A *108*, 12711-12716.

Sinden, R.R., Carlson, J.O., and Pettijohn, D.E. (1980). Torsional tension in the DNA double helix measured with trimethylpsoralen in living E. coli cells: analogous measurements in insect and human cells. Cell *21*, 773-783.

Sivolob, A., and Prunell, A. (2004). Nucleosome conformational flexibility and implications for chromatin dynamics. Philos Transact A Math Phys Eng Sci *362*, 1519-1547.

Sudhanshu, B., Mihardja, S., Koslover, E.F., Mehraeen, S., Bustamante, C., and Spakowitz, A.J. (2011). Tension-dependent structural deformation alters single-molecule transition kinetics. Proc Natl Acad Sci U S A *108*, 1885-1890.

Wang, M.D., Schnitzer, M.J., Yin, H., Landick, R., Gelles, J., and Block, S.M. (1998). Force and velocity measured for single molecules of RNA polymerase. Science *282*, 902-907.